MOLECULAR MECHANISMS OF RENAL EFFECT OF SGLT2 INHIBITOR AND GLP-1 RECEPTOR AGONIST ON CELLULAR MODEL OF PROXIMAL TUBULAR CELLS

Ninčević, Vjera

JOSIP JURAJ STROSSMAYER UNIVERSITY OF OSIJEK

FACULTY OF MEDICINE

Vjera Ninčević

MOLECULAR MECHANISMS OF RENAL EFFECT OF SGLT2 INHIBITOR AND GLP-1 RECEPTOR AGONIST ON CELLULAR MODEL OF PROXIMAL TUBULAR CELLS

Doctoral dissertation

Osijek, 2022.

JOSIP JURAJ STROSSMAYER UNIVERSITY OF OSIJEK

FACULTY OF MEDICINE

Vjera Ninčević

MOLECULAR MECHANISMS OF RENAL EFFECT OF SGLT2 INHIBITOR AND GLP-1 RECEPTOR AGONIST ON A CELLULAR MODEL OF PROXIMAL TUBULAR CELLS

Doctoral dissertation

Osijek, 2022.

Mentor: Assoc.Prof. Ines Bilić Ćurčić, Ph.D.

Co-Mentor: Prof. Ashraf Abdou Tabll, Ph.D.

The dissertation contains 133 pages.

POSVETA

Hvala Ti, predobri Isuse, što si me vodio kroz put ustrajnosti, odricanja i izazova u proteklim godinama istraživanja.

Hvala mami i tati, sestri i bratu na ljubavi, podršci i razumijevanju. Vi ste bili moja stijena.

Hvala mojoj ljubavi, mojem zaručniku Stipi na potpori i snazi u završnom dijelu ovog maratona. S tobom je svaki teški trenutak postajao podnošljiviji i ljepši.

Hvala mojoj rodbini i prijateljima na ogromnoj podršci, brizi i svakoj molitvi.

Hvala mojoj mentorici izv. prof. dr. sc. Ines Bilić Ćurčić koja je bila uz mene, bdijela nad mojim radom i uistinu pokazala što znači biti voditelj, prijatelj i velika podrška. Hvala Vam!

Hvala mojem komentoru prof. dr. sc. Ashraf Tabl koji je usprkos daljini uvijek porukama podrške i savjetima pratio moj rad.

Hvala prof. dr. sc. Martini Smolić što je vodila cijeli tim i mene kroz različite pustolovine istraživanja i koja me je mudrim savjetima usmjeravala.

Hvala mojim kolegama, posebno Tei Omanović Kolarić i Miloradu Zjaliću koji su uvijek bili uz mene i pomogli mi na putu odrastanja u doktora znanosti.

I još jednom hvala Tebi, ljubljeni Isuse, što si uvijek i zauvijek moja snaga, put, istina i život.

Ovo djelo posvećujem Njemu!

PREFACE

Thank you, dear Jesus, for leading and guiding me in paths of endurance, forcefulness, and all the challenges in the previous years of research.

I thank my Mom and Dad, my sister, and my brother for love, support, and understanding. You were my rock.

Thank you, my love, my fiancé, Stipe for support and strength in the final part of this marathon. With you, every difficult moment became more bearable and more beautiful.

I also thank my relatives and friends for their tremendous support, concern, and prayer.

Thank you, my mentor, Associate Professor Ines Bilić Ćurčić for standing by me, watching over my work and showing what it means to be a facilitator, a friend, and a great supporter. Thank you!

Thank you, Professor Ashraf Table, who, despite the distance, always followed my work with messages of support and advice.

Thank you, Professor Martina Smolić, for leading the entire team and myself through various adventures of research and for guiding me with words of wisdom.

Thank my colleagues, especially Tei Omanović Kolarić and Miloradu Zjaliću who have always been with me and helped me on my way to growing up as a doctor of science.

And thank you again, beloved Jesus, for always being my strength, the way, the truth, and the life.

I dedicate this work to Him!

Table of contents

Abbreviation list:

AMPK	AMP-activated protein kinase
ARB	angiotensin receptor blocker
ATP	adenosine triphosphate
BP	blood pressure
cAMP	cyclic adenosin monophosphate
cAMP-PKA	cAMP-dependent protein kinase
CANTATA-SU	Canagliflozin Treatment And Trial Analysis - Sulfonylurea
CANVAS	Canagliflozin Cardiovascular Assessment Study
CARMELINA	The Cardiovascular and Renal Microvascular Outcome Study With Linagliptin
CAROLINA	Cardiovascular Outcome Study of Linagliptin
CKD	chronic kidney disease
CNS	central nervous system
COX-1	cyclooxygenase-1
COX-2	cyclooxygenase-2
CV	cardiovascular
CVOT	cardiovascular outcomes trials
CYP1A2	cytochrome P450 1A2
CYP2C9	cytochrome P450 2C9
CYP2D6	cytochrome P450 2D6
D3OG	dapagliflozin 3-O-glucuronide
DECLARE-TIMI 58	Dapagliflozin Effect on Cardiovascular Events (DECLARE) - Thrombolysis in Myocardial Infarction (TIMI) 58
DKD	diabetic kidney disease
DMT1	diabetes mellitus type 1
DMT2	diabetes mellitus type 2
DN	diabetic nephropathy
DPP4	dipeptidyl peptidase-4
EASEL	Evidence for Cardiovascular Outcomes With Sodium Glucose Cotransporter 2 Inhibitors in the Real World
eGFR	estimated glomerular filtration rate
ELIXA	Evaluation of Lixisenatide in Acute Coronary Syndrome
EMA	European Medicines Agency

Empa	Empagliflozin
EMPA-REG OUTCOME	Empagliflozin Cardiovascular Outcome Event Trial in Type 2 Diabetes Mellitus Patients
EMT	epithelial-mesenchymal transition
ESC	European Society of Cardiology
EXAMINE	Examination of Cardiovascular Outcomes with Alogliptin versus Standard of Care
EXSCEL	Exenatide Study of Cardiovascular Event Lowering
F-actin	filamentous actin
FBS	fetal bovine serum
FDA	Food and Drug Administration
FIGHT	functional Impact of GLP-1 for Heart Failure Treatment
FN	fibronectin
GFR	glomerular filtration rate
GI	gastrointestinal
GLP-1	glucagon-like peptide-1
GLP1 RA	glucagon-like peptide-1 receptor agonist
GLUT2	glucose transporter 2
GPx	glutathione peroxidase
GSH	glutathione
GSSG	glutathione disulfide
HF	heart failure
HFrEF	HF with reduced ejection fraction
HG	high glucose
HIF-1α	hypoxia-inducible factor 1-alpha subunit
HK2 cells	human kidney 2 cells
IL6	interleukin 6
IL8	interleukin 8
JAKs	Janus kinases
LEADER	Liraglutide Effect and Action in Diabetes: Evaluation of Cardiovascular Outcome Results
LIRA-RENAL	Liraglutide Safe in Diabetes With Renal Failure

LIVE	The Effect of Liraglutide on Left Ventricular Function in Chronic Heart Failure Patients With and Without Type 2 Diabetes Mellitus
LLC-PK1	Pig Kidney Epithelial cells
MACE	major adverse cardiovascular events
MET-REMODEL	Metformin and Its Effects on Left Ventricular Hypertrophy in Normotensive Patients With Coronary Artery Disease
MTT	[3-(4, 5-dimethyl-2-thiazolyl) -2, 5-diphenyl -2H- tetrazolium bromide]
NAD(P)H	nicotinamide adenine dinucleotide phosphate
NFkB2	nuclear factor kappa B subunit 2
NHE3	sodium-hydrogen exchanger isoform 3
NS	nitrosative species
p-Akt	phosphorylation and activated Akt
PKA	protein kinase A
PKC	protein kinase C
PPAR-γ	peroxisome proliferator-activated receptor gamma
PT	proximal tubules
PTCs	proximal tubular epithelial cells
RAAS	renin–angiotensin–aldosterone system
ROS	reactive oxygen species
SAVOR	Saxagliptin Assessment of Vascular Outcomes Recorded
SAVOR-TIMI 53	Saxagliptin Assessment of Vascular Outcomes Recorded in Patients with Diabetes Mellitus (SAVOR)–Thrombolysis in Myocardial Infarction (TIMI) 53
SGLT1	sodium-glucose cotransporter 1
SGLT2	sodium-glucose cotransporter 2
SGLT2i	sodium glucose lowering transporter2 inhibitors
SIRT1	Sirtuin-1
STAT	signal transducer and transcription activator
STAT3	signal transducer and activator of transcription 3
SUSTAIN-6	Trial to Evaluate Cardiovascular and Other Long-term Outcomes With Semaglutide in Subjects With Type 2 Diabetes

	After Acute Coronary Syndrome During Treatment With Lixisenatide
DM	diabetes mellitus
T1DM	type I diabetes mellitus
T2DM	type II diabetes mellitus
TECOS	Trial Evaluating Cardiovascular Outcomes with Sitagliptin
TGFβ	transforming growth factor β
TIMI	thrombolysis in myocardial infarction
TNF-α	tumor necrosis factor alpha
UTI	urinary tract infections

1. INTRODUCTION

Diabetic nephropathy (DN) is a serious chronic complication of type I and type II diabetes mellitus (T1DM and T2DM) and is one of the major causes of kidney failure, resulting in an increase in dialysis and kidney transplantations worldwide. The number of people living with diabetes is rising across the globe and the International Diabetes Federation estimates the total number at 382 million. In the global prevalence of 382 million people with diabetes mellitus (DM), 5–10% of them have T1DM. Diabetic kidney disease (DKD) has been shown to potentially lead to end-stage renal disease in 30–40% of diabetic patients (1, 2), which means that genetic variations may affect the onset and progression of DM and kidney damage.

Development and progression of diabetic nephropathy are most probably triggered by interactions between metabolic and haemodynamic changes brought on by the onset of diabetes (3), but also by other contributing factors such as genetic predisposition (3), hyperglycemia-induced generation of reactive oxygen species (ROS) (3, 4) and inflammation (5).

Diabetic kidney disease potentially leads to end-stage renal disease in 30–40% of people with DM (2), which implies that genetic variations may affect the onset and progression of DM and end-stage renal disease. Large-scale genome research has been carried out to identify potential candidate genes relevant for DM and diabetic kidney disease (6). There are more than 14 genes that have been identified as key contributors in diabetic kidney disease development, including those involved in lipid metabolism (*ADIPOQ*), glucose metabolism (*GCKR*) and angiogenesis (*EPO* gene promoter), those influencing kidney structure and function (*SHROOM3*), genes affecting inflammation and oxidative stress (*TGF-β1*), genes involved in the functioning of the renin-angiotensin-aldosterone system (*AGTR1*), and other genes (7). However, the full effects of these genes and their variants have not been completely elucidated.

Tissue damage in DM is caused primarily by inflammation and concentration of constantly elevated circulating blood glucose and its metabolites as a result of high levels of oxidative and nitrosative stress in the kidneys (8, 9). The effects of oxidative stress have also been described in the context of other kidney diseases, such as urolithiasis (10). High ROS and nitrosative species (NS) production may damage nuclear and mitochondrial DNA, trigger

apoptosis and lead to endoplasmic reticulum stress; it is also involved in apoptotic and necrotic cell death pathways in key cell types, for example in podocytes (8).

Both T1DM and T2DM involve similar structural changes to the kidney brought on by diabetic kidney disease, but in the case of T2DM they are more heterogeneous and their clinical presentation is less predictable (11), likely because T2DM involves longer exposure to hyperglycemia before diagnosis, older age of patients and treatment with renin-angiotensin system inhibitors before the actual onset of diabetes (12). These structural changes appear in different sections of the kidney. The change that appears earliest is the thickening of the glomerular basement membrane and it is usually observed from 1.5 to 2 years after the patients' diagnosis of T1DM. The change that follows is the thickening of the capillary and tubular basement membrane (13-16). Subsequent glomerular changes are manifested through mesangial matrix expansion, loss of endothelial fenestrations, and loss of podocytes with pedicel effacement (13). Mesangial matrix expansion is first observed from 5 to 7 years after the onset of diabetes (15-18). Progression of DM brings about segmental mesangiolysis, which is thought to be associated with the development of Kimmelstiel-Wilson nodules and microaneurysms (19, 20). Similar subepithelial deposits could also be observed in Bowman's capsule and renal tubules. Glomerular filtration rate, hypertension, and albuminuria in diabetes are closely linked to mesangial expansion and, to a lesser extent, to the thickness of the glomerular basement membrane (13).

1.1.Oxidative stress

Oxidative stress plays a central role in the development and progression of DN (21). Reactive oxygen radicals, including superoxide anion, are generated in the kidneys as a result of hyperglycemia, which leads to oxidative stress caused by NADPH oxidase, the most important source of superoxide anions in diabetes mellitus (22-24). NADPH generation is reduced by increasing cAMP concentration and by activating PKA (25); it appears that cAMP-PKA pathway activation is an important process in inhibiting NADPH -dependent superoxide generation. GLP-1 receptor activation stimulates adenylate cyclase and increases cAMP generation; increased cAMP levels activate PKA, which inhibits NADPH and oxidative stress. That leads to the conclusion that GLP-1RAs prevent oxidative stress within the kidneys (26, 27). Furthermore, recombinant human GLP-1 inhibits protein kinase C (PKC) but enhances protein kinase A (PKA), which in turn reduces oxidative stress both in

the tubules and in the glomerulus (28). Oxidative stress activates fibrogenic cytokines such as TGF-β1 and CTGF, which leads to the proliferation of mesangial cells and extracellular matrix. Oxidative stress decreases the level of nitric oxide, which results in damage to the glomerular endothelium and charge of the glomerular barrier, causing the development of albuminuria (29-31).

1.2.TGF-beta

TGF-beta is a pro-inflammatory cytokine that appears to be responsible for glomerular and tubular damage. Its activated receptor phosphorylates Smad transcription factors, which play a role in gene regulation linked to cell differentiation, increase inhibition, and epithelial-mesenchymal transition (EMT) (32). Hyperglycaemia can cause transcription and secretion of collagen genes in the mouse cortical tubule cell line and can stimulate interstitial fibroblasts to increase the synthesis of fibrillar collagens and extracellular matrix (ECM) via the autocrine system of TGF-β1 (33). The TGF-β receptor acts by phosphorylating Smad transcription factors that are involved in gene regulation in the context of cell differentiation, growth inhibition, and EMT (32). When human proximal tubule cells and cortical fibroblasts are exposed to high glucose (HG) concentrations, that may directly stimulate cell growth and collagen synthesis, separately from glomerular, haemodynamic, or vascular pathology (32). A number of studies have indicated that fibronectin production as a response to HG is mediated through polyols in LLC-PK1 cells (34) and that glucose present in the hexosamine pathway acts as a mediator in ECM generation through stimulation of TGF-β (33). It also promotes oxidative stress, with PI3K/Akt pathway leading to tubular dysfunction. Hypoxia increases collagen production, TIMP1 expression and inhibits MMP2 activity (ECM deposition). It also causes activation of the plasminogen activator inhibitor-1 (PAI-1) through the nuclear accumulation of hypoxia-inducible factor 1-alpha subunit (HIF-1α) and NF-κB. This effect synergistically increases TNF-α, which points to a synergistic relationship between hypoxia and inflammation in tubular damage in DN (35).

1.3.GLP-1 agonists in diabetic nephropathy

1.3.1 GLP-1 RA classes and mechanism of action

There are two classifications of glucagon-like peptide-1 (GLP-1) receptor agonists (RAs); one according to origin: human or reptile (36, 37), and second according to the duration of action: short-acting (exenatide and lixisenatide) and long-acting agonists (dulaglutide, Liraglutide, semaglutide, albiglutide) (36, 37). GLP-1 RAs have been approved for treating people with type 2 diabetes mellitus (T2DM) and are administered subcutaneously (36). Semaglutide in oral form has been available on the market since 2020 (38). GLP-1 RAs are currently desirable treatment options, particularly those with a long duration of action, not only because of their metabolic efficacy (lowering of blood glucose levels, weight loss, etc.), but also because of the potential positive extraglycaemic effects on the process of atherosclerosis, endothelial dysfunction, and cardiovascular outcomes. Generally speaking, GLP-1 RAs have different beneficial effects when used in the treatment of T2DM: stimulation of glucose-dependent insulin secretion, inhibition of β-cell apoptosis and acceleration of β-cell proliferation, promotion of satiety by acting directly on the central nervous system, inhibition of gastric motility and emptying, weight loss (26, 37, 39, 40). Various other effects are still the subject of research such as lowering of systolic and diastolic blood pressure and lipid profile improvement (36, 41-45). The two groups differ primarily in the fact that short-acting GLP-1 RAs mainly decrease postprandial plasma glucose by delaying gastric emptying, while long-acting agonists predominantly show insulinotropic and glucagonostatic effects, which is why they have a significantly greater effect on fasting blood glucose concentration. Long-acting agonists have been shown by various meta-analyses as being more effective in lowering HbA1c in comparison with short-acting agonists (36, 44, 46-50). Specifically, these studies have shown that the greatest lowering of HbA1c levels was linked to Liraglutide and semaglutide administered once per week, while the smallest average lowering was observed with albiglutide (51). Comparison of their effects on weight loss reveals the same results (36). Compared with exenatide, Liraglutide has certain advantages, which include reduced frequency of nausea and vomiting (shorter presence of gastrointestinal side effects early on in the treatment), more efficient lowering of glycaemic parameters, and improvement of homeostasis model assessment of β-cell function (37). In general, the most common side effects of GLP-1 RA treatment are gastrointestinal (nausea, vomiting, diarrhea), reactions at the injection site (more significant with albiglutide and lixisenatide), and immunogenicity (exendin-4 derivates exhibit a greater likelihood of being linked to the

development of antibodies to medications in comparison with GLP-1 RAs modified from human GLP-1 (36, 52, 53). However, the mentioned side effects are not serious or long-lasting and they are rarely the reason for stopping treatment, especially due to the high efficacy of such medications.

1.3.2. Potential nephroprotective effects of GLP-1 agonists

Diabetes is one of the most pronounced public health issues, with the number of patients increasing dramatically. One of the consequences of diabetes is diabetic nephropathy, a chronic kidney disease, which is the leading cause of end-stage renal disease in western countries (54). GLP-1 RAs are proposed/presented as a desirable treatment option, not only owing to their glycemic and extraglycemic effects described above, but also due to their nephroprotective effects in DM2, which have been confirmed by numerous studies. In the study conducted by Yin, W. et al., it was demonstrated that GLP-1 RAs reduce albuminuria (high levels of albumin in the urine), improve tubule function and have a positive effect on tubulointerstitial injuries in the rat model of diabetic nephropathy (55). GLP-1 RAs suppress the expression of tubular TNF-α, MCP-1, type I collagen, α-SMA and fibronectin (FN), identified as a key role player in the onset of diabetic nephropathy (55). Moreover, the level of C-peptide, which is described in the literature as having an important role in the suppression of tubulointerstitial fibrosis (56), is increased through the action of GLP-1 RAs and may be one of the factors used to alleviate the process of tubulointerstitial and tubular injury in GK rats with developed diabetic nephropathy (55). A study by Kodera, R. et al. demonstrated the numerous benefits of exendin-4, primarily the prevention of macrophage infiltration, decrease in protein levels of intercellular adhesion molecule-1 (ICAM-1) and type IV collagen in the glomeruli, reduction of *Nox4* gene expression and nuclear factor-kB (notable for its effect on the crosstalk between inflammation and oxidative stress) in renal tissue (56). In addition, Liraglutide affects the inhibition of NAD(P)H oxidase through the generation of cAMP, which is followed by activation of PKA or Epac2 (57-59). All of these effects were blocked by the GLP-1R antagonist (42).

On the other hand, a different study conducted on HK-2 cells showed decreased expression of profibrotic factors (α-SMA, type I collagen, fibronectin) and inflammatory mediators (TNFα) as a result of GLP-1 Ras action (54). In addition, the effects of NF-κB and p38MAPK (two important pathways in the pathogenesis of renal fibrosis) are inhibited by

GLP-1RAs (54). Many studies have shown the effect of GLP-1RAs on maintaining water and electrolyte homeostasis, proposing inhibition of intestinal NHE3 activity as one of the probable mechanisms (60). The above NHE3 exchanger is located in the proximal tubules of kidneys and, by inhibiting its activity, GLP-1RAs induce natriuresis and diuresis (61). Thus, following the addition of the GLP-1R-exendin-9 blocker, a reduction was observed in terms of sodium and water excretion by the kidneys (61). Likewise, exendin-9 is associated with a mild reduction of the glomerular filtration rate (GFR), although an increase in GFR as a result of increasing proximal tubule reabsorption would be expected. Next is the inhibition of tubuloglomerular feedback signal for reabsorption and reduction of afferent arteriolar resistance (62). GLP-1RA that enhanced glomerular hyperfiltration increases glomerular filtration rate and, ultimately, electrolyte excretion (61). All of the mentioned studies indicate positive effects of GLP-1RAs on diabetic glomerular, tubulointerstitial and tubular nephropathy and suggest potential clinical use of such medications in the treatment of diabetic nephropathy. Seeing that streptozotocin-induced diabetic models in mice are not ideal for evaluating chronic complications of diabetes, a study was recently conducted on KK/Ta-Akita mice, which are particularly sensitive to kidney damage as a result of oxidative stress. It showed that Liraglutide treatment increases cAMP levels, activates PKA and inhibits NAD(P)H oxidase activity, which leads to reduced albuminuria and decreased proliferation of mesangial cells, increased levels of nitric oxide and improvement of glomerular filtration rate (63). Improvement of renal function was independent of changes to insulin secretion, glucose levels and other metabolic parameters, which confirms that Liraglutide treatment has a direct antioxidative and protective effect on renal function. The renal function relating benefits of Liraglutide treatment, specifically the reduction of proteinuria and albuminuria, have also been demonstrated in studies conducted on humans (64, 65).

1.3.3. Assessment of nephroprotective effects of GLP-1 receptor agonists in clinical trials

Treatment of patients with chronic kidney disease represents a major challenge in everyday clinical practice. Kidney damage can have a significant effect on a large number of medications for lowering blood glucose levels, which leads to dose reduction or stopping the use of medications (65). Therefore, it is preferable that antidiabetic medications, in addition to glycaemic control, have beneficial effects on kidneys and prevent/slow the progression of

diabetic nephropathy. Attention is now focused on less well-known non-glycaemic mechanisms of action of different generations/classes of antidiabetic medications. Recent clinical trials have indicated that glucagon-like peptide-1 (GLP-1) agonists have significant effects on the kidneys. In addition to their ability to lower blood glucose levels, GLPI-1 receptor agonists also have different non-glycaemic characteristics, such as enhanced natriuresis, lowering of blood pressure and anti-inflammatory effects (66). Such diversity of pharmacological effects of GLP-1 analogues implies the existence of potential mechanisms with direct renoprotective effects, which is the focus of this research. The LIRA-RENAL trial examined the efficacy and safety profile of Liraglutide in diabetics with moderate renal impairment (estimated glomerular filtration rate eGFR 30–59 ml/min/1.73 m^2) (65). The addition of Liraglutide reduced HbA1c more than in the placebo group (-1.05% compared to -0.38). Patients treated with Liraglutide experienced no worsening of renal function compared to those in the placebo group. In Liraglutide-treated patients, a minor increase in albuminuria was assessed as the urine albumin-to-creatinine ratio was observed in week 26, although this was not statistically significant. A more extensive and longer observational study of the effects of Liraglutide treatment on patients' outcomes with diabetic nephropathy was Liraglutide Effect and Action in Diabetes: Evaluation of Cardiovascular Outcome Results (LEADER) (66). In this trial, Liraglutide reduced the risk of new onset nephropathy by 22% in comparison with the placebo group. Considering that Liraglutide is proteolytically degraded at the tissue level, there are no differences in pharmacokinetic properties in people with normal and those with reduced renal function, meaning there is no danger of drug accumulation in people with impaired kidney function (67-69). The LIRA-RENAL study confirmed the safety of Liraglutide therapy in full treatment dose for people with DM2 and moderately reduced renal function (glomerular filtration rate $\geq$ 30 mL/min), while a mild increase of Liraglutide serum concentration was observed in patients with end-stage chronic kidney disease, with an increased risk of gastrointestinal side effects (65, 70).

There was no difference in the effect of Liraglutide on composite renal outcomes between subgroups of patients with increased renal risk at baseline. Obviously, the renal benefits of Liraglutide do not depend on the stage of chronic kidney disease. Subjects in the LEADER trial were patients with macroalbuminuria from baseline value to the onset of persistent albuminuria at the endpoint, while in the Evaluation of Lixisenatide in Acute Coronary Syndrome (ELIXA) trial focus was on renal outcomes of treatment in patients that only had normoalbuminuria or microalbuminuria (71). The primary focus of this randomized,

double-blind trial was the effect of lixisenatide, a short-acting GLP-1 agonist, on cardiovascular outcomes in 6068 patients with type 2 diabetes who experienced a recent acute coronary event. In addition to cardiovascular safety, the inclusion of lixisenatide in standard treatment also showed a beneficial effect on renal outcomes. The renoprotective effect was seen in a lower rate of increase of the urine albumin-to-creatinine ratio, 34% in the placebo group in comparison with 24% in the group that received lixisenatide. There was no significant difference between the two groups in terms of eGFR decrease or doubling of serum creatinine, while the total incidence of renal side effects was low in both groups. It seems that the difference in pharmacokinetics of GLP-1 analogues, the short-acting ones in comparison with the long-acting ones, does not affect composite renal outcomes of treatment (72).

Similar results were reported in the AWARD-7 trial, investigating the effect of long-term action of the GLP-1 analogue dulaglutide in comparison with insulin glargine on renal outcomes in the treatment of patients with type 2 diabetes and moderate to severe CKD (73). A total of 577 participants were randomly assigned to three groups, one treated with dulaglutide 1.5 mg, one with dulaglutide 0.75 mg and one with insulin glargine. After 52 weeks of treatment, drop in eGFR was less prominent in patients treated with dulaglutide in comparison with the insulin-treated group. Albuminuria reduction was similar among all groups, with a greater reduction of the urine albumin-to-creatinine ratio in patients treated with dulaglutide. Although dulaglutide increased weight loss, both in terms of adipose and muscle tissue, the study confirmed the independent beneficial effects of GLP-1 analogues on the kidneys. To summarize, GLP-1 analogues as antidiabetic medications significantly affect composite renal outcomes, primarily in the case of new-onset macroalbuminuria. Numerous prior studies reported the development of albuminuria as being an independent predictor of diabetic nephropathy progression followed by deterioration of estimated glomerular filtration rate and end-stage renal disease development (73-75). A decrease in macroalbuminuria occurrence in diabetic patients could partly be explained by improvement in glycaemic control achieved by adding GLP-1 agonists to antidiabetic treatment due to harmful effects of high glucose levels on increased glomerular protein filtration rate and compromised tubular reabsorption (76). Another possible mechanism of GLP-1 renoprotective effects may be the inhibition of inflammation-related pathways. The anti-inflammatory and antioxidative effects of GLP-1 analogues have been unambiguously shown by preclinical studies (63, 77) and implied in the LIRA-RENAL trial, where the group treated with Liraglutide showed lower

levels of the inflammation marker hsCRP in comparison with the group treated with placebo. While the actual mechanism of beneficial renal effects of GLP-1 agonists has yet to be elucidated, it could be concluded that combined effects of glucose-lowering treatment and extra-glycaemic effects are involved.

1.4. Mechanism of action of SGLT2 inhibitors and their potential nephroprotective mechanism of action: Empagliflozin, dapagliflozin, canagliflozin

Inhibitors of the sodium/glucose cotransporter 2 (SGLT2) are newly developed oral antidiabetics used in the treatment of type 2 diabetes (78). Glucose reabsorption occurs in proximal tubules via sodium-dependent glucose transporters (SGLT), which are located on the apical side of proximal tubules, contrary to concentration gradient transporting glucose simultaneously with sodium, through the basolateral pump Na, K-ATPase (67, 79). SGLT2 is almost exclusively expressed at one site, in renal proximal tubules, therefore its selective inhibition leads to renal glucose excretion and lowering of plasma glucose levels without affecting other metabolic processes (68). Sodium/glucose cotransporter 2 (SGLT2) is the primary luminal glucose transporter, situated in the S1 and S2 segments of proximal tubules (PT), absorbing nearly 90% of glucose filtered by the glomeruli; it is minimally expressed in other cells. Sodium/glucose cotransporter 1 (SGLT1) is situated in the S3 segment and absorbs the rest of glucose (10%) (69). SGLT2 in the apical membrane is linked with GLUT2 in the basolateral membrane. In normoglycaemic conditions, the two together reabsorb up to 90% of filtered glucose (80). Increased RAAS activity observed with SGLT2i may be explained by volume contraction as a result of this type of treatment (81). However, reduction of GFR with SGLT2i is likely a consequence of the increase in afferent tone controlled by tubuloglomerular feedback (82). Furthermore, maximum renoprotection from glomerular injury, proteinuria and renal fibrosis was achieved with a combination of luseogliflozin (SGLT2 inhibitor) and lisinopril (ACE inhibitor) (68). A potential mechanism of action of SGLT2 inhibitors involves inhibition of glucose influx into renal proximal tubular cells, implicated in the development of diabetic nephropathy (83-85). Histological changes observed in the glomerulus are crucial in the development of DN, but changes observed in the tubulointerstitium more commonly correspond to impaired renal function (80). SGLT2 inhibitor medications dapagliflozin, canagliflozin and Empagliflozin are useful for reducing hyperglycaemia and achieving better glycaemic control, offering extraglycemic benefits such

as weight and blood pressure (BP) reduction (86). SGLT2 inhibitors have good oral bioavailability, a long half-life that allows administration once daily, low accumulation index, lack of active metabolites and restricted renal elimination (87). Furthermore, drug-drug interactions are negligible (88). The risk of hypoglycaemia is practically non-existent due to unique mechanism of action not affecting insulin secretion and gluconeogenesis. There are certain implications that SGLT2 inhibition improves beta-cell function, possibly through reduction of glucotoxicity (89, 90). Glucose excretion in urine results in loss of extra calories leading to weight reduction or even mitigation of weight gain associated with insulin or sulphonylurea therapy. In hypertensive patients, SGLT2 inhibitors cause a decrease in blood pressure, most likely due to enhanced excretion of glucose, sodium and water (91). Orally administered dapagliflozin is quickly absorbed, typically achieving peak plasma concentrations in 1–2 hours; it is metabolized mainly in the liver and kidneys by uridine diphosphate-glucuronosyltransferase-1A9 (UGT1A9) into the main inactive metabolite dapagliflozin 3-O-glucuronide (D3OG). Dapagliflozin is not excreted by kidneys and drug-drug interactions are moderate to none (85, 92). Dapagliflozin improves glycaemic control, reduces body weight and has a diuretic effect on lowering blood pressure (88). Effects of dapagliflozin on lowering blood pressure could be used in the treatment of obese hypertensive patients with T2DM, especially patients with difficulties in regulation of arterial hypertension (89). A common side effect of SGLT2i is an increased risk of urinary tract infections (UTI), but the infections are generally mild to moderate. No dose correlation exists between glucosuria and UTIs (93). The bioavailability of oral canagliflozin is nearly 65%; it is absorbed immediately after oral administration in a dose-dependent manner across a dose range of 50–300 mg. The medication is to a great extent (99%) bound to albumin. Canagliflozin is generally metabolized into two inactive O-glucuronide metabolites (88, 94). Unlike other SGLT2 inhibitors, canagliflozin also modestly inhibits sodium/glucose cotransporter 1 (SGLT1) postponing absorption of glucose in the intestines subsequently lowering postprandial glucose and insulin levels (95). Canagliflozin treatment is also linked to UTIs and symptomatic vulvovaginal adverse events in female T2DM patients (96). Empagliflozin is absorbed quickly when administered in single oral doses, reaching Cmax after 1.0–2.0 h (97). No drug-drug interactions were observed between Empagliflozin and other oral antidiabetic medications, cardiovascular medications or other narrow therapeutic index medications (87, 88). Paradoxical increase of endogenous glucose production was observed with Empagliflozin treatment of patients with T2DM in the post-absorptive and postprandial state and that was also observed with dapagliflozin (98). Nonetheless,

Empagliflozin significantly reduces fasting plasma glucose levels (87). A moderate increase in the incidence of genital infections was observed with Empagliflozin, but there was no increase in the number of urinary tract infections (97). The SGLT2i's antihyperglycemic potential is in direct proportion to the glomerular filtration rate (GFR) and is diminished in chronic kidney disease (CKD). Still, available research shows that SGLT2 inhibitors contribute to nephroprotection in diabetes (86, 99-101). Hyperglycaemia causes increased Na^+ reabsorption in proximal tubules and decreased Na^+ delivery to the macula densa, with subsequent vasodilation of the afferent arteriole, increase in glomerular pressure and hyperfiltration (66, 102). SGLT2i have a nephroprotective effect in patients with diabetes type 2 independent of CKD (103-106). Renal benefits mediated by SGLT2 inhibitors cannot be attributed only to glycaemic improvement, but are also mediated via haemodynamic effects including plasma volume reduction, lowering of systemic blood pressure and glomerular filtration pressure, and reduction of renal hypoxia; and metabolic effects such as weight loss (107). Renal benefits of SGLT2i have been recently proven in landmark clinical trials regardless of diabetes mellitus in patients with CKD (108) and heart failure (109). Molecular pathways of direct protective effects of SGLT2 inhibitors are still not elucidated. Kidney inflammation, a process directly engaged in the pathogenesis of CKD regardless of underlying disease could have a key role in this context (110). In addition, increased influx of Na^+ to the macula densa as a result of SGLT2 inhibition initiates tubuloglomerular feedback, which reoccurs in afferent vasoconstriction, lowered glomerular pressure and albuminuria reduction by 30–50% (92).

1.4.1. Evidence of nephroprotection in vitro and in animal models

A significant increase in SGLT2 mRNA and glucose transporter activity was observed in cultured human proximal renal tubular cells of type 2 diabetes patients (111). In addition, earlier studies on human proximal tubular cells (HK-2) indicated that SGLT2 inhibition led to a decrease in the proinflammatory and fibrotic markers caused by hyperglycemia (86). Those in vitro findings show that SGLT2 inhibitors can be nephroprotective in diabetes inhibiting glucose delivery to proximal tubular cells (112). Earlier, the use of SGLT2 inhibitors in db/db mice – dapagliflozin in males (113) and tofogliflozin in females (114) diminished advanced albuminuria, parallel with the effect of losartan in the latter study, and lowered the plasma glucose level to < 15 mmol/L. On a sample of Empagliflozin-treated male db/db mice, Lin et

al. similarly reported a reduction in albuminuria and glomerular sclerosis, together with substantial improvement of hyperglycaemia (115). Vallon et al. also demonstrated that Empagliflozin administered to male Akita mice with type 1 diabetes reduced albuminuria, renal hypertrophy and inflammatory markers, in proportion to lowering blood glucose levels (112). Furthermore, the effect of SGLT2 inhibition on diabetic nephropathy, independent of the lowering of blood glucose levels, was observed in diabetic eNOS knockout mice (116). Proximal tubular cells exposed to the urine of diabetic patients showed increased expression of SGLT2 (111), while studies conducted on obese Zucker rats demonstrated that diabetes causes enhanced RNA expression of SGLT2 and SGLT1 in the kidneys (117). Different medications are associated with changes in the SGLT1 and SGLT2 expression, like HNF1α and SGK1 (67), while upregulation of SGLT2 expression was observed when proximal tubular cells were exposed to the transforming growth factor β (TGFβ), a profibrotic cytokine (118). After exposure for 96–120 hours, interleukin-6 (IL-6) and tumour necrosis factor-α (TNF-α) increased the expression of SGLT2 in cultured renal cell lines (119), and glucose-induced increased SGLT2 expression was shown through the protein kinase A (PKA) and the protein kinase C (PKC) dependent pathway (120, 121).

Furthermore, the actions of sodium/glucose cotransporters and the renin-angiotensin-aldosterone system are intertwined. In animal studies, losartan, an angiotensin receptor blocker (ARB), lowered SGLT2 expression in diabetic rats with a normal or high salt intake diet (122). In diabetic rats, GLUT2 expression was increased in diabetes and translocated to the luminal surface of proximal tubular cells, enhancing glucose reabsorption (69). Decrease of GLUT9 levels, glucose / uric acid exchanger, could also contribute to improving renal outcomes in diabetic patients (123-125). Moreover, expression of some profibrotic genes was decreased by Empagliflozin, similar to metformin, a first-line anti-diabetic medication. Gallo et al. demonstrated that the threshold for lowering blood glucose levels may be necessary for achieving full renoprotection in diabetes, considering the fact that Empagliflozin affected certain fibrotic markers, but did not affect albuminuria or glomerular sclerosis. Thus, Gallo et al. proposed that in order to achieve maximum nephroprotection in diabetes, appropriate and stable lowering of blood glucose levels, including higher and/or multiple daily doses of SGLT2 inhibitors in combination with RAS inhibitors, may be required (126). The anti-inflammatory potential of SGLT2 inhibitors was previously demonstrated in diabetic animals (127-129) and human studies (130, 131), as well as cell culture models of hyperglycaemia (86). In animal studies, the improvement in glomerular and tubulointerstitial damage was

associated with the anti-inflammatory properties of SGLT2 inhibitors (125, 132). This has only recently been proven in normoglycaemic conditions in the *in vitro* model. The inhibitory effect that Empagliflozin (Empa) has on IL-1β-induced MCP1/CCL2 and endothelin-1 expression on mRNA and protein in normoglycaemic conditions was shown in two independent human proximal tubular cell lines (HPTC) – HK-2 and RPTEC/TERT1. Both genes are involved in the early ethiopathogenesis of diabetic and non-diabetic kidney impairment (133-137). Genetic and pharmacological inhibition of those two genes could have renal benefits previously demonstrated in animal (133, 135, 138-142), and human models (141, 143, 144) with kidney disease. In a study by Maayah, et al. survival benefit in Empa-treated mice subjected to LPS-induced septic shock was observed corroborating the anti-inflammatory effect of Empa, independent of antihyperglycaemic potential. Improved survival could be to some extent attributed to suppression of kidney and systemic inflammation and reduction of acute kidney injury (145). A study by Pirklbauer, M. et al. showed that the expression of several genes involved in the inflammatory response in IL-1β-induced normoglycaemic HPTCs (10 ng/mL) – HK-2 and RPTEC/TERT1 cells were diminished with the Empa addition. This transcriptomic methodology revealed new genes such as CXCL8/IL8, LOX, NOV, PTX3 and SGK1 through which SGLT2i could have a direct anti-inflammatory effect independent of their antihyperglycaemic effect offering nephroprotection (146).

Sirtuin family (one to seven) of nicotinamide adenine dinucleotide (NAD+)-dependent deacetylases, a homolog of yeast Sir2 has been demonstrated to play a significant role in a diversity of cellular functions. Sirtuin-1 (SIRT1), the mammalian Sir2 ortholog is upregulated by caloric regulation and resolves the durability effect of calorie restriction by control of glucose and lipid metabolism and regulates gluconeogenesis and mitochondria biogenesis by deacetylating/ activating PGC-1a (147). Variations in the expression of SIRT1 protein that can be found in the brain, heart, kidney, liver, etc. are critical in some diseases, including metabolic disease, cardiovascular disease, and cancer. SIRT1 exerts renoprotective effects in DKD in part through the deacetylation of transcription factors involved in the disease pathogenesis, such as p53, FOXO, RelA/p65, NF-κB, STAT3, and PGC1α/PPARγ. HG induced an increase in SGLT2 and decrease SIRT1 expression. Activation of SGLT2 reduces SIRT1 expression by inducing excessive glucose access into proximal tubules under diabetic conditions. Inhibition of SGLT2 reversed HG induced SIRT1 downregulation (148, 149). Diminished SIRT1 expression leads to increased acetylation and activation of transcription

factors, such as STAT3, p53, NF-κB, and PGC1α, enhancing inflammation, senescence/apoptosis, and mitochondrial dysfunction of renal cells like podocytes. The podocyte-specific overexpression of SIRT1 attenuated proteinuria and kidney injury in an experimental model of DKD, further confirming SIRT1 as a potential target to treat kidney disease (150). SIRT3 is expressed in the mitochondrial matrix and is the main regulator of the entire organelle acetylome (151). It has been described as a crucial regulator of the mitochondrial dynamics in renal cells and has an important role in controlling proximal tubular cell homeostasis, regulating microtubule network-dependent trafficking of useful mitochondria among renal tubular epithelial cells, an action that maintains the right cellular bioenergetic form and antioxidant protection (152). It has been demonstrated recently that recovery of SIRT 3 level by SGLT2 inhibitors leads to suppression of abnormal glycolysis (153). Induced by oxidative stress, SIRT6 is drafted to the spots of DNA double-strand cracks via ADP-ribosylation, improving its repair (154). SIRT7 is expressed in the basolateral membrane and has the capacity to deacetylate KCC4 (K1/Cl2 cotransporter) in the collecting duct and restore the pH balance in the time of metabolic acidosis. The positive effect of SIRT7 on KCC4, proposes that sirtuin has a role in acid-base and renal electrolyte balance. Sirtuins maintain renal homeostasis and their downregulation leads to chronic and acute kidney diseases (155). Expression of SIRT 1,3,6 and 7 through different renal compartments is shown in Figure 1.4.1.a

The signal transducer and transcription activator (STAT) are a family of transcription factors activated by tyrosine phosphorylation via Janus kinases (JAKs). Phosphorylation initiates the dimerization of proteins that move into the nucleus, bind to DNA and regulate the transcription of target genes (156). The members of the STAT family are involved in a number of cell differentiation processes and regulate tissue-specific gene expression (157). Transcription factors such as signal transducer and activator of transcription 3 (STAT3) are activated under diabetic conditions. Sirutin – 1 negatively balances the transcriptional activity of STAT3. The growth hormone induces JAK phosphorylation and consequent activation of STAT5 protein, which induces PPAR-γ expression (158). The JAK2 / STAT3 pathway is activated during early adipogenesis and is responsible for achieving maximal differentiation potential, presumably through modulation of C / EBP-β transcription (159). Although STAT3 is mainly prevalent in the cytosol and nucleus, there is growing evidence that it can also be found in mitochondria where it affects cellular respiration (160).

PPAR-γ belongs to the family of nuclear hormone receptors and ligandome is an activated transcription factor. It binds to specific areas on DNA, known as the peroxisome proliferator response elements (PPRE), as heterodimer with retinoid X receptor (RXR) that modulates the transcription of genes involved in lipid metabolism(161). PPAR-γ is a type of ligand-activated nuclear transcription factor (162) associated with obesity, fat tissue differentiation, and insulin resistance. PPAR-γ is bound to PPRE even when it is not active, and by activating endogenous (unsaturated FA) or synthetic (drugs) ligands, PPAR-γ releases corepressors and binds coactivators. In this way, ligand-dependent transcriptional activation of nearby genes occurs, which is the basic mechanism by which PPAR-γ ligands stimulate the transcription of PPAR-γ cyan genes (163). PPAR-γ is considered to be a major regulator of the adipogenesis process (164) and in addition, plays a dominant role in glucose metabolism and the inflammatory processes (165). Activation of PPAR-γ stimulates adiponectin expression and gene mutations in the PPAR-γ result in insulin resistance and lipodystrophy (166). PPAR-γ exerts its effect through two isoforms, PPAR-γ2 whose expression is limited to adipose tissue and PPAR-γ1 which can be found in other tissues (167). Moreover, PPAR-γ represents one of the target molecules of euglycemic agents, such as thiazolidnediones (168).

Diabetes-induced decrease in SIRT1 expression enhances apoptosis via stimulation of the p53 pathway (169). The favorable effects of SRT2104 (small-molecule activator of SIRT1) on DN are reported in recent studies. P53, placed in the proximity of SRT2104 was recognised as the major target of SIRT1 by accelerating DN. In the latest articles, the pathogenic impact of P53 was discovered in chronic complications of DM, such as nephropathy(170, 171), retinopathy (172), cardiomyopathy (172) and peripheral artery disease. Moreover, P53 also has the capacity to activate oxidative stress (173).

The most important mediator in the progress of diabetic nephropathy is TGF-β (174). TGF- β, after binding to its receptors, signals through two next mediators; Smad2 and Smad3 in order to utilize its biological activities, such as ECM production. Moreover, TGF- β1 also encompasses an inhibitory Smad7 that balances activation of Smad 2/3 competition and degradation in a negative way, through the ubiquitin-proteasome degradation mechanism (175, 176). Studies have shown that Smad7 can inhibit inflammation and renal fibrosis by blocking the activation of TGFβ/Smad and nuclear factor-kB (NF-kB) signaling pathway (177, 178). On the other hand, inhibition of Smad7 promotes inflammation and renal fibrosis (179), thus suggesting that Smad7 could be the most important therapeutic agent and regulator for renal fibrosis and inflammation (180).

Akt is a significant mediator of insulin activity. Beginning with insulin stimulation, Akt controls the uptake of glucose in adipocytes, liver, muscle and other tissues by advancing the translocation of glucose transporters from intracellular space to the plasma membrane. Furthermore, Akt has been established as a fundamental gene necessary for maintaining regular glucose homeostasis. Mice absent of this gene have increased insulin resistance as noticed in T2DM (181). Glycogen synthase kinase-3β, a protein downstream of Akt, is broadly associated with the control of mitochondrial functions (182). Akt is activated by phosphorylation and activated Akt (p-Akt) can conversely control GSK3β (182). Renoprotective effects of emodin against diabetic nephropathy in rat models are mediated via PI3K/Akt/GSK-3β (183). Akt has been investigated regarding its role in the worsening hyperglycemia inducing renal glomerular hypertrophy and apoptosis (184). Akt can directly phosphorylate GSK-3β at Ser9 negatively controlling its kinase activity, while the active form of GSK-3β may phosphorylate VDAC1 on threonine 51 leading to reduced HK-II binding to mitochondria. Inactivation of GSK-3β by Akt thereby preserves the integrity of mitochondria (185).

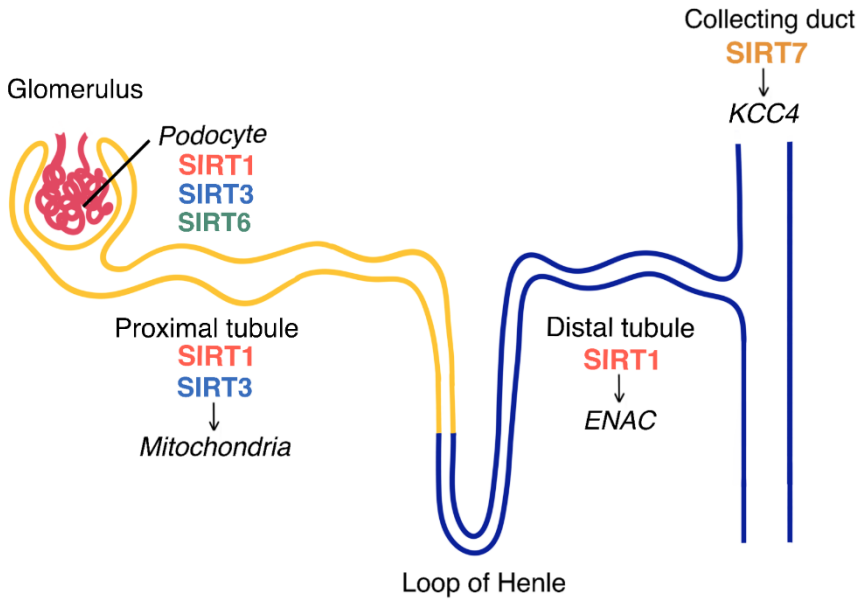

Figure 1.4.1. a Sirtuins are expressed in different kidney sections.

SIRT1, SIRT3, and SIRT6 are responsible for the functional and structural integrity of podocytes in the glomerulus. SIRT1 is ubiquitously expressed in the whole nephron and plays an important part in maintaining sodium and water balance via epithelial sodium channel (ENaC) thea-subunit of aquaporin 2-positive cells located in the distal nephron. SIRT1 and SIRT3 are mostly found in the proximal tubule and are accountable for the functional integrity of mitochondria. Acid-base control and electrolyte transport are mediated by SIRT7, located in the collecting duct, due to deacetylation of the K1/Cl2 cotransporter KCC4. The figure was made by the author.

1.4.2. Assessment of nephroprotective effects of SGLT2 inhibitors in clinical trials

Currently, short-term research assuring the renal safety of SGLT2 inhibitor medications is available, but no long-term data are confirming their beneficial effects on kidneys (125). Effects of SGLT2 inhibitors on albuminuria reduction have been demonstrated in various studies (92, 186, 187), but the actual precise mechanism remains unclear, though it appears independent of changes in eGFR, systolic blood pressure, body weight or HbA1c (92). A placebo-controlled study showed that 100 mg of canagliflozin per day reduced albuminuria by about 22% (187), while 25 mg/day of Empagliflozin reduced albuminuria in approximately 35% of patients with chronic kidney disease and type 2 diabetes mellitus (187). SGLT2 inhibitors and RAS-based medications such as ACE inhibitors or ARBs clearly have different mechanisms of action and different outcomes in the renal system. Considering their complementary effects on kidneys, SGLT2 inhibitors and ACE inhibitors/ARBs should have a synergistic effect. In a new experimental study, the combination of RAAS blockers and SGLT2 inhibitors correlated with nephroprotective effects in diabetic nephropathy, in contrast to such medications administered individually (188). Another study from Heerspink et al. conducted on patients with hypertension and diabetes used RAAS inhibitor treatment in combination with 10 mg/day of dapagliflozin, showing a reduction of albuminuria by about 35% in comparison with placebo. It is interesting to note that the above reductions were independent of changes in systolic blood pressure, body weight, HbA1c or eGFR (92). Reduction of serum uric acid levels is another model indicative of SGLT2i mechanisms of nephroprotection. It has been demonstrated that elevated uric acid levels or hyperuricemia are correlated with the possibility of kidney damage in diabetes (132, 189, 190) causing microvascular complications in diabetes(191, 192). Clinical relevance of increased excretion

of serum uric acid level induced by SGLT2 inhibitors has been demonstrated in several studies (193-195). For example, the EMPA-REG trial showed that in diabetic patients whose glomerular filtration rate was estimated at no less than 30 ml per minute, Empagliflozin significantly decreased deterioration or sudden nephropathy, need for kidney transplantation or dialysis, or the doubling of serum creatinine level in comparison with placebo, while further analysis showed albuminuria reduction (71).

In the CREDENCE trial, nearly all patients included (99%) were treated with ACE inhibitors or ARBs in comparison with other trials (80%) (196) and their eGFR ranged from 30 to < 90 ml per minute. The trial was stopped early, based on positive results of the planned interim analysis, since the relative risk of composite renal outcomes decreased by 34% and the relative risk of end-stage renal disease decreased by 32%. These data show that renoprotection was achieved through the entire spectrum of eGFR levels, which re-established the nephroprotective effect, independent of renal function at baseline. Nephroprotective effects of SGLT2 inhibitors may also benefit cardiovascular outcomes through neurohormonal activation and fluid volume reduction (196, 197).

As recently confirmed in a meta-analysis including all trials with SGLT2i in diabetic patients, the risk of dialysis, transplantation or death resulting from kidney disease (hard renal outcomes) was significantly reduced in patients treated with SGLT2 inhibitors (198). Up until recently, SGLT2 inhibitors were not indicated for treatment of diabetic patients with eGFR lower than 45 ml/min per 1,73 m², only due to their lower antihyperglycaemic effect (107, 199). Based on the evidence of the renoprotective effect in the above mentioned trials such limitations became questionable (200). This was confirmed in the latest clinical trials including diabetic and non-diabetic patients with heart failure and preserved ejection fraction (201, 202) demonstrating improvement of hard renal outcomes in the lower spectre of eGFR, 30 and 20 mL/min/1.73 m^2 in the EMPEROR-Reduced and DAPA-HF trial respectively. The final proof that renoprotective effect was independent of the antihyperglycemic effect was provided by the DAPA-CKD study indicating that dapagliflozin reduced renal events in patients with CKD with or without DM who were on maximally tolerated doses of angiotensin-converting enzyme inhibitor/angiotensin-receptor blocker. Beneficial effects were observed on non-CV and all-cause mortality (108).

1.5. Implications of the potential synergy of GLP-1 RAs and SGLT2 inhibitors for prevention of kidney disease

Totally 30% of patients with diabetes develop severe renal impairment despite available treatment options for achieving adequate control of blood pressure and renin-angiotensin-aldosterone system blockade (100, 203). Consequently, new treatment measures and polytherapy are necessary for the prevention and treatment of diabetes-related complications. Recently published studies have demonstrated a reduction of new-onset albuminuria in patients treated with GLP-1 receptor agonists (204). This could be mediated through GLP-1 receptors, found in multiple types of kidney cells, which could be responsible for the increase in natriuresis and glomerular filtration rate as well as afferent vasodilation (62). Despite the natriuretic effect, research into the mechanism of action and clinical trials have failed to demonstrate that renal haemodynamic vasoconstriction in response to treatment with GLP-1 RAs resulted in overall neutral effects of GFR. Nevertheless, treatment of diabetic patients with GLP-1 RAs undoubtedly leads to albuminuria reduction, most likely as a result of suppression of inflammation-related pathways (203). Natriuresis could be achieved by the complementary action of these two classes of drugs, although mechanisms of action involved in the albuminuria reduction somewhat differ. The synergistic effect of SGLT2 inhibitors and GLP-1 receptor agonists on the improvement of renal function may be achieved in two ways: by direct effects on the kidney itself and through extrarenal effects including improvement in glucose control, blood pressure reduction and weight loss. GLP-1 receptor agonists and SGLT2 inhibitors both stimulate natriuresis in proximal tubules through action at different sites; SGLT2 inhibition leads to increased natriuresis, while GLP-1 receptor agonists stimulate natriuresis by inhibiting the NHE3 (sodium-hydrogen exchanger 3) transporter in proximal tubules (205) as shown in Figure 1.5.a.

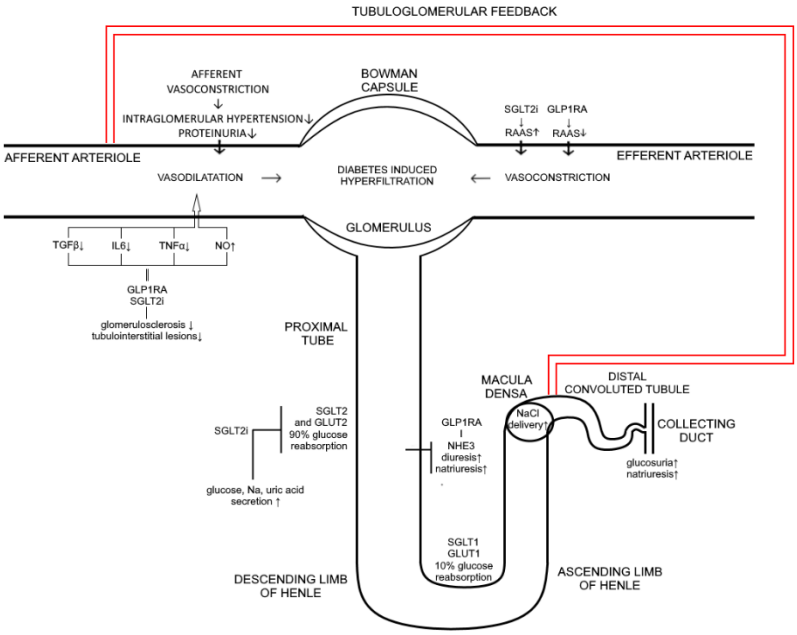

Figure 1.5.a Mechanism of action of SGLT2i and GLP 1RA on the kidney.
SGLT2 and GLUT2 transporters are inhibited by SGLT2i preventing sodium and glucose transport and subsequently provoking natriuresis, diuresis, glucosuria, and uric acid excretion. Likewise, diuresis and natriuresis are also induced by GLP 1RA through NHE3. Sodium influx to macula densa increases leading to vasoconstriction of the afferent arteriole, reduction of intraglomerular pressure and proteinuria via tubuloglomerular feedback. Production of proinflammatory markers such as Il6, TGFβ, TNFα involved in glomerusclerosis is inhibited by GLP 1RA and SGLT2i, leading to afferent vasoconstriction (through stimulation of NO). RAAS activity is inhibited with GLP 1RA therapy triggering efferent vasodilatation. On the contrary, SGLT2i induced natriuresis and volume depletion lead to RAAS activity suppression pointing to tubuloglomerular feedback as the main culprit of beneficial effect on intraglomerular pressure. The figure was made by the author.

SGLT2i; sodium glucose-lowering transporter2 inhibitors, GLP1 RA; glucagon-like peptide 1 receptor agonist, GLUT 2; glucose transporter 2, NHE3, sodium-hydrogen exchanger isoform 3, TGFβ; transforming growth factor β, IL6; interleukin 6, TNFα; transforming nuclear factor α, RAAS, *renin–angiotensin–aldosterone system*

1.6. Cardioprotective effects of GLP 1 RA

According to the most recent guidelines on diabetes and pre-diabetes of the European Society of Cardiology (ESC) published in 2019, GLP 1 RA with proven CV benefit (Liraglutide, dulaglutide, semaglutide) and inhibitors of the sodium/glucose cotransporter 2 (SGLT2) – canagliflozin, dapagliflozin and Empagliflozin – are recommended as the treatment of choice for patients with type 2 diabetes mellitus (DMT2) and cardiovascular (CV) disease with the aim of reducing the incidence of undesirable CV events. The Food and Drug Administration (FDA) and the European Medicines Agency (EMA) demand assessment of CV safety of every new antihyperglycemic medication on the market examined in cardiovascular outcomes trials (CVOT). The primary outcome is defined as a composite of 3 point major adverse cardiovascular events (MACE - death from cardiovascular causes, nonfatal myocardial infarction and nonfatal stroke). Available data from CVOTs examining GLP 1RA demonstrated significant reductions in 3 point MACE for Liraglutide (LEADER) (206), albiglutide (HARMONY) (207), dulaglutide (REWIND) (208) and subcutaneous semaglutide (SUSTAIN 6) (76). Noninferiority was shown for lixisenatide in the ELIXA trial possibly due to a shorter half-life compared to long-acting GLP1 RA (209). The same results were obtained in the EXSCEL trial examining exenatide once-weekly which could be explained with a higher discontinuation rate due to the complexity of delivering the device and GIT side effects (210). CKD and CVD in diabetes have similar pathophsyiological background- haemodynamic and metabolic disturbance as well as chronic inflammation. As already mentioned, long-acting GLP 1 RA has a beneficial effect on body weight and blood pressure as well as hyperglycemia thus improving haemodynimcs, endothelaila dysfunction and reducing inflammation. Cardiovascular protection was also demonstrated in animal and human studies of GLP-1 receptor agonists showing improvement of ischaemic myocardial damage and left ventricular dysfunction along with plaque stabilization. (211-214)

1.7. Cardioprotective effects of inhibitors of sodium/glucose cotransporter 2

As previously described, SGLT2i block proximal tubular reabsorption of sodium, resulting in negative sodium balance, reduction of plasma volume and lowering of arterial blood pressure thus changing haemodynamics (215-217). As a consequence, preload and afterload reduction take place. In addition, SGLT2i produce an increase in ketone bodies offering alternative energy sources to myocardiocites thus improving cardiac function (218, 219). Also, it is entirely plausible that inhibition of Na^+/H^+ exchange via NHE1 by SGLT2i

leads to an increase of mitochondrial calcium. Furthermore, NHE3 in the proximal tubule which is increased in heart failure, is also inhibited by SGLT2i suggesting a mutual cardio-renal protective pathway (220-222). Empagliflozin decreases myocardial cytoplasmic Na^+ through inhibition of the cardiac Na^+/H^+ exchanger in rats and rabbits. Besides, reduction of myocardial fibrosis has been observed with SGLT2i in rat models (223). Dapagliflozin, a selective SGLT2 inhibitor, attenuated cardiac fibrosis by regulating the macrophage polarization via STAT3 signaling in infarcted rat hearts (224-227).

In the EMPA-REG OUTCOME trial, patients were randomly assigned to receive 10 mg or 25 mg of Empagliflozin or placebo once per day. The primary outcome included 3 point MACE. The secondary outcome was hospitalization for unstable angina. The study included 7,020 patients, with a median follow-up of 3.1 years. There were no significant differences between groups concerning myocardial infarction or stroke rates. However, in the Empagliflozin group, rates of death resulting from cardiovascular causes were significantly lower (3.7% in comparison with 5.9% in the placebo group; 38% relative risk reduction), as was hospitalization for HF (2.7% and 4.1%, respectively; 35% relative risk reduction) and death from any cause (5.7% and 8.3%, respectively; 32% relative risk reduction). There were no significant differences between groups concerning the secondary outcome (28). A subanalysis of this study investigated the effects of Empagliflozin on clinical outcomes in patients with DMT2, established cardiovascular disease, and chronic kidney disease. The outcomes were defined as cardiovascular death, hospitalization for HF, hospitalization for any cause, and death from any cause. In patients with major kidney diseases, compared to placebo, Empagliflozin reduced the risk of cardiovascular death by 29%, the risk of death from any cause by 24%, the risk of hospitalization for HF by 39% and the risk of hospitalization for any cause by 19% (228). This implies that cardiorenal benefits are independent of the glucose-lowering potential of SGLT2i since the hypoglycemic potency of these drugs is diminished in CKD. Similar has been shown in the CANVAS trial (229). Investigating cardiovascular safety of canaglifozin demonstrating reduction in 3 point MACE, but no effect on cardiovascular death as opposed to EMPA-REG OUTCOME trial. On the other hand, dapagliflozin and ertugliflozin reduced the risk of heart failure (HF). However, there was no effect on atherosclerotic CVD as was established in DECLARE-TIMI 58 and VERTIS trials respectively (230). Cardiovascular and renal outcomes section of 'The VERTIS CV Trial Cardiovascular Outcomes Following Ertugliflozin Treatment in Patients with Type 2 Diabetes Mellitus and Atherosclerotic Cardiovascular Disease. Available

evidence suggests that the protective effect of SGLT2i on 3-point MACE is restricted to patients with already established CVD, while class benefit exists for HF independent of CVD presence (231). Furthermore, the beneficial effect on HF and 3-point MACE is further emphasized in patients with DMT2 and CKD (eGFR <60 mL/min/1.73 m^2) (232).

Recently, results from two large-scale studies have been published demonstrating improved outcomes in patients with HF with reduced ejection fraction (HFrEF) treated with dapagliflozin and Empagliflozin (DAPA-HF and EMPEROR-Reduced, respectively) independent of the presence of diabetes (109, 202). Both trials reported a reduced rate of hospitalizations for HF, but only in DAPA-HF favourable effect on mortality risk was noted.

Based on the evidence in the above trials, the guidelines of the European Society of Cardiology (ESC) propose SGLT2i and/or GLP 1 RA as the treatment of choice for patients with diabetes and proven cardiovascular disease or risk, which is contrary to the deeply-rooted practice of using metformin as the first choice for DMT2 treatment (233).

2. HYPOTHESIS

Treatment with both SGLT2 inhibitor and GLP-1 receptor agonist will demonstrate renoprotective effect through downregulation of TGF β expression and altered protein expression related to insulin and leptin signaling pathways in a model of diabetic nephropathy.

3. RESEARCH OBJECTIVES

The main objectives of this study:

- Establishing cell culture model of diabetic nephropathy of proximal tubule cells.
- Determination of cell viability and oxidative status of the cells.
- Measuring expression levels of genes related to the level of cellular damage caused by the treatment.
- Measuring protein levels related to insulin and leptin signaling pathways to determine its activation regarding the treatment and induced nephrophaty.
- Determination of cell morphology changes and extracellular matrix levels caused by the treatment and induced diabetic nepthropathy.

The specific aims of this study:

- To establish a cell culture model of diabetic nephropathy on proximal tubule cells by incubating the cells with glucose (HG30) and a combination of glucose and H_2O_2 (HG30/ H_2O_2) (control vs HG30 and HG30/ H_2O_2)
- To determine the viability of proximal tubule cells in *in vitro* model of DN after treatment with Liraglutide and Empagliflozine by MTT analysis and live cell counting using a Neubauer hemocytometer (HG30 vs HG30/Lira10 and HG30/Lira20; HG30/ H_2O_2 vs HG30/H_2O_2/Lira10 and HG30/H_2O_2/Lira20; HG30 vs HG30/Empa100 and HG30/Empa500; HG30/H_2O_2 vs HG30/H_2O_2/Empa100 and HG30/H_2O_2/Empa500)
- To evaluate oxidative stress by measuring total glutathione (tGSH) in *in vitro* model of DN after treatment with Liraglutide and Empagliflozine
- To determine the expression of genes (*TGF-beta1*) involved in *in vitro* model of DN after treatment with Liraglutide using RT-PCR method
- To determine the expression of proteins (Akt, pAkt, GSK3β, pGSK3β, p53, p-p53, pSTAT3, SMAD7, and PPAR-γ) involved in *in vitro* model of DN after treatment with Empagliflozin
- To measure TGF-β transcription in *in vitro* model of DN after treatment with Liraglutide and Empagliflozine

- To measure the extracellular matrix (ECM) in *in vitro* model of DN after treatment with Liraglutide and Empagliflozine
- To measure influence on cell morphology in *in vitro* model of DN after treatment with Liraglutide and Empagliflozine by visualizing the F-actin cytoskelet with *Rhodamine* Phalloidin stain

4. MATERIAL AND METHODS

4.1.Study design

- The study was designed as a randomised controlled trial. There were two sets of experiments: one with Liraglutide and the other with Empagliflozine. In each experiment there were three different groups. The first group was the same in both experiments, cells treated with HG30 and HG30/ H_2O_2 were compared to control cells; in the second group cells treated with HG30 were compared to cells treated with HG30/Lira10 and HG30/Lira20, or HG30/Empa100 and HG30/Empa500. In the third group, cells treated with HG30/ H_2O_2 were compared to cells treated with HG30/H_2O_2/Lira10 and HG30/H_2O_2/Lira20; or HG30/H_2O_2/Empa100 and HG30/H_2O_2/Empa500.

4.2.Material

Pig proximal kidney tubular epithelial cells (LLC-PK1, Manassas, VA, USA) below the 30th passage were used in all experimental procedures. Supplemental properties of chemicals and manufacturer details are written in brackets after first mentioning.

4.3. Methods

4.3.1. Cultivation of the cells

The commercially available LLCPK1 cell line was isolated from the kidney of a healthy, male, Hampshire pig aged between 3 and 4 weeks. Cell line demonstrates endothelial morphology with few distinctions. The cells can occasionally grow in the form of domes, creating several layers of cells appearing as rings (234). During growth, cells show differentiated morphology and a polarized appearance with a brush border on the apical side, a thin basal membrane on the base side, with a close interconnection between cells (235). The cell line has characteristics of proximal tubule-specific properties in the kidney - Na + dependent transmission system, enzymes of apiary membranes, including alkaline phosphatase and γ-glutamyl transferase (236). It is a generous gift from Professor Carl Verkoelen's laboratory at the Urology Clinic of Erasmus Medical Center in Rotterdam, The Netherlands. Dulbecco's modified Eagle medium, DMEM was supplemented with 1 % of 100x Penicillin streptomycin, and 10 % of FBS. The culturing protocol was as follows:

1. 9 mL of growth medium was transferred in a 100 mm cell culture dish.
2. Tubes with frozen cells were taken from a liquid nitrogen tank.
3. Tubes with frozen cells were defrosted for 2 minutes in the water bath heated up to 37 °C.
4. The defrosted cell suspension was transported by sterile pipette into a growth medium in the Falcon tube.
5. The cell suspension was centrifuged at room temperature at 140 x g for 6-minutes.
6. Supernatant was discarded and 5 ml of fresh complete medium was pipetted and cells were resuspended.
7. Cells were counted in the Neubauer chamber and diluted to obtain the final concentration of 100 000 cells/mL.
8. Upon dilution cells were transferred to 100 mm Petry dish.
9. The next day growth medium was replaced with the same volume of a fresh medium.
10. Cells were grown to 80-85 % confluency.
11. After reaching the required confluent state, the medium was removed, and cells were trypsinized with 5 mL of trypsin solution for 5 minutes.
12. A fresh growth medium (5mL) was added to trypsin/cell suspension to block the enzyme, and everything was transferred to a 15 mL falcon tube centrifuged at room temperature at 140 x g for 6-minutes.
13. Cells were resuspended in 10 mL of fresh complete growth medium and the supernatant was discarded.
14. Cells were counted in the Neubauer chamber to obtain the final concentration of 150 000 cells/mL and the cell suspension was transferred to a 100mm Petry dish.
15. Cells were grown to 80-90 % confluency and then used for further experiments.

4.3.2. Establishment of *in vitro* cell culture mimic model of diabetic nephropathy on proximal tubule cells

LLC-PK1 cells were sub-cultivated in Dulbecco's modified Eagle medium (DMEM, Capricorn Scientific) supplemented with 10% fetal bovine serum (FBS/ Thermo Fisher Scientific Cat.No. 16000036) and 1× antibiotic solution (penicillin / streptomycin/Thermo Fisher Scientific Inc., Waltham, MA, USA) at 37 °C in a humidified atmosphere of 5% CO_2 v/v in air. When LLC-PK1 cells reach 80-90% confluence they were exposed to pathophysiological mediators mimicking DN: high glucose and oxidative stress. To examine

the effect of normal (NG) and high glucose (HG) the cells were plated in 6 well plates at density 1.5 x10^5 cells/cm^2 and treated with glucose (D-(+)-Glukoza, pro analysis (Kemika, Zagreb) at different concentrations (1.5, 30 mM) during 24 hours. To induce oxidative stress, the cells were treated with 0.5 mM H_2O_2 (Grammol, Zagreb, Croatia, Cat.No. 7722-84-1) in combination with HG for 24 hours (30/0.5mM). In the same experiment, the cells were treated with a combination of glucose and different concentrations of GLP-1 receptor analogue (Novo Nordisk Liraglutide Victoza 6mg/ml) (30mM/10nM, 30/20nM) and a combination of glucose, H_2O_2 and Liraglutide (30/0.5mM/10nM, 30/0.5mM/20nM). In another set of experiments, LLC-PK1 cells were treated with glucose at different concentrations (1.5, 30 mM) and combination of glucose and H_2O_2 (30/0.5mM) during 24 hours. The cells were then treated with the combination of glucose and sodium/glucose cotransporter-2 inhibitors (Empagliflozin 10 mg Cat. No. A12440) (30mM/100nM, 30/500nM) and combination of glucose, H_2O_2 and Empagliflozin (30/0.5mM/100nM, 30/0.5mM/500nM). The cells were seeded in 96 or 6 well plates in the specified concentration whereas the 96 well-plated cells were used for the MTT experiment while 6 well-plated cells were for all other experiments.

On the first day of the experiment, the cells were plated at density 1.5 x10^5 cells/cm^2 in 6 well plates. The cells were incubated overnight and on the second day when reaching confluency, the medium was changed to DMEM without FBS with appropriate concentrations of glucose and H_2O_2 in combination with different concentrations of Liraglutide (described above) or Empagliflozin (described above). On the third day of the experiment, the medium was removed from all wells, the PBS was washed, the cells were trypsinized with 500 µL of trypsin which was then deactivated with 500 µL of the medium. In some methods described below cells were detached using scrapers. In each experiment there were three different groups. The first group is untreated cells, cells exposed to glucose only and glucose and H_2O_2. The second group is cells treated with Liraglutide 10 and 20 nM in combination with glucose and H_2O_2. In the third group, cells were treated with Liraglutide 10 and 20 nM in combination with glucose only. In another set of experiments in the first group of untreated cells, cells were exposed to glucose only and glucose and H_2O_2. The second group is cells treated with Empagliflozin 100 and 500 nM in combination with glucose and H_2O_2. In the third group, cells were treated with Empagliflozin 100 and 500 nM in combination with glucose only. All experiments were made in three independent biological replicates.

4.3.3. Assessment of damaged tubular cell viability in *in vitro* mimic model of DN

Damaged tubular cell viability in *in vitro* model of DN in LLC-PK1 cells (previously described protocol) was determined by the Erythrosin B color exclusion test. Cells were counted using a Neubauer hemocytometer. Transparent cytoplasm was present in living cells, while dead cells had a reddish cytoplasm.

The extent of proximal tubular damage in DN and drug effect on cell viability was determined by an MTT colorimetric test. MTT assay is extensively used in testing cytotoxicity, cell viability, and cell proliferation. It relies on functional NAD(P)H-dependent oxidoreductase enzymes found in mitochondrial of all living cells. These enzymes reduce yellow water-soluble tetrazolium bromide into purple water-insoluble formazan crystals. The amount of produced crystals usually correlates with the number of live cells (237). MTT stock solution was prepared as follows: 100 mg of tetrazolium bromide powder (Cruz chemicals, Dallas, Texas, USA) was dissolved in 20 mL of 1×PBS. The solution was sterilized using a 0.2 μm syringe PES filter (Nalgene ™ Thermo Fisher Scientific Waltham, Massachusetts, United States. Aliquots (1 mL) were frozen at -20 °C and protected from the UV light. The cells were plated on 96-well plates at density $1.5x10^5$ cells/mL and treated with different compounds according to the aforementioned protocol. After 24 hours 10 μL of MTT stock solution was pipetted into each well, resulting in 0.5 mg/mL of tetrazolium bromide concentration. The plate was placed in an incubator for 4-hours to make formazan crystals. After incubation time, in each well with MTT stock solution, 100 μL of MTT solvent (Sigma Aldrich) was added, and formazan crystals were dissolved by repeated pipetting in and out 10-15 times. Absorbance was read at a wavelength of 595 nm using a microplate reader (iMarkTM Microplate Absorbance Reader; Bio-Rad, Hercules, California, USA). The absorbance value from the control group was set as 100% and the values from treatment groups were expressed as a percentage of control.

4.3.4. Measurement of cellular reduced glutathione (GSH) concentration in *in vitro* mimic model of DN in proximal tubule cells.

Glutathione (GSH) is the cell's main thiol antioxidant. The oxidized form of glutathione is glutathione disulfide (GSSG). Glutathione is present in high concentrations in the cytosol, nucleus, and mitochondria and is the main soluble antioxidant in these cell sections (238). GSH in the nucleus maintains a reduction of the critical proteins needed for

the repair and expression of DNA (239). The main protective mechanisms of GSH from oxidative stress are: GSH is a co-factor of several enzymes detoxifying oxidative stress (e.g. Glutathione peroxidase (GPx)); it participates in the transport of amino acids through a plasma membrane; it purifies hydroxyl radicals, detoxifying hydrogen peroxide, and lipid peroxides via the catalytic activity of glutathione peroxidase. Therefore, the concentration of GSH can be used as a suitable measure of oxidative stress in cells (240). To determine the level of free radicals accumulating in the cells, the concentration of glutathione (GSH) was measured (241). Oxidative stress of cells was evaluated by measuring total glutathione (tGSH) concentration spectrophotometrically (242). On the first day of the experiment, the cells were plated at a density of $1.5x10^5$ cells/ mL in 6-well plates and treated with different compounds according to the aforementioned protocol. On the third day, GSH concentration was determined using a commercially available colorimetric kit according to the manufacturer's protocol (Glutathione Assay Kit, Signa-Aldrich, Saint Louis, MO, SAD). Cells were scraped, detached from dish surface, and centrifuged at 140 x g for 7 minutes at 4 ºC. Obtained pellet was used for this experiment and supernatant for measuring TGF-β expression (described below). The cell pellet was resuspended in 1x PBS, centrifuged at 600 x g for 5 minutes at 4 ºC and the supernatant was removed. Pellet was then transported to the microcentrifuge tubes, 3 volumes of the 5% SSA Solution was added to the pellet, each tube was vortexed for 5 sec, frozen and thawed twice (frozen at -80ºC for 10 minutes and thawed at 37ºC for 6 min) and left for 5 minutes in the refrigerator. The content was then centrifuged at 10 000 x g for 10 minutes. The amount of 50 ul of supernatant was measured and stored at 2-8 ºC before the next step (if the assay could not be performed within 2 hours, the content was stored at -70 ºC for a maximum of 10 days). The supernatant was used to measure GSH concentration and it was placed in a 96-well polystyrene plate. 10 µl of sample and 150 µl of working solution (prepared according to the manufacturer's instructions) were added to each well. The content was gently mixed, incubated for 5 minutes at room temperature and after that 50 ul of NADPH was added to each well. The response was measured using a microplate reader (iMarkTM Microplate Absorbance Reader) at 412 nm. Results are shown in nanomoles per milliliter of sample.

4.3.5. Determining *TGF-beta 1* gene expression level involved in signaling pathways of tubular damage in *in vitro* mimic model of DN in proximal tubule cells.

Total RNA was isolated by TRI Reagent (T9424, Sigma Aldrich, St. Louis, USA) according to the manufacturer's protocols. Cells were added to 350 µL of high guanidine thiocyanate buffer and vortexed briefly to achieve lysation and homogenization. Then 350 µL of 70% ethanol was added. The entire sample was then transferred to a centrifugation column and centrifuged at 10,000 rpm for 15 seconds to allow RNA to bind to the column membrane. The column was then washed three times to remove any impurities and cell debris from the membrane. The centrifuge column was placed in a new centrifuge tube and 40 µL of distilled water was added to the column and centrifuged at 10,000 rpm for 1 minute to dissolve the RNA in water. Total RNA was stored at -20 ° C. The concentration of RNA was determined from isolated total RNA samples and the synthesis of the first cDNA strand was started using a commercial kit (PrimeScript First Strand cDNA Synthesis Kit, Takara Bio, Inc.) according to the manufacturer's instructions. The resulting cDNA was stored at -20 ° C until preparation for PCR. The obtained cDNA was quantified by polymerase chain reaction (PCR) transcription using a commercial kit according to the manufacturer's instructions (Taq PCR Core Kit, Qiagen, Hilden, Germany). β-actin was used as an internal control. The synthesized cDNA was amplified using specific primer sequences as follows: TGF-β1 (sense 5' -CTGAGGCTCAAGTTAAAAG -3' antisense 5' GAACCCGTTAATTTCCAC -3'.) and β-actin (sense 5'-TGCGGGACATCAAGGAGAAG-3'; antisense 5'-AGTTGAAGGTGGTCTCGTGG3'). PCR conditions were: for TGF-β1 denaturation at 94 °C for 3 min, annealing at 47 °C for 45 s, elongation at 72 °C for 1 min in 30 cycles; for β-actin denaturation at 94 °C for 3 min, annealing at 58 °C for 45 s, elongation at 72 °C for 1 min in 30 cycles. PCR products were run on a 2% agarose gel stained with Syber Safe (Invitrogen, Thermo Fisher Scientific Inc., Waltham, MA, USA) according to the manufacturer's protocols and visualized using a Gel Imaging System (ChemiDocTM Imaging System, Bio-Rad, Hercules, California, USA) and semiquanfied by Image Lab software (version 5.2.1. build 11, BioRad, Hercules, CA, USA). Results are shown as percentages compared to untreated control.

4.3.6. Protein analysis and Western blot method in *in vitro* mimic model of DN in proximal tubule cells.

In order to isolate proteins in a sample electrophoresisbased on mass was performed. Sodium dodecyl sulphate (SDS) and dithiothreitol or β-mercaptoethanol were used for denaturation of proteins. Samples were run on an acrylamide gel. The gel consists of two different gels: one with 5 % acrylamide/bis-acrylamide (AA/Bis) and the other with 12% of AA/Bis concentration.

Table 4.3.6.1. Prepared solutions used in the western blot method (243).

Solution name	Abbreviation	Composition
Phosphate buffered saline 1x	1x PBS	137mM of NaCl, 2.7 mM of KCl, 10 mM of Na_2HPO_4, 1.8 mM oh KH_2PO_4 (All chemicals from GramMol, Zagreb, Croatia)
Homogenization buffer	HB	1x PBS, 0,32m sucrose, 1mM PMSF, 5mM NaF, 1mM Na_3VO_4, 1mM EDTA (All chemicals from Sigma-Aldrich, Saint Louis, MO, SAD), 1 tablet of complete mini protease inhibitor per 10 mL of buffer (Roche, Basel Switzerland)
10 % SDS	/	10g of SDS Acrylamide (Sigma-Aldrich, Saint Louis, MO, SAD)/100mL distilled water
Western blot sample buffer	/	0.35M Tris-HCl, pH 6.8, 10 % SDS, 30 % glycerol, 9.3 % DTT
3M Tris-HCl	/	36.342 g of tris base, up to 100 mL of dH2O, pH 8.8
1M Tris-HCl	/	12.114 g of tris base, up to 100 mL of dH2O, pH 6.8
30 % Acrylamide/Bis-acrylamide	AA/Bis	30 % Acrylamide(Sigma-Aldrich, Saint Louis, MO, SAD) , 2.7 % Bis-
1.5 % Ammonium persulphate	APS	1.5g Ammonium persulphate (Sigma-Aldrich, Saint Louis, MO, SAD) in 100 mL of distilled water

Table 4.3.6.1. Prepared solutions used in the western blot method (243) continued

Electrophoresis buffer	/	25mM Tris-Base (Fisher scientific, Waltham, Massachusetts, USA), 192mM glycine (Fisher scientific, Waltham, Massachusetts, USA), 0.1 % SDS in distilled water
Towbin blotting buffer	/	25mM Tris-Base, 192mM glycine, 20 % methanol in distilled water
Blocking solution	/	3 % BSA (Sigma-Aldrich, Saint Louis, MO, SAD) in 1x PBST

LLC-PK1 cells were plated on a 75 cm^2 petri dish and grown to 80-90% confluency in DMEM medium plus 10% FBS and treated with different compounds according to the aforementioned protocol. Every next step needs to be done with precooled solutions and on ice. PBS (500ul) was added to each well, and cells were scraped using a cell scraper. Scraped cells were moved in a 1.5 mL Eppendorf tube and centrifuged at 130g for 5-minutes at 4 °C (centrifuge: Sigma 1-15 PK, St. Louis, Missouri, United States). The supernatant was separated, followed by the addition of 600 µL of homogenization buffer. Ultrasonic homogenizer Bandelin Sonopuls 2070 (BANDELIN electronic GmbH & Co. KG, Berlin, Germany) was used for cell homogenization on ice, cycle set at 9 and 100 % of the power for 15 seconds. In order to separate extracellular matrix and insoluble remains, the homogenate was centrifuged for 15 minutes at 1000g at 4 °C (centrifuge: Sigma 1-15 PK, St. Louis, Missouri, United States). The supernatant was transferred in a 0.5 mL Eppendorf tube and stored at -80 °C.

Bradford protein assay was used for protein content measurement prior final preparation of gel samples. Bradford protein assay exploits the reaction of Coomassie blue G 250 in an acidic solution with aromatic groups of amino acids. After binding to amino acids the dye absorption maximum is shifted from 465 nm to 595 nm (161). 50 mg of Coomassie blue G 250 powder (Carl Roth Karlsruhe, Germany) was dissolved in 50 mL of methanol (Carlo Erba, Milan, Italy), followed by the addition of 100 mL of 85 % phosphoric acid (Sigma, St. Louis, Missouri, United States) and distilled water up to 1 litre was capped on top of the prepared solution. To extract undissolved dye powder, the reagent was filtered through

a 0.2 µm PES filter (Nalgene ™ Thermo Fisher Scientific Waltham, Massachusetts, United States) and stored at 4 °C.

Samples were pipetted in technical triplicates on a 96 well plate (Thermo Fisher Scientific Waltham, Massachusetts, United States). 1 µL of the standard sample and 250 µL of Bradford reagent was pipetted to each well. Samples were incubated at room temperature for 15 minutes and read at the iMark microplate reader (Bio-rad, Hercules, California, United States) at 595 nm. The calibration curve was plotted from obtained values of absorption value measured in standard 7 was subtracted from measured values of the rest of the standards, and a linear equation was calculated.

The same procedure as described above for sample reparation was used to determine the concentration of proteins in samples. The absorption value measured in standard 7 was subtracted from the samples' measured values. Triplicates were averaged to a single value. Protein concentrations were calculated from corrected and averaged absorption values used in a linear equation.

Dillution of sample aliquots to 1 mg/mL was achieved with 1x PBS buffer. Western blot sample buffer was added in a 1:5 ratio - buffer to sample. Aliquots were heated up to 100 °C for 5-minute in a heat block (Eppendorf Thermomixer Compact; Eppendorf, Hamburg, Germany). Samples were then cooled down and stored at 4 °C.

Western blot analysis gels were the discontinuous type consisted of 5 % of AA/Bis in stacking gel and 12 % of AA/Bis in resolving gel primed in Tris-Glycine buffer with the addition of 1.15 % of 2,2,2-Trichloroethanol (Merck, Darmstadt, Germany) for the stain-free method (162,163). Gels were loaded as follows: 5 µL of protein standard in the first well (SeeBlue 2 Plus, Thermo Fisher Scientific Waltham, Massachusetts, United States) and 10 µL of the sample in each well of the gel resulting in a total protein load of 20 µg. Electrophoresis was performed in Hoeffer's mighty small electrophoresis system (Hoeffer inc. San Francisco, California, United States) using a continuous current of 15 mA per gel for 3 hours electrophoresis buffer. Cooling fluid was circulated through the central block to ensure a constant temperature of 4 °C.

Once electrophoresis was completed, stacking gel was cut from gel cassettes upon removal from the electrophoresis system, following activation of bottom stain-free gels in the ChemiDoc™ Imaging system (BioRad Hercules, California, United States) using automated imaging protocol for 45 seconds for visualisation of proteins within the gel. Gel tri-halo

components are attached to amino acid tryptophan enabling detection of proteins. Proteins were blotted in the TE22 Mighty small transfer tank (Hoeffer inc. San Francisco, California, United States) for 2 hours at 200mA continuous current in Towbin blotting and transferred from gel to 0.45 μm pore size polyvinyl difluoride (PVDF) membrane (Thermo Fisher Scientific Waltham, Massachusetts, United States). The cooling of the system was constant ensuring a temperature of 4 °C. Next, visualization of proteins was performed using the ChemiDoc™ Imaging system (BioRad Hercules, California, United States) for the imaging of PVDF membrane-containing proteins.

The next step was immunodetection. Blockade of nonspecific reactions achieved by 3% bovine serum albumin in 1x PBS buffer with Tween detergent (PBST) solution used for all antibodies and tertiary complex dilutions. The membrane was then incubated in the primary antibody solution (Akt, pAkt – Ser 473, GSK3 α/β, pGSK3 α/β, p53, p-p53, pSTAT3, SMAD7, PPAR-γ) overnight on a shaker at + 4 ° C in the dilutions shown in Table 4.3.6.2. Membranes were washed for 10 minutes 3 times in PBST buffer and incubated in biotin labeled secondary antibody for 2 hours at room temperature (Table 4.3.6.3.) After incubation, membranes were again washed in PBST buffer (3x 10 minutes) and incubated in the streptavidin-HRP complex for 1 hour at room temperature. Washing of secondary antibodies and the streptavidin-HRP complex was carried out 3 times for 10 minutes in PBST buffer. Cemiluminescent detection solution was used for visualisation (Immobilon ® Forte Western HRP Substrate, Millipore Burlington, Massachusetts, USA) according to the manufacturer's instructions. The signal was detected using the ChemiDoc™ Imaging system (BioRad Hercules, California, United States) according to the manufacturer's instructions. The captured images were stored in digital form. Glyceraldehyde 3-phosphate dehydrogenase (GAPDH) was used as an internal control.

Table 4.3.6.2. List of primary antibodies used in the Western blot method.

Antibody label	Full name of the antibody	Antibody classification	Host species	Manufacturer and catalog number	Dilution used for Western blot
Akt	anti-protein kinase B	IgG monoclonal	Mouse	Cell signaling Danvers, Massachusetts, USA Cat. No.2920S	1:1000

Table 4.3.6.2. List of primary antibodies used in the Western blot method-continued.

pAkt – Ser 473	anti-protein kinase B – phosphorylated on serine 473	IgG monoclonal	Rabbit	Cell signaling Danvers, Massachusetts, USA Cat. No. 9271S	1:1000
GSK3 β	Anti-glycogen synthase kinase 3 alpha + beta	IgG monoclonal	Rabbit	Cell signaling Danvers, Massachusetts, USA Cat. No. 676S	1:1000
pGSK3 β	Anti-glycogen synthase kinase 3 - tyrosine 279 phosphorylated GSK3alpha and tyrosine 216 phosphorylated GSK3beta	IgG polyclonal	Rabbit	Thermo Fisher Waltham, Rockford, USA Cat. No. OPA1-03083	1:1000
p53	Anti-p53 antibody	IgG monoclonal	Rabbit	Cell signaling Danvers, Massachusetts, USA Cat. No. 527S	1:1000
p-p53	Anti-p53 - phosphorylated on serine 33	IgG polyclonal	Rabbit	Cell signaling Danvers, Massachusetts, USA Cat. No. 526S	1:1000
pSTAT3	Anti-signal transducer and activator of transcription 3 - phosphorylated on tyrosine 705	IgG monoclonal	Rabbit	Cell signaling Danvers, Massachusetts, USA Cat. No. 145S	1:1000

Table 4.3.6.2. List of primary antibodies used in the Western blot method-continued.

SMAD7	Anti-sterile alpha motif domain containing 7	IgG polyclonal	Rabbit	Sigma-Aldrich, St. Louis, MO, USA Cat. No. HPA028897	1:1000
PPAR-γ	Anti-peroxisome proliferator-activated receptor gamma	IgG polyclonal	Rabbit	Sigma-Aldrich, St. Louis, MO, USA Cat. No. SAB45O2262	1:1000

Table 4.3.6.3. List of secondary antibodies and tertiary complex used in Western blot method.

Antibody label	Full name of the antibody	Antibody classification	Host species	Manufacturer and catalog number	Dilution used for Western blot
αMO-biotin	Anti-mouse antibody labeled with biotin	IgG	Goat	Jackson immune research West Grove, Pennsylvania, USA Cat. No. 115-065-071	1:20000
αRB-HRP	Anti-rabbit antibody labeled with HRP	IgG	Goat	Jackson immune research West Grove, Pennsylvania, USA Cat. No. 111-035-144	1:20000
SA-HRP	Streptavidin peroxidase polymer, Ultrasensitive	-	-	Sigma-Aldrich, St. Louis, MO, USA Cat. No. S2438	1:1000

A publicly available ImageLab 6.0 computer program compatible with the Chemidoc system was used for visualization and quantification of the protein expression in specific solution (αMO-biotin, αRB-HRP, SA-HRP). Quantitative analysis of protein signals was accomplished using images of total and individual proteins uploaded to the computer program ImageLab. The obtained values of signal intensity of specific protein expression was further used for statistical analysis.

4.3.7. Measurement of TGF-β concentrations in *in vitro* mimic model of DN in proximal tubule cells.

Total TGF-β1 was measured using Human/Mouse/Rat/Porcine/Canine TGF-beta 1 Quantikine ELISA Kit (Cat No. DB100B) according to the manufacturer's instructions. On the first day of the experiment, the cells were plated at a density of $1.5x10^5$ cells/ mL of medium in 6-well plates and treated with different compounds according to the aforementioned protocol. On the third day, cells were scraped and detached from the cultured dish surface, centrifuged at 140 x g for 7 minutes at 4 ºC and obtained supernatant was used for measurement of TGF-β expression. The first step was the sample activation procedure. 1N HCL was added to 100 ul of cell supernatant and mixed well followed by incubation at room temperature for 10 minutes. The acidified sample was then neutralized by adding 20 ul of 1.2 N NaOH/0.5 M HEPES, vortexed for a minimum of 10 seconds and the immunoassay procedure was immediately started(244).

4.3.8. Measurement of ECM expression in *in vitro* mimic model of DN in proximal tubule cells.

LLC-PK1 cells were plated on a 75 cm^2 petri dish and grown to 80-90% confluency in DMEM medium plus 10% FBS and treated with different compounds according to the aforementioned protocol. Cells were scraped and detached from the cultured dish surface, transferred in a 15 mL Falcon tube and centrifuged at 140 x g for 7 minutes at 4 ºC. The supernatant was discarded and the pellet (250 ul) was washed with Ammonia acetate (150 mM) and homogenized on ice with an ultrasonic homogenizer Bandelin Sonopuls 2070 (BANDELIN electronic GmbH & Co. KG, Berlin, Germany) for 15 seconds, cycle set at 9 and 100 % of the power. Homogenate was centrifuged for 15 minutes at 1000g at 4 °C

(centrifuge: Sigma 1-15 PK, St. Louis, Missouri, United States). In each tube of a homogenized aqueous solution, 750 ul of 25% saturated $(NH_4)_2SO_4$ was added and incubated overnight at 4°C under constant agitation. The next day, samples were centrifuged at 21 000 x g 40 minutes at 4 ºC, and collagen was isolated. The supernatant was discarded and the pellet was solubilized in 1mL of 0.5M HAc (acetic acid) leaving aliquots of collagen from the culture medium. 100 ul of collagen aliquots were transferred in 2 mL conic tubes, homogenized for 5 seconds, cycle set at 9 and 100 % of the power, and precipitated with 1 mL of 50 uM (69 ug/mL) dye Sirius Red (Sigma – Aldrich Chemical Co., Saint Louis, EUA) solution in 0,5 M acetic acid. Samples were vortexed, incubated for 30 minutes at room temperature to achieve spontaneous precipitation, and then centrifuged for 40 minutes at 21 000 x g. The supernatant was disposed and the pellet was diluted in 1mL 0,1N KOH for 15 minutes at room temperature. Absorbance was measured at 490 nm wavelength.

4.3.9. Coverslips preparation

The coverslips were washed with a washing solution containing 1 portion of 30 % hydrogen peroxide (Kemika, Zagreb, Croatia) mixed with 9 portions of concentrated (96 %) sulfuric acid (Kemika, Zagreb, Croatia) (245).

1. 100 coverslips were placed in a 300 mL Erlenmeyer flask (20×20mm square), and glass slides were washed with a washing solution
2. Tender spinning ensured coverage of all coverslips with the washing solution, repeated 3 times in 30 minutes.
3. Next, acid was dilluted in a 5L-bucket of distilled water. An additional 200 mL of distilled water was needed to further dilute leftover acid in the flask with glass slides.
4. Glass slides were then washed with water.
5. 200 mL of distilled water was added into a flask and put on an orbital shaker (100 rpm) for 1 hour.
6. Next, the remaining water was discarded, and a fresh batch of 200 mL of distilled water was poured. The washing sequence was repeated 5 times more (6 hours of washing, in total).
7. After washing, distilled water was thrown away, and drying of coverslips was performed as follows: 100 mL of ACS or HPLC grade methanol was added and the flask was spun for 5 minutes. Methanol was then thrown away.

8. Flask top was covered by aluminum foil, followed by dry sterilization of coverslips at 270°C for 5 hours.
9. Then one cover slip was put in each well of 6 well plates with sterile forceps. Coverslips were treated with poly-D-Lysine, used (Sigma Aldrich, St. Louis, MO, USA) as an adhesive molecule necessary to guarantee firm cell attachment.
10. 5 mg of poly-D-lysine powder was dissolved in 5 ml of sterile deionised water in a final concentration of 1 mg/ml to prepare Poly-D-Lysine stock.
11. Next, sterile deionised water 1:200 was used for stock dilution. 1.25 ml of working solution was pippeted to each well.
12. Poly-D-lysine was removed after incubation for 1 hour.
13. Coverslips were dried overnight in sterile conditions under UV-C light

4.3.10. Measurement of treatment effects on cell morphology in *in vitro* mimic model of DN in proximal tubule cells by visualizing the F-actin cytoskelet with Rhodamine Phalloidin stain.

LLC-PK1 cells were grown on glass cover-slips inside a petri dish to reach 80-90% confluency in DMEM medium plus 10% FBS. and treated with different compounds according to the aforementioned protocol. LLC-PK1 cell morphology (F-actin cytoskelet) was visualized using Phalloidin stain (Rhodamine Phalloidin Reagent (ab235138)) as follows: on the third day, the cell culture medium was aspirated carefully avoiding cell detachment from the plate surface. Cells were then fixed in 2% formaldehyde (2.5 mL per each well) at 4ºC for 30 minutes. 0.1% Triton X-100 in PBS 1x was added into the fixed cells for 5 minutes at room temperature t permeabilize the membrane. Cells were washed 3 times every 10 minutes in PBS 1x. Conjugate the working solution, 250 µL of 1X Phalloidin was added to each well of fixed cells. Cells were incubated in dark, at room temperature for 60 minutes. Nuclei were counterstained using DAPI (1 µg/mL in methanol). Subsequently, cells were rinsed 2-3 times with PBS 1x. The cells were analyzed using an AxioSkop 2 MOT Microscope (Car Zeiss, Göttingen, Germany) equipped with fluorescence and Zeiss filter sets 15 and 01 and mounted Olympus DP 70 camera (American laboratory trading, Inc., East Lime, CT, USA). Cell images were obtained by using a 40× objective adjusted against negative stain control with mounted and without postacquisition enhancement of images. Total and immunopositive nuclei were counted in ImageJ software using QuantIF ImageJ macro. https://www.mdpi.com/1999-4915/11/2/165/htm.

4.4.Statistical analysis

Statistical analyses were performed using One-way ANOVA with Post-hoc Tukiey HSD; p-values of <0.05 were considered statistically significant. Statistical program Statistica 12 (Tibco, Palo Alto, California USA). The normality of data distribution was determined with the Shapiro-Wilk test. T-test was used to determine the significance of the difference between the two samples in the case of a normal distribution of results in the population. The option of t-test type depended on the size and whether the samples were dependent or independent. The conclusion about the differences between the two independent continuous random variables distributions was based on the Mann-Whitney-Wilcoxon test if the distribution of the results was not normal. In the case of more than two samples, and depending on the nature of the results, parametric or nonparametric analysis of variance (ANOVA) was used. Friedman test was used for multiple dependent samples and the Kruskal-Wallis test was used as a nonparametric analysis for multiple independent samples. In all analyses, the p-value was determined with $p <0.05$ or $p <0.001$. Statistics applies to all of these experiments. A sample in minimal biological triplicate was used for each statistical analysis.

5. RESULTS

In the first set of our *in vitro* experiments, the LLC-PK1 cell line was cultured in normal glucose as a control (NG; 1.5 mM), high glucose (HG; 30 mM), the combination of glucose and H_2O_2 (30mM/0.5mM), a combination of glucose and Liraglutide (30mM/10nM, 30mM/20nM) and combination of glucose, H_2O_2 and Liraglutide (30mM/0.5mM/10nM, 30mM/0.5mM/20nM) for 24 h. In another set of experiments, LLC-PK1 cells were treated also with glucose at different concentrations (1.5, 30 mM) and combination of glucose and H_2O_2 (30mM/0.5mM), a combination of glucose and Empagliflozin (30mM/100nM, 30mM/500nM) and combination of glucose, H_2O_2 and Empagliflozin (30mM/0.5mM/100nM, 30mM/0.5mM/500nM). All experiments were made in triplicates for consistency of the results.

5.1. Establishment of the cell culture model of diabetic nephropathy: assessment of the toxic effect of the high glucose and hydrogen peroxide and renal effects of Liraglutide and Empagliflozin.

The control group of cells was cultured under normoglycemic conditions (NG), and the other groups were experimental. In cells treated with HG30 and HG30/H_2O_2 there was a decrease in cell survival, although the difference did not reach statistical significance. Furthermore, the addition of Liraglutide in both concentrations HG30 and HG30/H_2O_2 treated cells led to improvement in cell survival once again not reaching statistical significance (Figure 5.1.a). Also, cell viability assessed by MTT assay was decreased in cells grown in hyperglycemia due to induced cytotoxicity. A significant decrease in MTT levels compared with control ($p<0.01$; $p<0.001$) was observed after treatment with a combination of HG30/H_2O_2, and HG30 alone. Cell viability was improved with the addition of Liraglutide 10 nM to cells treated with HG30, while 20 nM had no effect, however, cell viability was significantly decreased in all experimental groups treated with H_2O_2 regardless of Liraglutide addition, as shown in Figure 5.1.c.

Cell survival was significantly lower in cells treated with HG30 only and HG30/H_2O_2 compared to control ($p<0.001$). The addition of Empagliflozin 100 and 500 nM to HG30/H_2O_2 treated cells showed significantly higher cell survival ($p<0.01$) compared to

HG30/H_2O_2 only treated cell line. On the other hand, Empagliflozin 100 and 500 nM in combination with HG30 improved cell survival compared to control and HG30 only treated cells, but the difference was not statistically significant (Figure 5.1.b).

In cells treated with Empagliflozin 100 and 500 nM in combination with HG30 only and HG30/H_2O_2 cell viability was significantly increased compared to cells treated with HG30 and H_2O_2 ($p<0.001$) (Figure 1.b). According to the MTT results, a significant reduction of cell viability was observed in cells treated with HG30/H_2O_2 combination ($p<0.001$), while the difference in the viability of cells treated with HG30 only was only numerical compared to control (Figure 5.1.d).

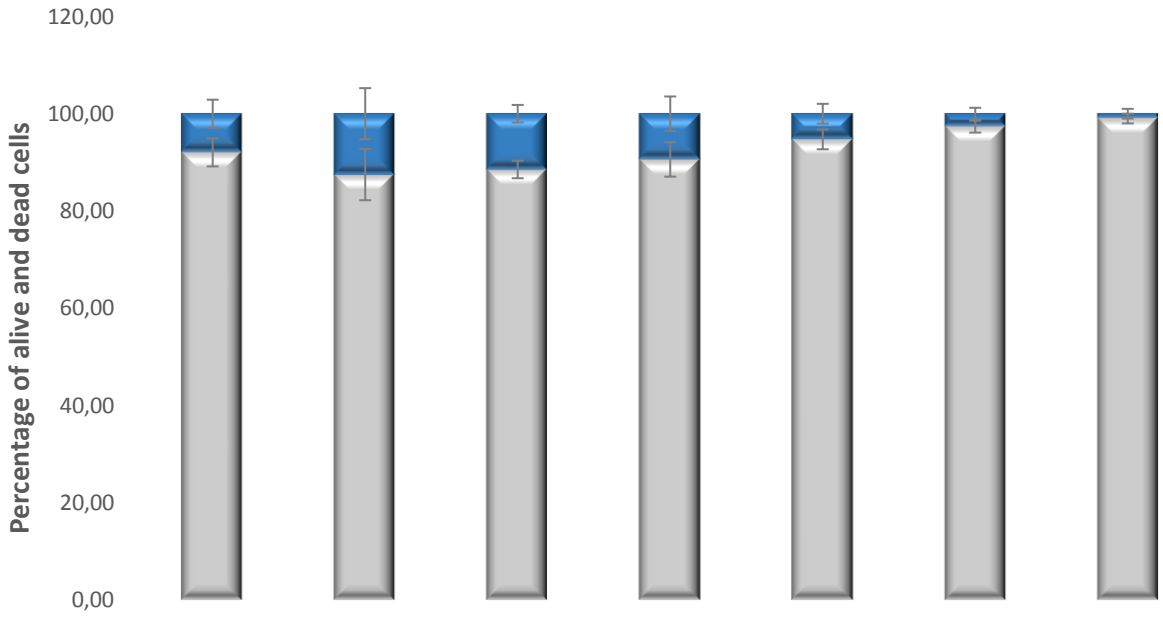

Glucose 30mM	-	+	+	+	+	+	+
H_2O_2 0.5 mM	-	-	+	+	+	-	-
Liraglutide 10nM	-	-	-	+	-	+	-
Liraglutide 20nM	-	-	-	-	+	-	+

Figure 5.1.a- Cell survival in the experimental LLC-PK1 treated cell lines (control vs HG30 and HG30/H_2O_2; HG30 vs HG30/Lira10 and HG30/Lira20; HG30/H_2O_2 vs HG30/ H_2O_2/Lira10 and HG30/H_2O_2/Lira20). Determined by the Erythrosin B color exclusion test 24 h after treatment; significance was analyzed on data regarding dead cells; Kruskal-Wallis test with Dunns post hoc test and Bonferroni correction. The data shown are representative of at least three independent experiments. Plus (+) sign indicates the addition of compounds and minus (−) sign lack of compounds in the experimental group compared to untreated control. Erythrosin B color exclusion test, pig proximal tubule cell line (LLC-PK1), HG (1.5 mM, 30 mM), H_2O_2 (0.5mM), Liraglutide (10 nM, 20 nM).

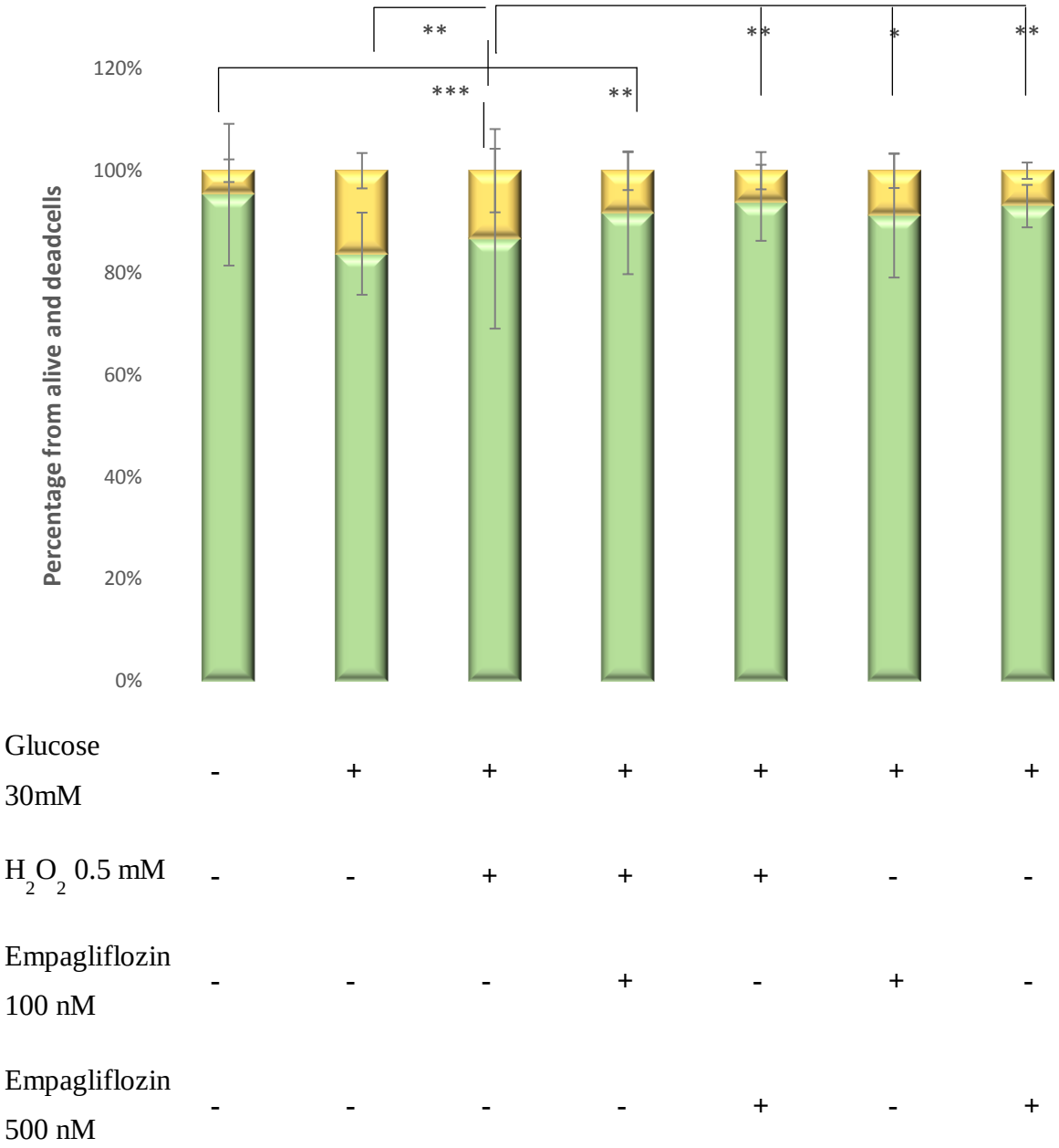

Figure 5.1.b- Cell survival in the experimental LLC-PK1 treated cell lines (control vs HG30 and HG30/H_2O_2; HG30 vs HG30/Empa100 and HG30/Empa500; HG30/H_2O_2 vs HG30/ H_2O_2/Empa100 and HG30/H_2O_2/Empa500). Determined by the Erythrosin B color exclusion test 24 h after treatment; significance was analyzed on data regarding dead cells. One-way ANOVA $_{F(6,34)\ 6.04,\ p=3.8\times10^{-4}}$ with Tukey HSD post hoc test; : *p<0.05, **p<0.01 ***p<0.001. The data shown are representative of at least three independent experiments. Plus (+) sign indicates the addition of compounds and minus (−) sign lack of compounds in the experimental group compared to untreated control. Erythrosin B color exclusion test, pig proximal tubule cell line (LLC-PK1), HG (1.5 mM, 30 mM), H_2O_2 (0.5mM), Empagliflozin (100 nM, 500 nM).

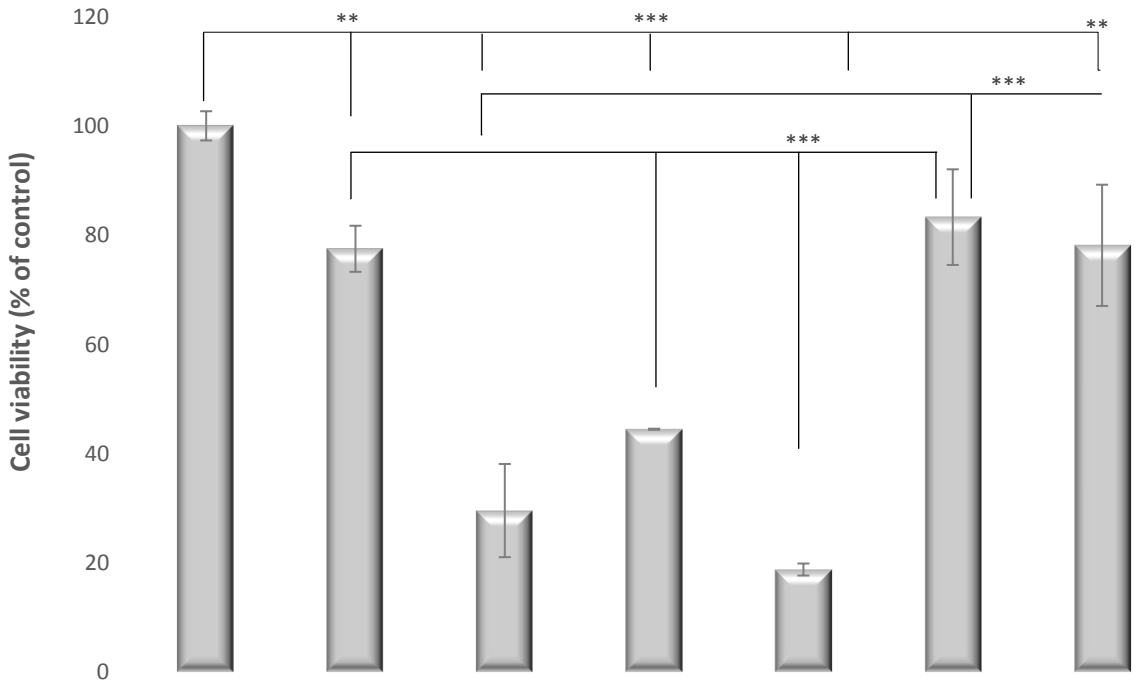

Glucose 30mM	-	+	+	+	+	+	+
H_2O_2 0.5 mM	-	-	+	+	+	-	-
Liraglutide 10nM	-	-	-	+	-	+	-
Liraglutide 20nM	-	-	-	-	+	-	+

Figure 5.1.c- Cell viability assessed by MTT assay in the experimental LLC-PK1 treated cell lines (control vs HG30 and HG30/H_2O_2; HG30 vs HG30/Lira10 and HG30/Lira20; HG30/H_2O_2 vs HG30/ H_2O_2/Lira10 and HG30/H_2O_2/Lira20). MTT measurements were done by spectrophotometry at 595 nm. One-way ANOVA $_{F(8,44)\ 67.66,\ p=9.26\times10}{}^{-19}$ with Tukey HSD post hoc test; : **p<0.01 ***p<0.001. Plus (+) sign indicates the addition of compounds and minus (−) sign lack of compounds in the experimental group compared to untreated control. MTT assay, pig proximal tubule cell line (LLC-PK1), HG (1.5 mM, 30 mM), H_2O_2 (0.5mM), Liraglutide (10 nM, 20 nM).

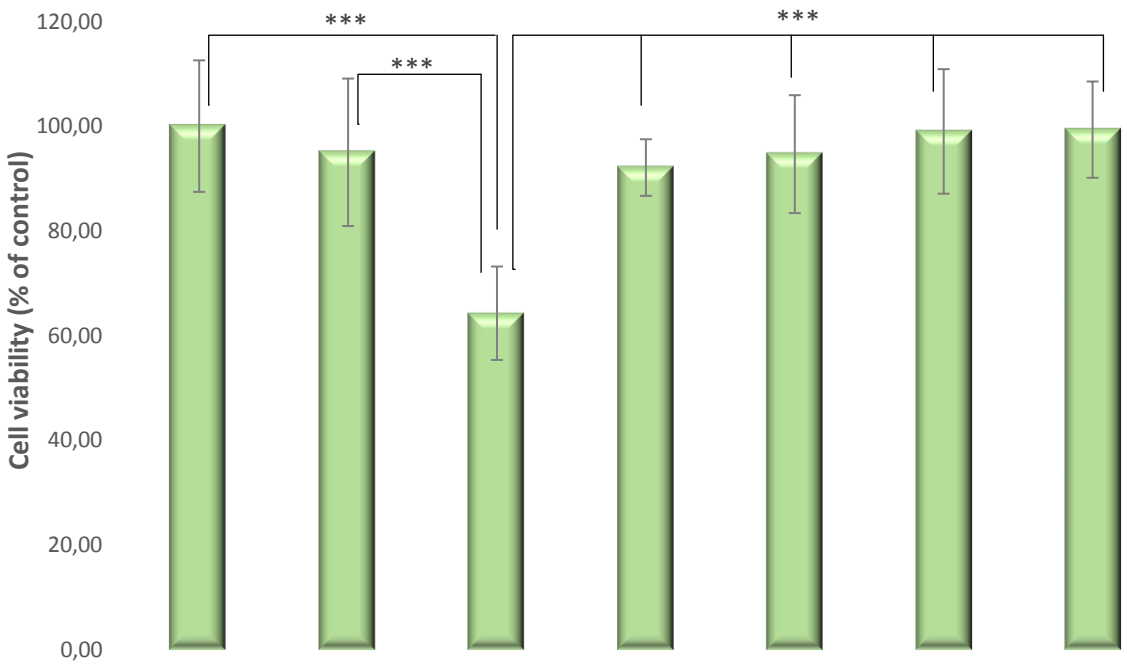

Glucose 30mM	-	+	+	+	+	+	+
H_2O_2 0.5 mM	-	-	+	+	+	-	-
Empagliflozin 100 nM	-	-	-	+	-	+	-
Empagliflozin 500 nM	-	-	-	-	+	-	+

Figure 5.1.d- Cell viability assessed by MTT assay in the experimental LLC-PK1 treated cell lines (control vs HG30 and HG30/H_2O_2; HG30 vs HG30/Empa100 and HG30/Empa500; HG30/H_2O_2 vs HG30/ H_2O_2/Empa100 and HG30/H_2O_2/Empa500). MTT measurements were done by spectrophotometry at 595 nm. One-way ANOVA $_{F(6,58)\ 11.59,\ p=3.41\times10^{-8}}$ with Tukey HSD post hoc test; ***p<0.001. Plus (+) sign indicates the addition of compounds and minus (−) sign lack of compounds in the experimental group compared to untreated control. MTT assay, pig proximal tubule cell line (LLC-PK1), HG (1.5 mM, 30 mM), H_2O_2 (0.5mM), Empagliflozin (100 nM, 500 nM).

5.2. Measurement of cellular glutathione (GSH) concentration in LLC-PK1 cell culture model of diabetic nephropathy

To evaluate cellular redox tone, GSH levels were measured in LLC-PK1 treated cell cultures in the above-mentioned subgroups, as shown in Figure 5.2.a. There was a significant decrease in GSH levels in cells treated with HG30 and HG30/ H_2O_2 compared to the untreated control ($p<0.001$) as expected. A significant increase of GSH was observed with the addition of Liraglutide 10 and 20 nM to cells treated with HG30/H_2O_2 compared to cells treated with HG30/ H_2O_2 only ($p<0.01$). However, the addition of Liraglutide (both 10 and 20 nM) to HG30 exposed cells had no significant effect on GSH levels, the difference was only numerical.

In another set of experiments with Empagliflozin, GSH levels were decreased in cells treated with HG30 and a combination of HG30/H_2O_2 compared to control (p=NS; $p<0.001$ respectively). With the addition of Empagliflozin 100nM and 500nM to HG30 treated cells recovery of GSH levels was observed compared to cells treated with HG30 only ($p<0.05$; p=NS respectively). Both doses of Empagliflozin (100 nm and 500 nM) led to an increase of GSH levels when added to HG30/H_2O_2 compared to HG30/H_2O_2 only treated cells (p=NS; $p<0.01$ respectively). Figure 5.2.b. Each experiment was repeated in minimal biological triplicate for consistency of the results.

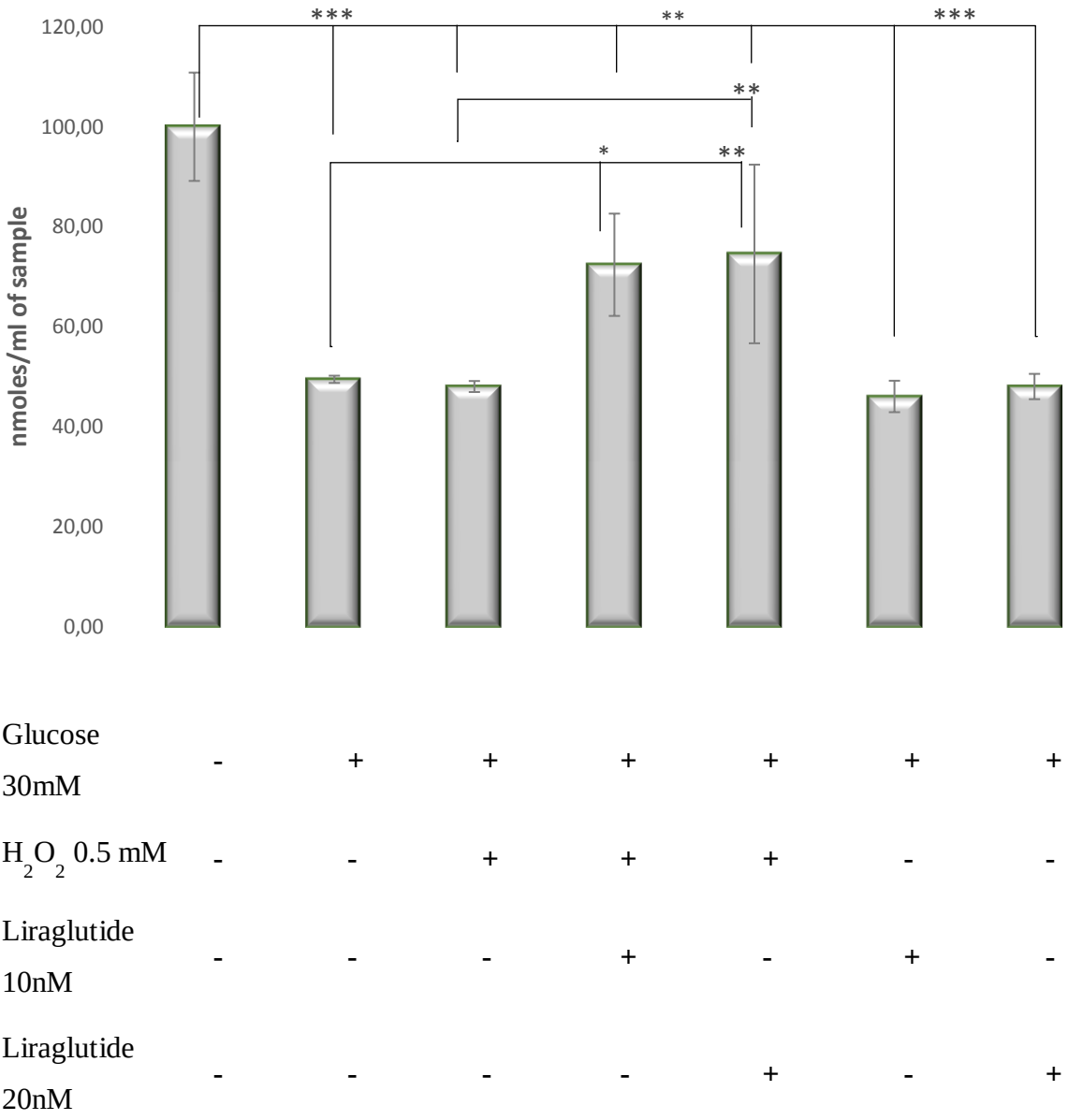

Figure 5.2.a- GSH levels in the experimental LLC-PK1 treated cell lines (control vs HG30 and HG30/H_2O_2; HG30 vs HG30/Lira10 and HG30/Lira20; HG30/H_2O_2 vs HG30/ H_2O_2/Lira10 and HG30/H_2O_2/Lira20). GSH measurements were done by spectrophotometry at 415 nm. One-way ANOVA $_{F(16,70)=43.68,\ p=4.137\times10^{-25}}$ with Tukey HSD post hoc test; The values are represented in micromol per milliliter as average with standard deviation ± SD. Bars assigned with asterisks are statistically significantly different *p<0.05, **p<0.01 ***p<0.001. Plus (+) sign indicates the addition of compounds and minus (−) sign lack of compounds in the experimental group compared to untreated control. The data shown are representative of at least three independent experiments. Cellular glutathione (GSH), pig proximal tubule cell line (LLC-PK1),HG (1.5 mM, 30 mM), H2O2 (0.5mM), Liraglutide (10 nM, 20 nM).

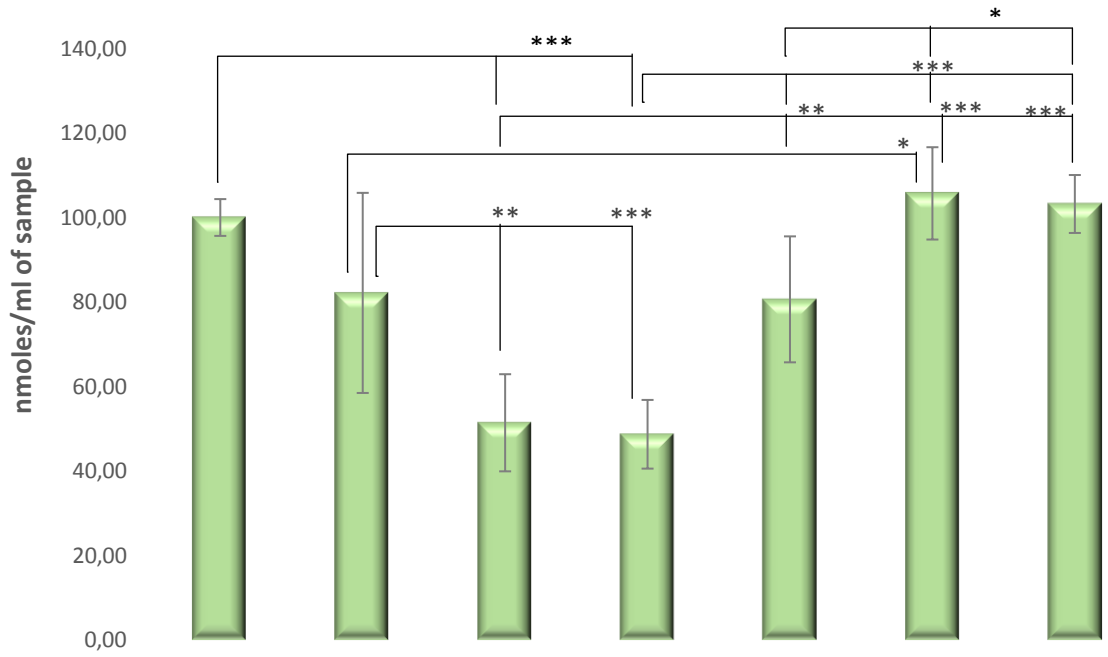

Glucose 30mM	-	+	+	+	+	+	+
H_2O_2 0.5 mM	-	-	+	+	+	-	-
Empagliflozin 100 nM	-	-	-	+	-	+	-
Empagliflozin 500 nM	-	-	-	-	+	-	+

Figure 5.2.b- GSH levels in the experimental LLC-PK1 treated cell lines (control vs HG30 and HG30/H_2O_2; HG30 vs HG30/Empa100 and HG30/Empa500; HG30/H_2O_2 vs HG30/ H_2O_2/Empa100 and HG30/H_2O_2/Empa500). GSH measurements were done by spectrophotometry at 415 nm. One-way ANOVA $F(6,47)=24.5,\ p=4.21\times10^{-12}$ with Tukey HSD post hoc test; The values are presented in micromol per milliliter as average with standard deviation ± SD. Bars assigned with asterisks are statistically significantly different *p<0.05, **p<0.01 ***p<0.001. Plus (+) sign indicates the addition of compounds and minus (−) sign lack of compounds in the experimental group compared to untreated control. The data shown are representative of at least three independent experiments. Cellular glutathione (GSH), pig proximal tubule cell line (LLC-PK1), HG (1.5 mM, 30 mM), H_2O_2 (0.5mM), Empagliflozin (100 nM, 500 nM).

5.3. Expression of *TGF-β1* in an LLC-PK1 cell culture model of diabetic nephropathy

TGF-β1 gene is related to inflammation and oxidative stress and plays an important role in the development of diabetic kidney disease**.** We performed an analysis of the regulated expression of TGF-β1 in LLC-PK1 cell culture model of diabetic nephropathy, as shown in Figure 5.3.a TGF-β1 mRNA expression, compared to untreated controls 24 h after treatment, as expected, was significantly higher in cells treated with 30 mM HG ($p<0.001$) while in cells treated with HG30/H_2O_2 difference was only numerical. TGF-β1 mRNA expression was significantly decreased in a combination of cells treated with Liraglutide 20 nM and HG30 compared to HG30 mM only ($p<0.001$). TGF-β1 expression was significantly decreased in cells treated with 10nM Liraglutide and HG30/H_2O_2 compared to cells treated with HG30/H_2O_2 ($p<0.001$). The addition of 20 nM Liraglutide to HG30/H_2O_2 treated cells had an insignificant effect on TGF-β1 mRNA expression compared to HG30/H_2O_2. Each experiment was repeated in minimal biological triplicate for consistency of the results.

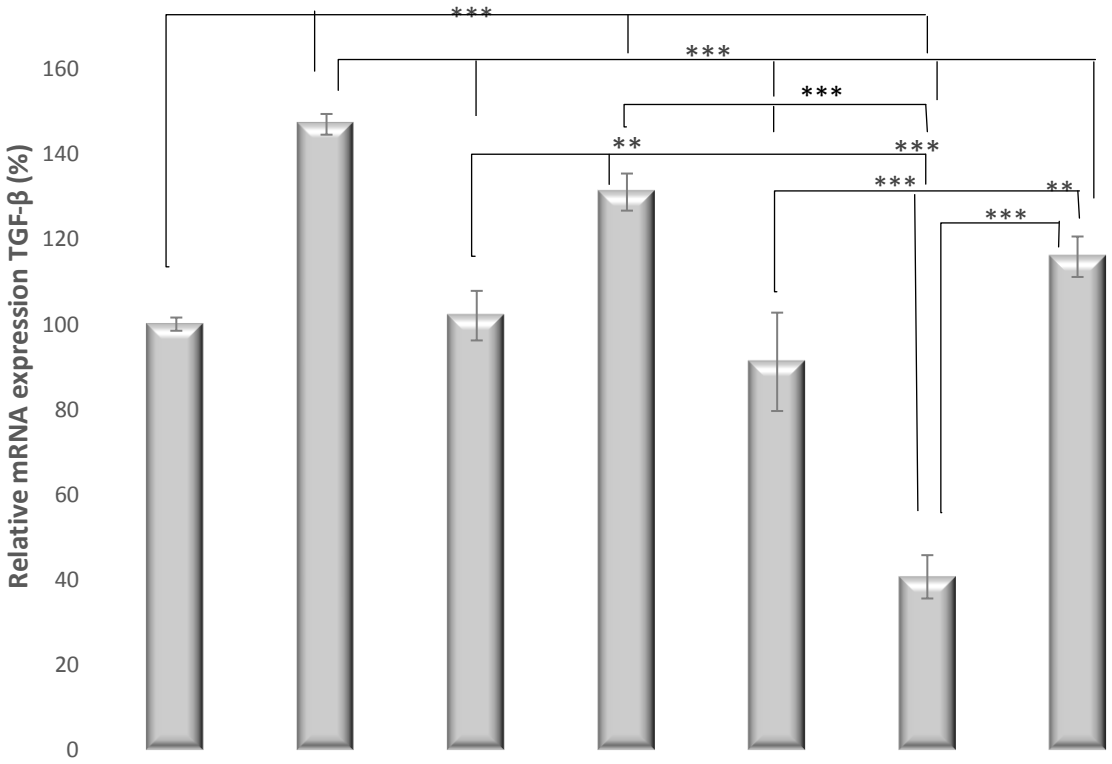

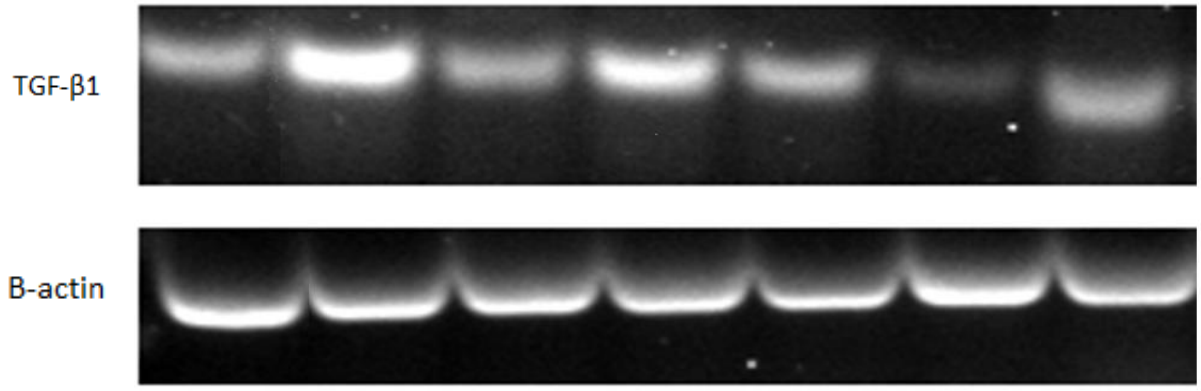

Glucose 30mM	-	+	+	+	+	+	+
H_2O_2 0.5 mM	-	-	+	-	-	+	+
Liraglutide 10nM	-	-	-	+	-	+	-
Liraglutide 20nM	-	-	-	-	+	-	+

Figure 5.3.a: **TGF-β1 gene in LLC-PK1 treated cell line** (control vs HG30 and HG30/H_2O_2; HG30 vs HG30/Lira10 and HG30/Lira20; HG30/H_2O_2 vs HG30/H_2O_2/Lira10 and HG30/H_2O_2/Lira20). **B**: Agarose gel electrophoresys images of TGF-β1 expression compared to β-actin expression. One-way ANOVA $F(7,23)=180.6,\ p=5.15\times10^{-14}$ with Tukey HSD post hoc test; **p<0.01, ***p<0.001 . The gene expression analysis was done by RT-PCR and obtained results were semi-quantified by ImageLab software. The values are represented as means ±SD. The data shown are representative of three independent experiments. *Transforming growth factor-beta* 1 (TGF-β1).

5.4. Measurement of protein expression in LLC-PK1 cell culture model of diabetic nephropathy

The protein expression levels of key regulators in diabetic nephropathy were further analyzed. The effects of glucose at different concentrations (1.5, 30 mM) and combination of glucose and H_2O_2 (30/0.5mM), a combination of glucose and Empagliflozin (30mM/100nM, 30/500nM) and a combination of glucose, H_2O_2 and Empagliflozin (30/0.5mM/100nM, 30/0.5mM/500nM) on the protein expression was examined using Western blot analysis.

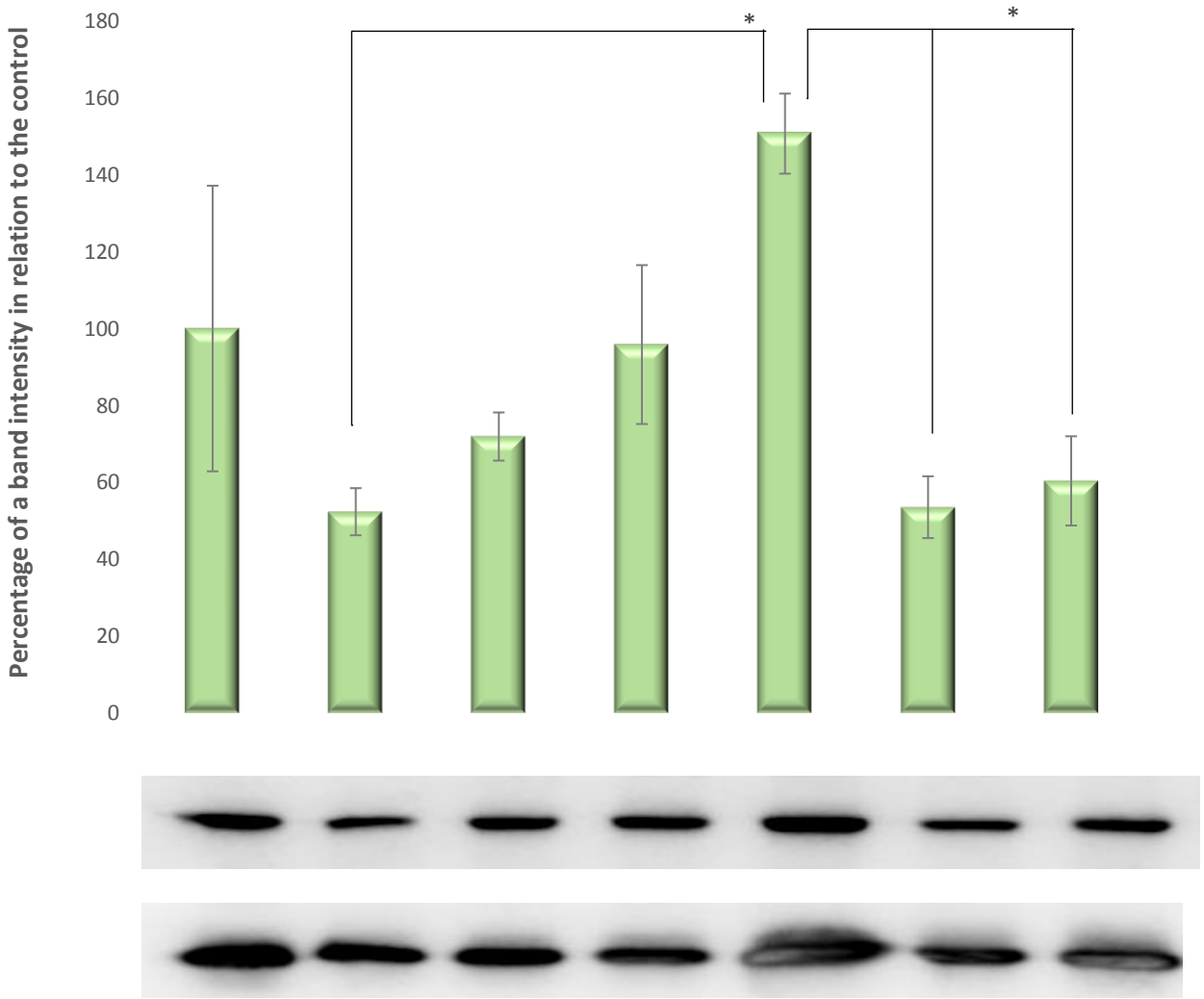

Glucose 30mM	-	+	+	+	+	+	+
H_2O_2 0.5 mM	-	-	+	+	+	-	-
Empagliflozin 100 nM	-	-	-	+	-	+	-
Empagliflozin 500 nM	-	-	-	-	+	-	+

Figure 5.4.a: **Protein expression p53 in LLC-PK1 treated cell line** (control vs HG30 and HG30/H_2O_2; HG30 vs HG30/Empa100 and HG30/Empa500; HG30/H_2O_2 vs HG30/ H_2O_2/Empa100 and HG30/H_2O_2/Empa500) determined by Western blot. Glyceraldehyde 3-phosphate dehydrogenase (GAPDH) was used as an internal control. The data are shown as the means ± SD (standard deviation) from three biological replicants. One-way ANOVA $F(6,20)=3.981,\ p=1.56\times10^{-2}$ with Tukey HSD post hoc test; *$p<0.05$; Plus (+) sign indicates the addition of compounds and minus (−) sign lack of compounds in the experimental group compared to untreated control. Western blot, pig proximal tubule cell line (LLC-PK1), HG (1.5 mM, 30 mM), H_2O_2 (0.5mM), Empagliflozin (100 nM, 500 nM).

In cells treated with HG30 and HG30/H2O2, there was no change in P53 protein compared to the control group. Only treatment with HG30/H2O2/Empa500 caused an increase in P53 protein expression relative to HG30/H2O2 and HG30/Empa100 and 500 treated group ($p<0.05$) as shown in Figure 5.4.a.

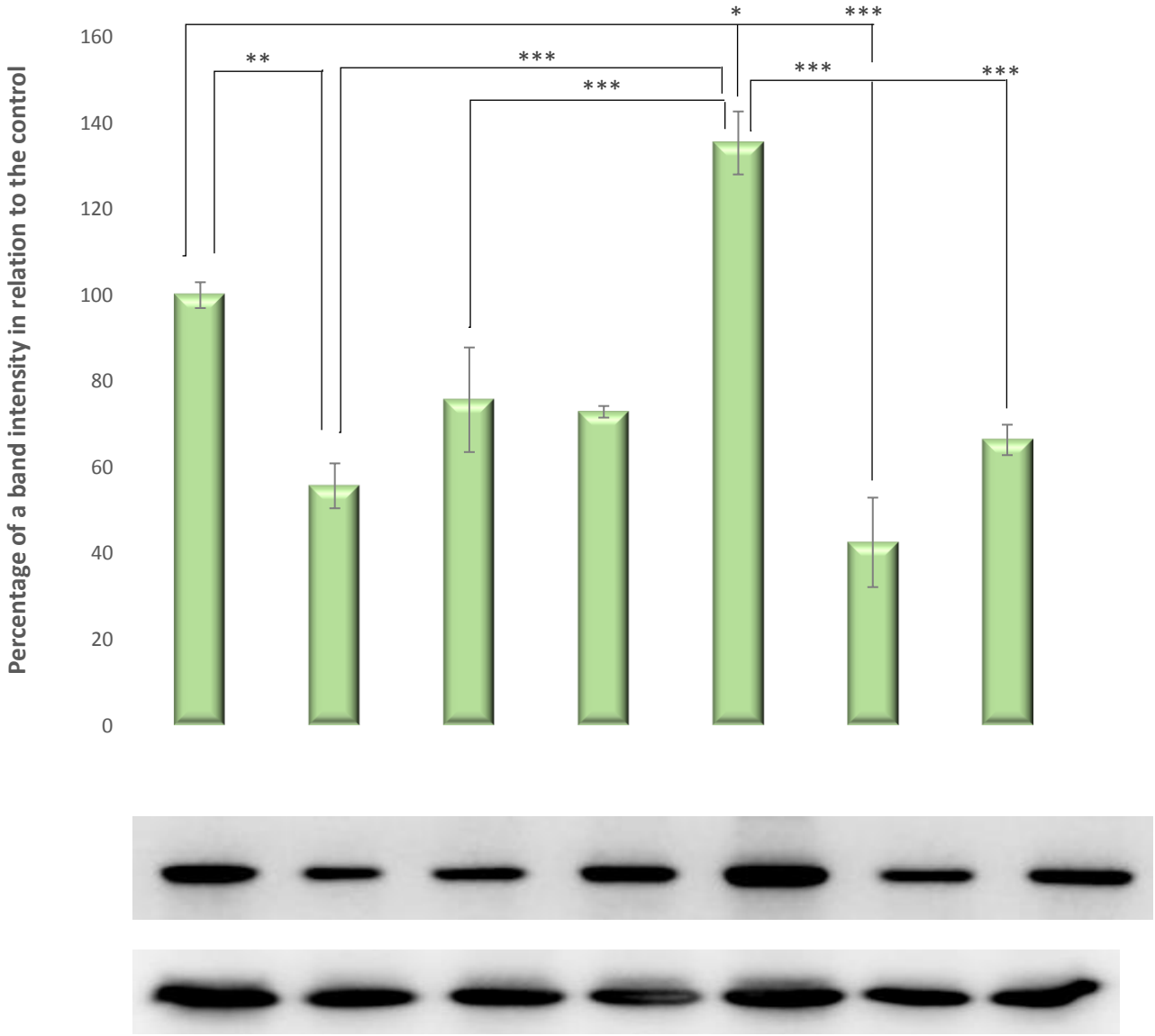

Figure 5.4.b: **Protein expression p-p 53 in LLC-PK1 treated cell line** (control vs HG30 and HG30/H_2O_2; HG30 vs HG30/Empa100 and HG30/Empa500; HG30/H_2O_2 vs HG30/ H_2O_2/Empa100 and HG30/H_2O_2/Empa500), determined by Western blot. Glyceraldehyde 3-

phosphate dehydrogenase (GAPDH) was used as an internal control. The data are shown as the means ± SD (standard deviation) from three biological replicants. One-way ANOVA $F(6,20)=18.46,\ p=6.56\times10^{-6}$ with Tukey HSD post hoc test; *p<0.05, **p<0.01; ***p<0.001. Plus (+) sign indicates the addition of compounds and minus (−) sign lack of compounds in the experimental group compared to untreated control. Western blot, pig proximal tubule cell line (LLC-PK1), HG (1.5 mM, 30 mM), H_2O_2 (0.5mM), Empagliflozin (100 nM, 500 nM).

In cells treated with HG30 ($p<0.01$) pP53 levels were decreased, while in cells treated with HG30/H2O2 there was no change compared to the control group. Only treatment with HG30/H2O2/Empa500 caused an increase in pP53 protein expression relative to all groups ($p<0.05$; $p<0.001$) as shown in Figure 5.4.b.

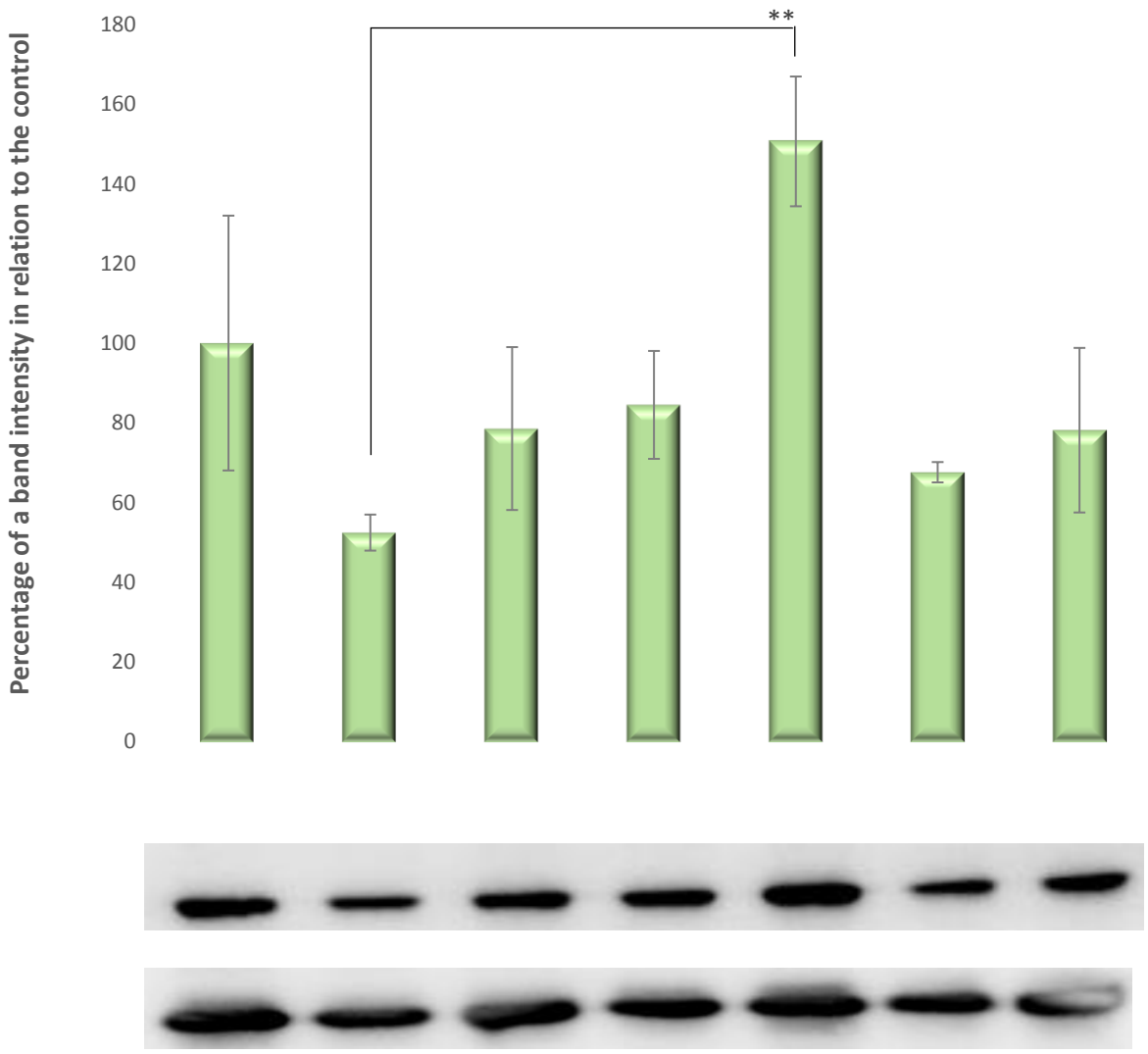

Glucose 30mM	-	+	+	+	+	+	+
H_2O_2 0.5 mM	-	-	+	+	+	-	-
Empagliflozin 100 nM	-	-	-	+	-	+	-
Empagliflozin 500 nM	-	-	-	-	+	-	+

Figure 5.4.c: **Protein expression PPARy in LLC-PK1 treated cell** (control vs HG30 and HG30/H_2O_2; HG30 vs HG30/Empa100 and HG30/Empa500; HG30/H_2O_2 vs HG30/H_2O_2/Empa100 and HG30/H_2O_2/Empa500), determined by Western blot.

Glyceraldehyde 3-phosphate dehydrogenase (GAPDH) was used as an internal control. The data are shown as the means ± SD (standard deviation) from three biological replicants. One-way ANOVA $F(6,20)=2.96,\ p=4.44\times10^{-2}$ with Tukey HSD post hoc test; **p<0.01. Plus (+) sign indicates the addition of compounds and minus (−) sign lack of compounds in the experimental group compared to untreated control. Western blot, pig proximal tubule cell line (LLC-PK1), HG (1.5 mM, 30 mM), H_2O_2 (0.5mM), Empagliflozin (100 nM, 500 nM).

A trend in the decrease of PPARG levels compared to control was observed in HG30 and HG30/H2O2-treated cells, however, the difference was not statistically significant. The effect on PPARG protein levels was more pronounced in HG30/H2O2 cells where Empagliflozin 500 was added relative to HG30 only treated cells ($p<0.01$) as shown in Figure 5.4.c.

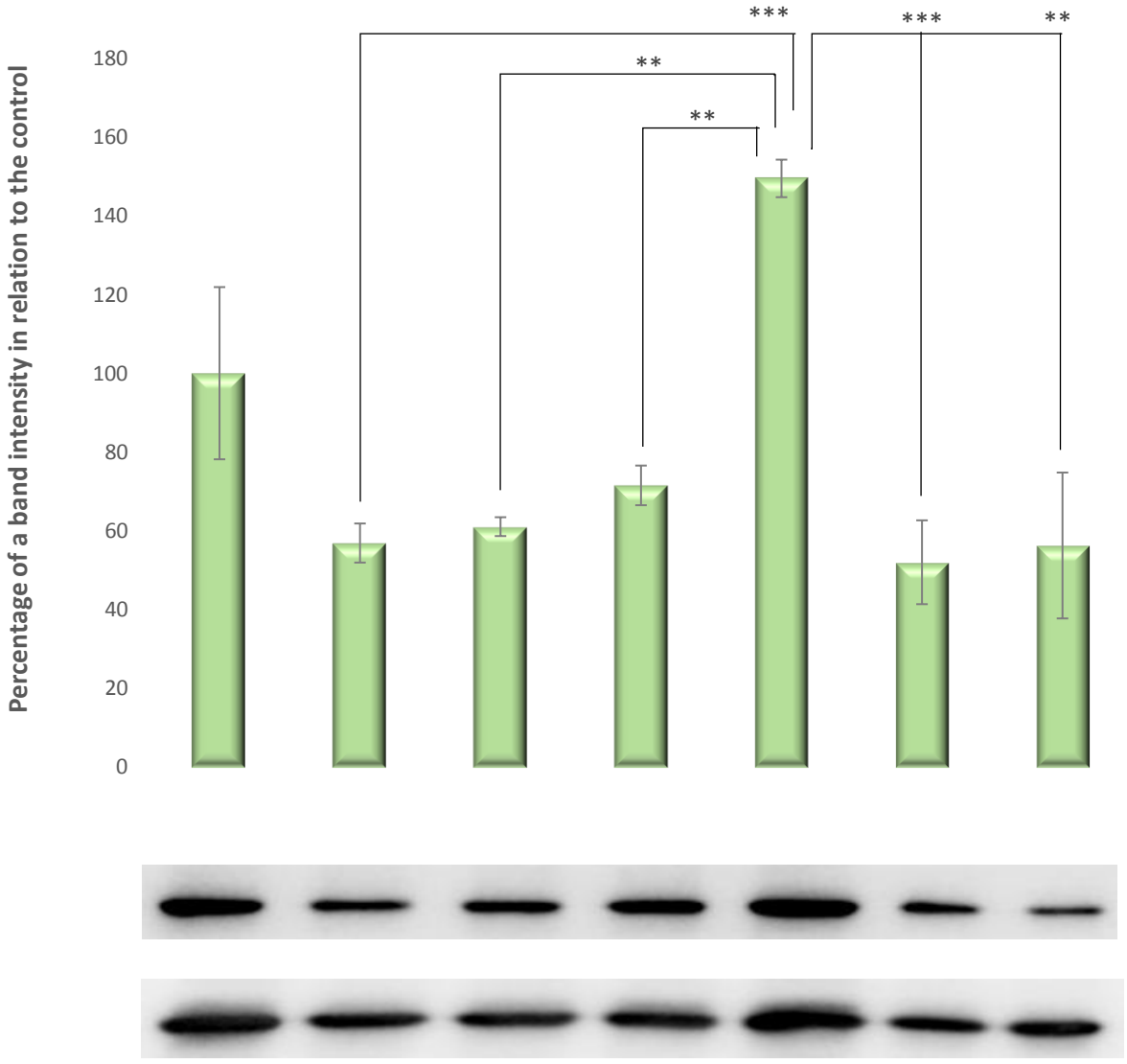

Glucose 30mM	-	+	+	+	+	+	+
H_2O_2 0.5 mM	-	-	+	+	+	-	-
Empagliflozin 100 nM	-	-	-	+	-	+	-
Empagliflozin 500 nM	-	-	-	-	+	-	+

Figure 5.4.d: **Protein expression p-STAT3 in LLC-PK1 treated cell line** (control vs HG30 and HG30/H_2O_2; HG30 vs HG30/Empa100 and HG30/Empa500; HG30/H_2O_2 vs HG30/ H_2O_2/Empa100 and HG30/H_2O_2/Empa500), determined by Western blot. Glyceraldehyde 3-phosphate dehydrogenase (GAPDH) was used as an internal control. The data are shown as

the means ± SD (standard deviation) from three biological replicants. One-way ANOVA $F(6,20)=8.659,\ p=4.64\times10^{-4}$ with Tukey HSD post hoc test; **p<0.01; ***p<0.001. Plus (+) sign indicates the addition of compounds and minus (−) sign lack of compounds in the experimental group compared to untreated control. Western blot, pig proximal tubule cell line (LLC-PK1), HG (1.5 mM, 30 mM), H_2O_2 (0.5mM), Empagliflozin (100 nM, 500 nM).

The level of pSTAT3 protein in HG30 and HG30/H202 treated cells remained unchanged relative to the control group. Treatment with HG30 / H202 / Empa500 increased STAT 3 levels significantly compared to all groups except control (p <0.01; p<0.001) as shown in Figure 5.4 d.

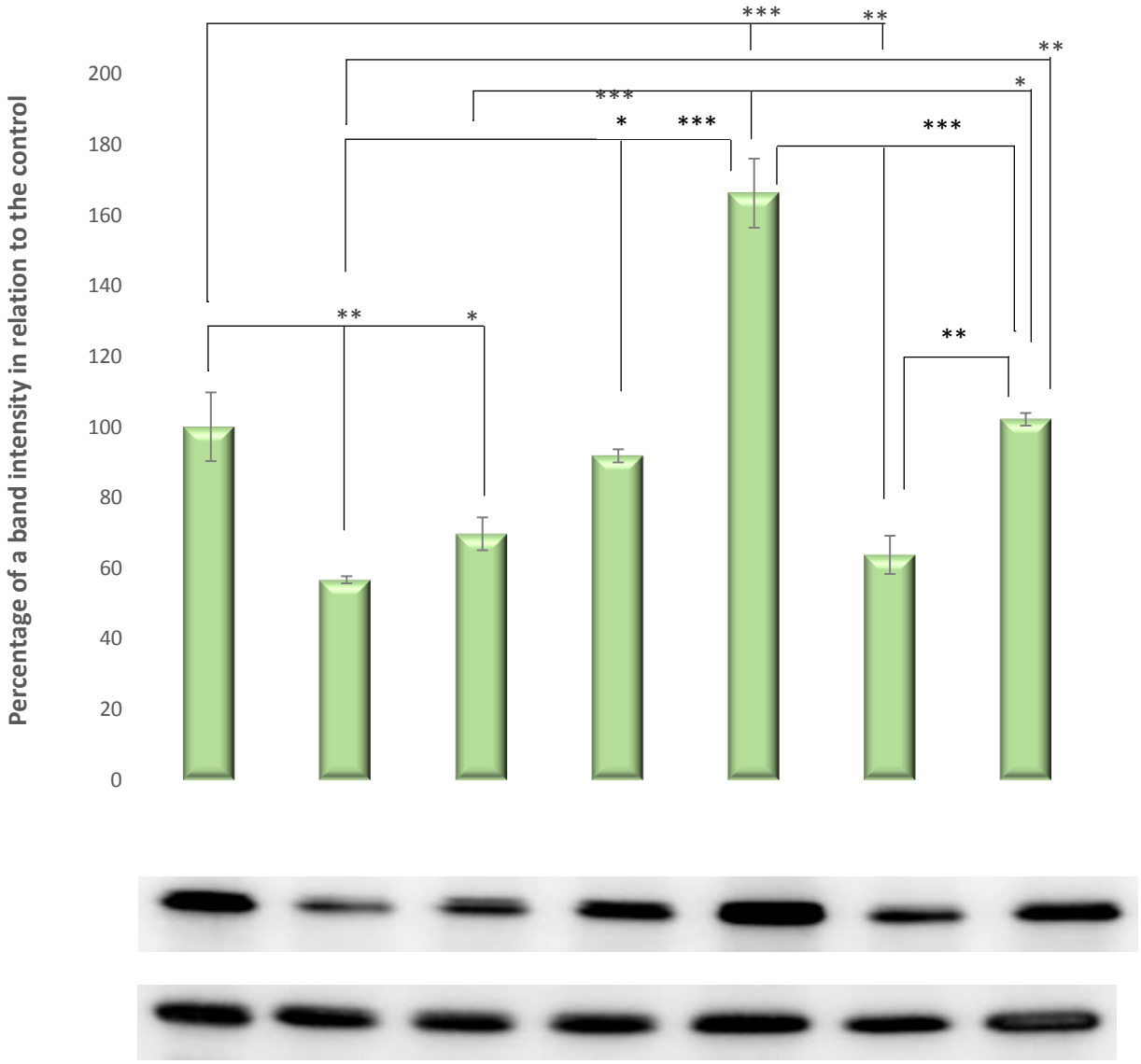

Glucose 30mM	-	+	+	+	+	+	+
H_2O_2 0.5 mM	-	-	+	+	+	-	-
Empagliflozin 100 nM	-	-	-	+	-	+	-
Empagliflozin 500 nM	-	-	-	-	+	-	+

Figure 5.4.e: Protein expression p-GSK3β in LLC-PK1 treated cell line (control vs HG30 and HG30/H_2O_2; HG30 vs HG30/Empa100 and HG30/Empa500; HG30/H_2O_2 vs HG30/ H_2O_2/Empa100 and HG30/H_2O_2/Empa500), determined by Western blot. Glyceraldehyde 3-phosphate dehydrogenase (GAPDH) was used as an internal control. The data are shown as

the means ± SD (standard deviation) from three biological replicants. One-way ANOVA $F(6,20)=38.49$, $p=6.48\times10^{-8}$ with Tukey HSD post hoc test; *p<0.05, **p<0.01; ***p<0.001. Plus (+) sign indicates the addition of compounds and minus (−) sign lack of compounds in the experimental group compared to untreated control. Western blot, pig proximal tubule cell line (LLC-PK1), HG (1.5 mM, 30 mM), H_2O_2 (0.5mM), Empagliflozin (100 nM, 500 nM).

A significant decrease in the p-GSK3β protein level was observed in cells treated with HG30 and HG30/H202 compared to the control ($p < 0.01$; $p < 0.05$). In addition, in the cells treated with HG30/H2O2/Empa500 protein expression was significantly increased compared to all groups ($p<0.05$; $p < 0.001$). Significantly increased protein expression relative to HG30 ($p < 0.01$) was observed in HG30 cells treated with Empa 500 as shown in Figure 5. 4.e.

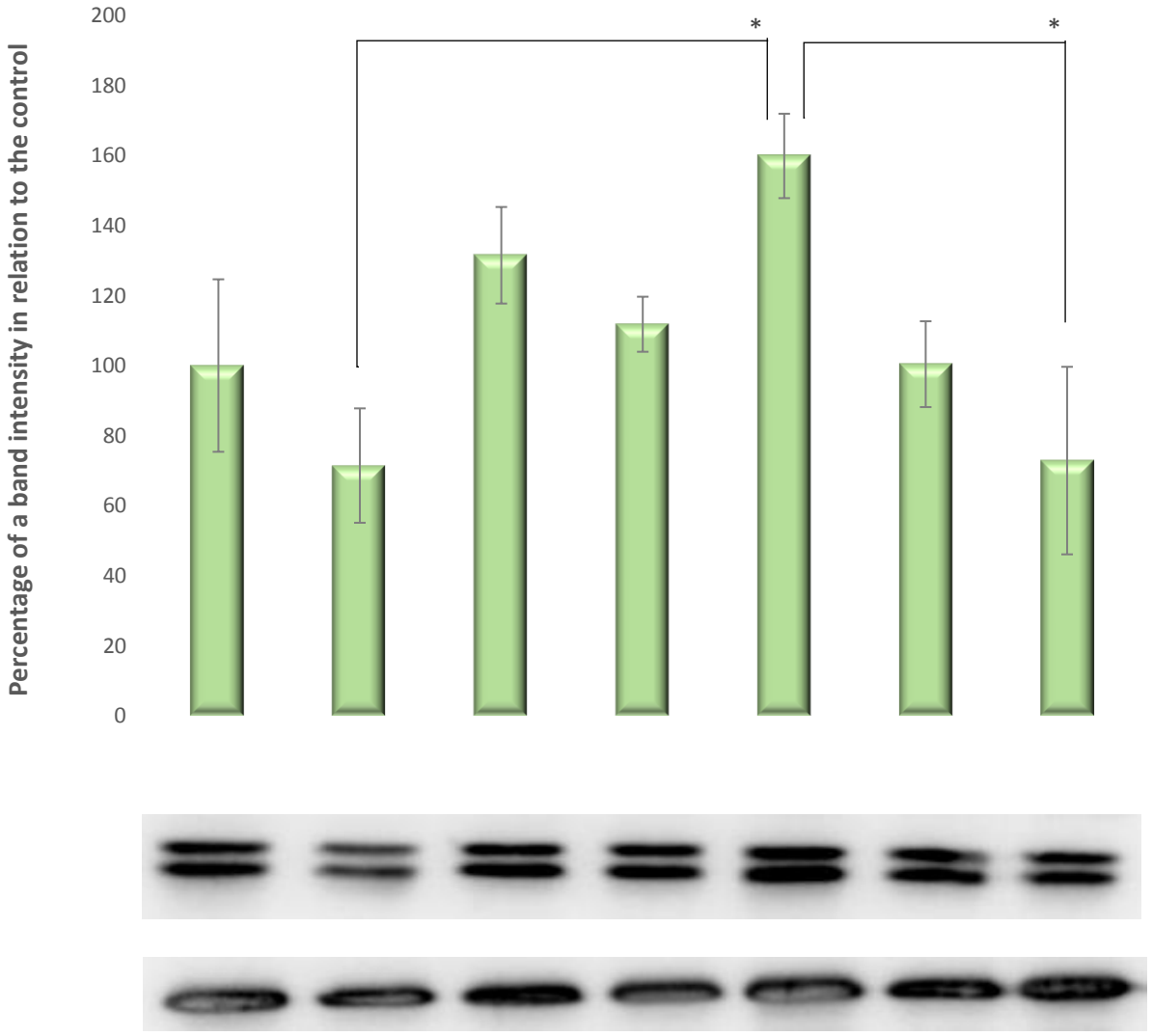

Glucose 30mM	-	+	+	+	+	+	+
H_2O_2 0.5 mM	-	-	+	+	+	-	-
Empagliflozin 100 nM	-	-	-	+	-	+	-
Empagliflozin 500 nM	-	-	-	-	+	-	+

Figure 5.4.f: Protein expression GSK3β in LLC-PK1 treated cell line (control vs HG30 and HG30/H_2O_2; HG30 vs HG30/Empa100 and HG30/Empa500; HG30/H_2O_2 vs HG30/ H_2O_2/Empa100 and HG30/H_2O_2/Empa500), determined by Western blot. Glyceraldehyde 3-phosphate dehydrogenase (GAPDH) was used as an internal control. The data are shown as

the means ± SD (standard deviation) from three biological replicants. One-way ANOVA $F(6,20)=3.241,\ p=3.27\times10^{-2}$ with Tukey HSD post hoc test; *$p<0.05$. Plus (+) sign indicates the addition of compounds and minus (−) sign lack of compounds in the experimental group compared to untreated control. Western blot, pig proximal tubule cell line (LLC-PK1), HG (1.5 mM, 30 mM), H_2O_2 (0.5mM), Empagliflozin (100 nM, 500 nM).

A slight increase in **GSK3β** protein levels was demonstrated in HG30/H2O2 treated cells compared to the control not reaching statistical significance. GSK3 Beta protein levels were increased in cells treated with HG30/H2O2/Empa500 compared to the HG30, HG30/Empa 500 ($p<0.05$) as shown in Figure 5.4.f.

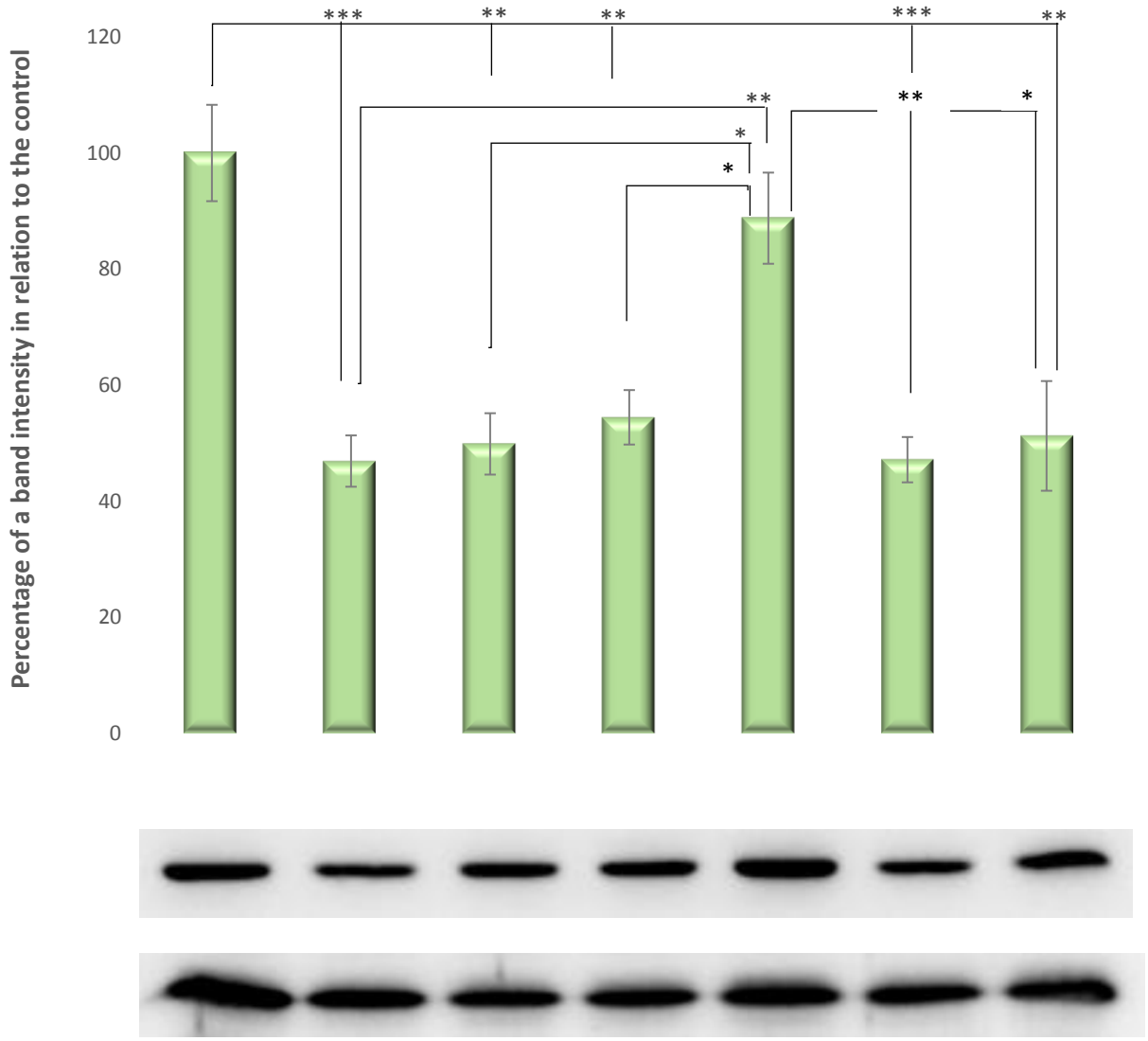

Glucose 30mM	-	+	+	+	+	+	+
H_2O_2 0.5 mM	-	-	+	+	+	-	-
Empagliflozin 100 nM	-	-	-	+	-	+	-
Empagliflozin 500 nM	-	-	-	-	+	-	+

Figure 5.4.g: Protein expression SMAD7 in LLC-PK1 treated cell line (control vs HG30 and HG30/H_2O_2; HG30 vs HG30/Empa100 and HG30/Empa500; HG30/H_2O_2 vs HG30/ H_2O_2/Empa100 and HG30/H_2O_2/Empa500), determined by Western blot. Glyceraldehyde 3-

phosphate dehydrogenase (GAPDH) was used as an internal control. The data are shown as the means ± SD (standard deviation) from three biological replicants. One-way ANOVA $F(6,20)=11.2,\ p=1.18\times10^{-4}$ with Tukey HSD post hoc test; *p<0.05, **p<0.01; *** p <0.001. Statistical significance was tested with one-way ANOVA. Plus (+) sign indicates the addition of compounds and minus (−) sign lack of compounds in the experimental group compared to untreated control. Western blot, pig proximal tubule cell line (LLC-PK1), HG (1.5 mM, 30 mM), H_2O_2 (0.5mM), Empagliflozin (100 nM, 500 nM).

A significant decrease in SMAD 7 protein expression was observed in HG30 and HG30 / H2O2-treated cells compared to the control (p <0.001; p <0.01). Protein levels were also increased in cells treated with Empa 500 with HG30 / H2O2 compared to all groups except control (p <0.05; p<0.01). Cells treated with HG30/Empa100 and 500 showed a slight increase in protein compared to HG30 alone, not reaching statistical significance as shown in Figure 5.4.g.

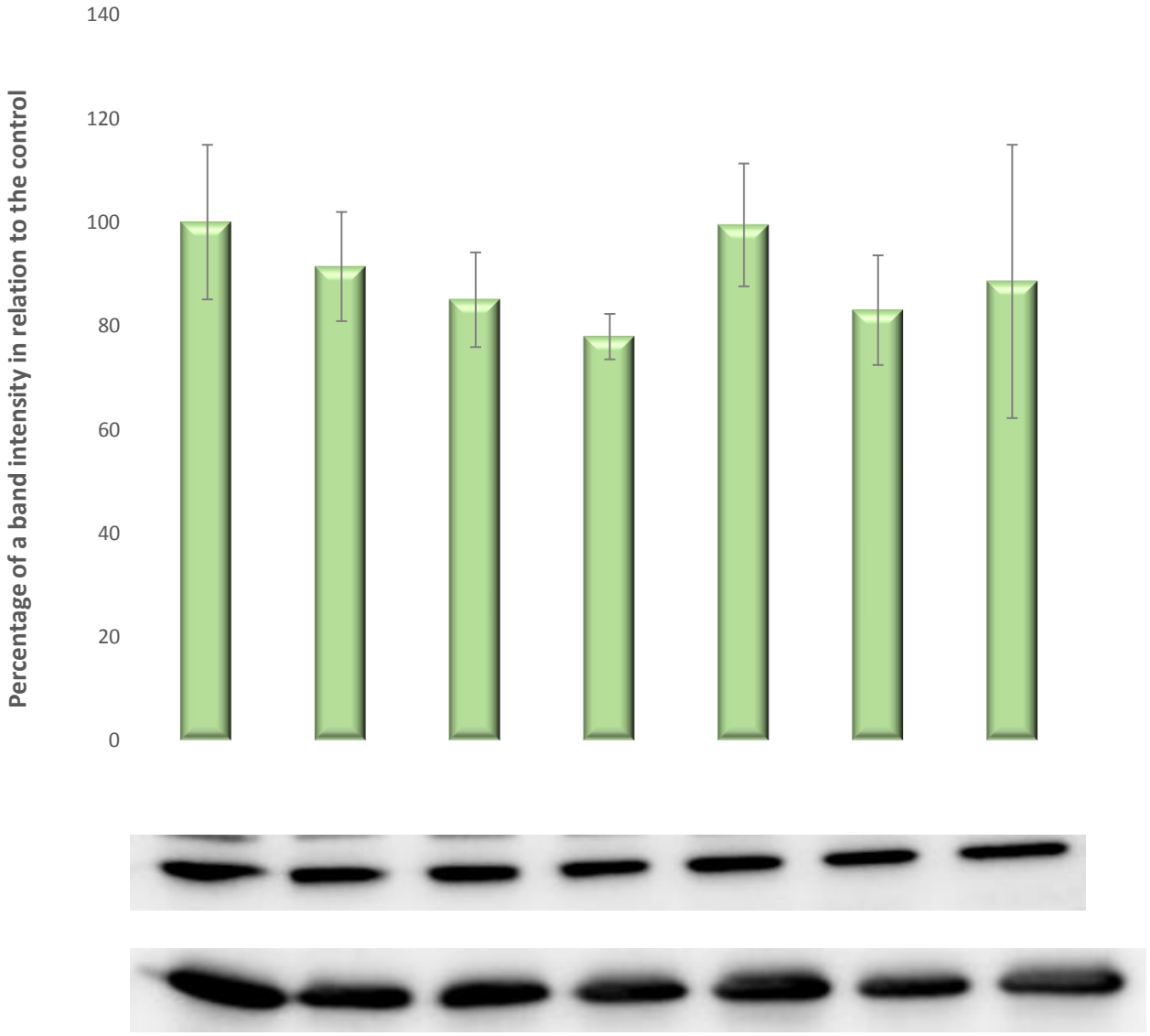

Glucose 30mM	-	+	+	+	+	+	+
H_2O_2 0.5 mM	-	-	+	+	+	-	-
Empagliflozin 100 nM	-	-	-	+	-	+	-
Empagliflozin 500 nM	-	-	-	-	+	-	+

Figure 5.4.h: Protein expression AKT in LLC-PK1 treated cell line (control vs HG30 and HG30/H_2O_2; HG30 vs HG30/Empa100 and HG30/Empa500; HG30/H_2O_2 vs HG30/

H_2O_2/Empa100 and HG30/H_2O_2/Empa500), determined by Western blot. Glyceraldehyde 3-phosphate dehydrogenase (GAPDH) was used as an internal control. The data are shown as the means ± SD (standard deviation) from three biological replicants. One-way ANOVA $F(6,20)=0.35$, $p=9.1\times10^{-1}$ with Tukey HSD post hoc test. Statistical significance was tested with one-way ANOVA. Plus (+) sign indicates the addition of compounds and minus (−) sign lack of compounds in the experimental group compared to untreated control. Western blot, pig proximal tubule cell line (LLC-PK1), HG (1.5 mM, 30 mM), H_2O_2 (0.5mM), Empagliflozin (100 nM, 500 nM).

Compared to control, there was no significant change in AKT expression across all experimental groups as shown in Figure 5.4.h.

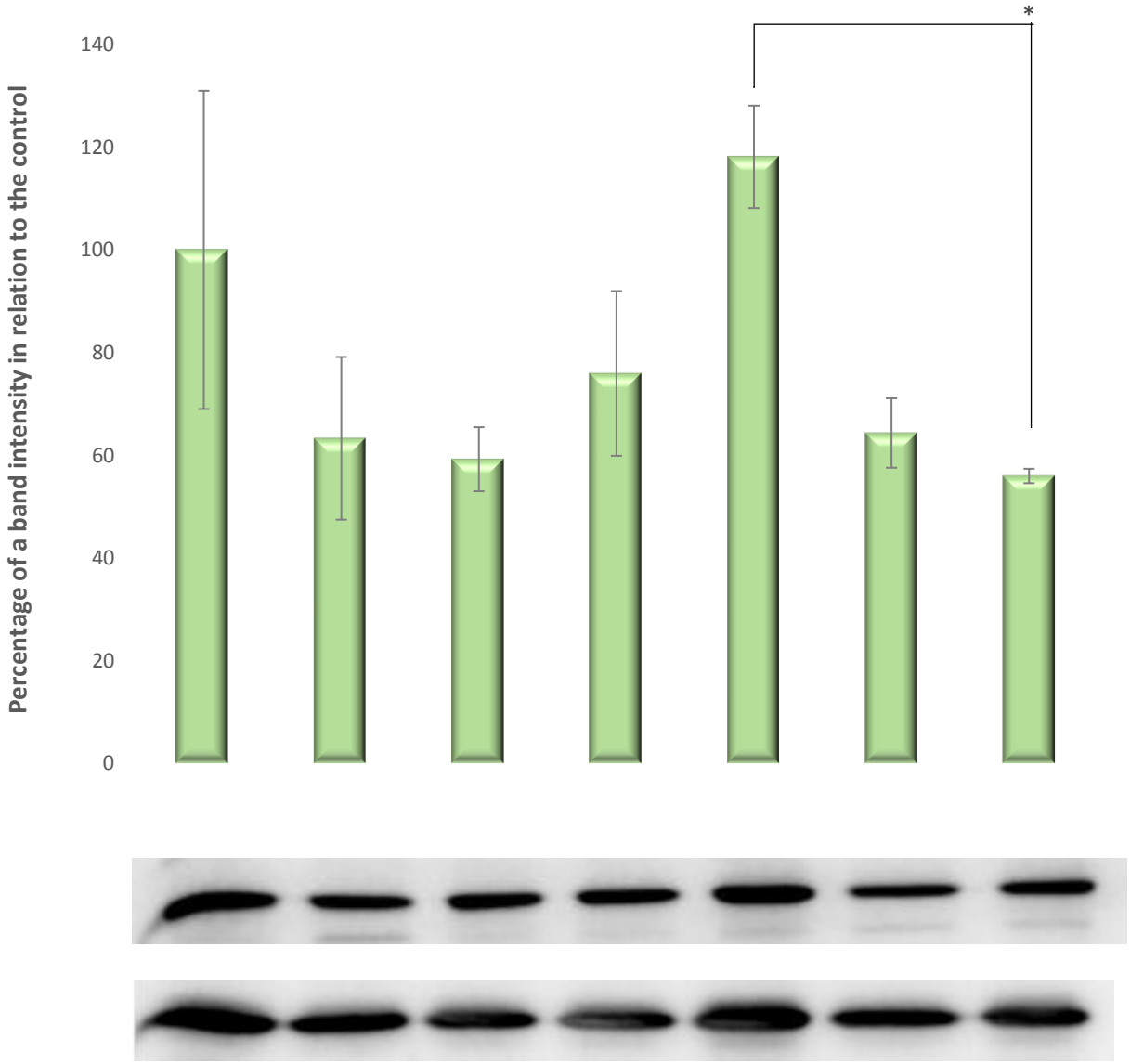

Glucose 30mM	-	+	+	+	+	+	+
H_2O_2 0.5 mM	-	-	+	+	+	-	-
Empagliflozin 100 nM	-	-	-	+	-	+	-
Empagliflozin 500 nM	-	-	-	-	+	-	+

Figure 5.4.i: Protein expression pAKT in LLC-PK1 treated cell line (control vs HG30 and HG30/H_2O_2; HG30 vs HG30/Empa100 and HG30/Empa500; HG30/H_2O_2 vs HG30/

H_2O_2/Empa100 and HG30/H_2O_2/Empa500), determined by Western blot. Glyceraldehyde 3-phosphate dehydrogenase (GAPDH) was used as an internal control. The data are shown as the means ± SD (standard deviation) from three biological replicants. One-way ANOVA $F(6,19)=3.349,\ p=3.21\times10^{-2}$ with Tukey HSD post hoc test; *$p<0.05$. Plus (+) sign indicates the addition of compounds and minus (−) sign lack of compounds in the experimental group compared to untreated control. Western blot, pig proximal tubule cell line (LLC-PK1), HG (1.5 mM, 30 mM), H_2O_2 (0.5mM), Empagliflozin (100 nM, 500 nM).

There was no change in pAKT protein expression in HG30 and HG30/H2O2 treated cells relative to the control. There was a statistically significant decrease of pAKT levels in cells treated HG30 / H2O2/ Empa 500 compared with cells exposed to HG30/Empa500 ($p<0.05$) as shown in Figure 5.4.i.

5.5. Measurement of TGF-β1 levels in a cell culture model of diabetic nephropathy

As expected, TGF-β1 levels were significantly increased in HG30 and HG30/ H_2O_2 treated cells compared to the untreated control ($p<0.001$ for all). Moreover, the addition of Liraglutide in both concentrations (10 and 20 nM) significantly decreased TGF-β1 levels in both, HG30 ($p<0.01$ for all) and HG30/ H_2O_2 ($p<0.05$ for all) treated cells. The results are shown in Figure 5.5.a.

In the second set of the experiments, treatment with HG30/ H_2O_2 led to a significant increase of TGF-β1 levels ($p<0.001$). On the other hand, treatment with HG30 increased TGF-β1 concentrations but the difference was not statistically significant. The addition of Empagliflozin in both concentrations led to a significant decrease of TGF-β1 levels when added to HG30/ H_2O_2 treated cells ($p<0.001$ for all). An insignificant increase was noted with the addition of both concentrations of Empagliflozin to HG30 treated cells. Each experiment was repeated in minimal biological triplicate for consistency of the results. The results are shown in Figure 5.5.b.

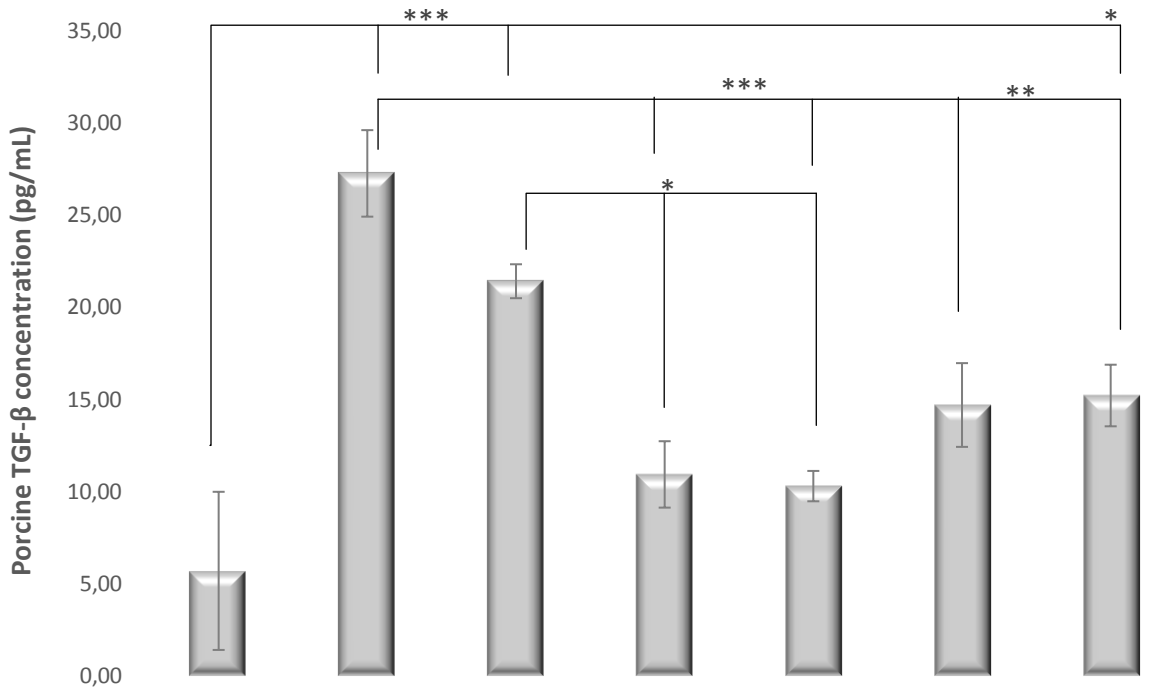

Glucose 30mM	-	+	+	+	+	+	+
H_2O_2 0.5 mM	-	-	+	+	+	-	-
Liraglutide 10nM	-	-	-	+	-	+	-
Liraglutide 20nM	-	-	-	-	+	-	+

Figure 5.5.a: Levels of TGF-β concentrations in the experimental LLCPK1 treated cell lines (control vs HG30 and HG30/H_2O_2; HG30 vs HG30/Lira10 and HG30/Lira20; HG30/H_2O_2 vs HG30/H_2O_2/Lira10 and HG30/H_2O_2/Lira20). TGF-β measurements were done by spectrophotometry at 450 nm. One-way ANOVA $_{F(7,23)=14.54,\ p=7.47\times10^{-6}}$ with Tukey HSD post hoc test; *p<0.05, **p<0.01, ***p<0.001. The values are represented in picogram per milliliter as average with standard deviation ± SD. Plus (+) sign indicates the addition of compounds and minus (−) sign lack of compounds in the experimental group compared to untreated control. The data shown are representative of at least three independent experiments TGF-β elisa, pig proximal tubule cell line (LLC-PK1), HG (1.5 mM, 30 mM), H_2O_2 (0.5mM), Liraglutide (10 nM, 20 nM).

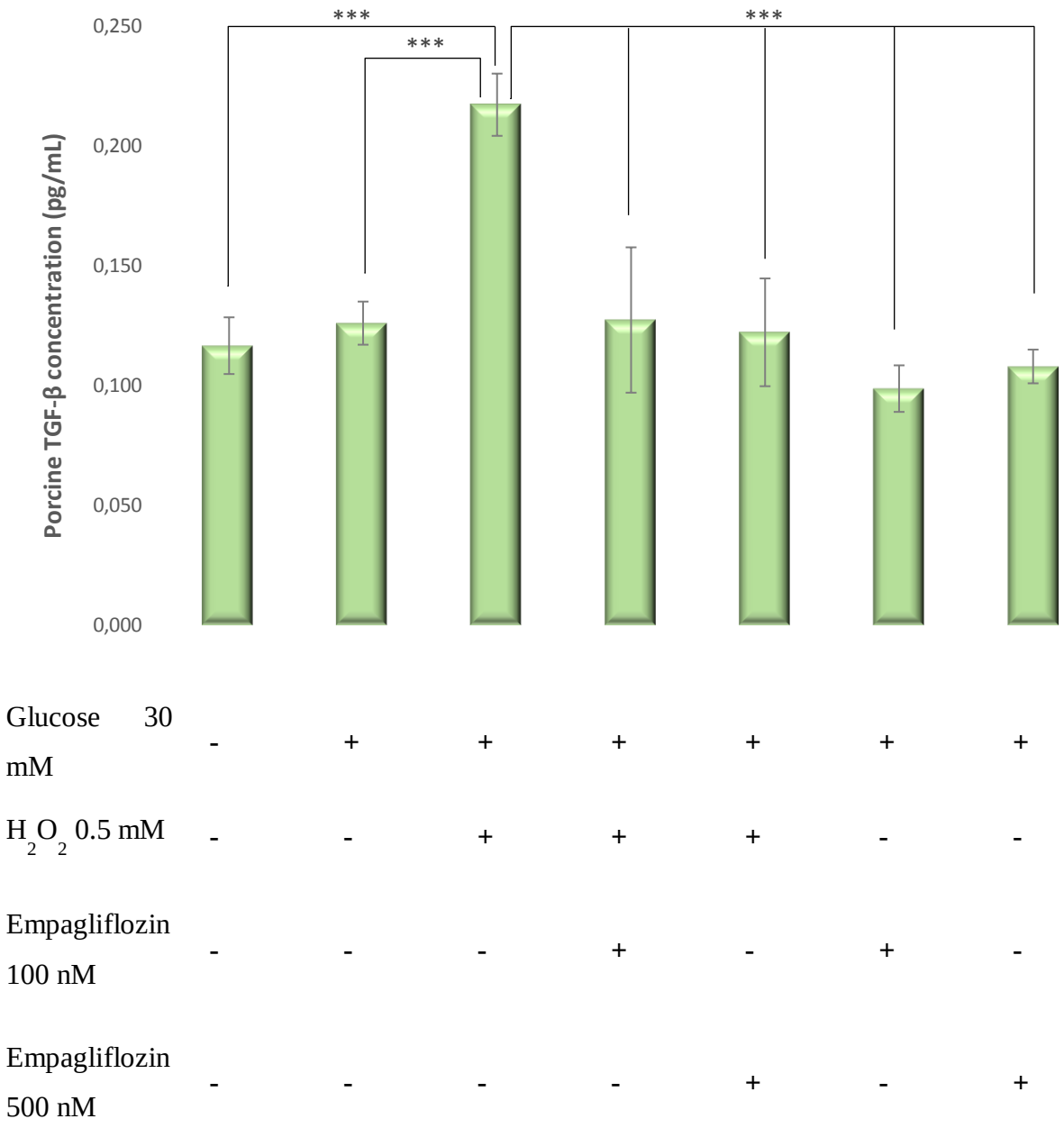

Figure 5.5.b: Levels of TGF-β concentrations from treated LLCPK1 cell lines (control vs HG30 and HG30/H_2O_2; HG30 vs HG30/Empa100 and HG30/Empa500; HG30/H_2O_2 vs HG30/ H_2O_2/Empa100 and HG30/H_2O_2/Empa500). TGF-β measurements were done by spectrophotometry at 450 nm. One-way ANOVA $_{F(6,36)=19.50,\ p=3.9\times10^{-9}}$ with Tukey HSD post hoc test; ***p<0.001. The values are represented in picogram per milliliter as average with standard deviation ± SD. Plus (+) sign indicates the addition of compounds and minus (−) sign lack of compounds in the experimental group compared to untreated control. The data shown are representative of at least three independent experiments TGF-β elisa, pig proximal tubule cell line (LLC-PK1), HG (1.5 mM, 30 mM), H_2O_2 (0.5mM), Empagliflozin (100 nM, 500 nM)

. 5.6. Measurement of ECM expression in a cell culture model of diabetic nephropathy

Synthesis of collagen was significantly increased in HG30/ H_2O_2 ($p<0.001$) treated cells when compared to control, while the addition of Liraglutide in both concentrations (10 nM and 20 nM) significantly decreased collagen concentrations compared to HG30/H2O2 treated cells ($p<0.001$ for all). Treatment with HG30 did not change the synthesis of collagen compared to control. The addition of Liraglutide 20 nM in cells treated with HG30 only, unexpectedly, significantly increased collagen synthesis compared to cells treated with HG30 only ($p<0.01$) while the same effect was observed with the addition of 10 nM of Liraglutide but the difference was not statistically significant as shown in Figure 5.6.a.

In the second set of experiments, the addition of HG30 and HG30/ H_2O_2 led to an insignificant decrease in collagen synthesis compared to control. Empagliflozin in 500 nM caused a slight increase in collagen synthesis when added to HG30/ H_2O_2 treated cells (p=NS) while the addition of 100 nM of Empagliflozin had no effect. The addition of 500 nM of Empagliflozin significantly increased collagen synthesis in cells treated with HG30 compared to cells treated with HG30 only ($p<0.01$), however the addition of 100nM of Empagliflozin had no effect. as shown in Figure 5.6.b. Each experiment was repeated in minimal biological triplicate for consistency of the results.

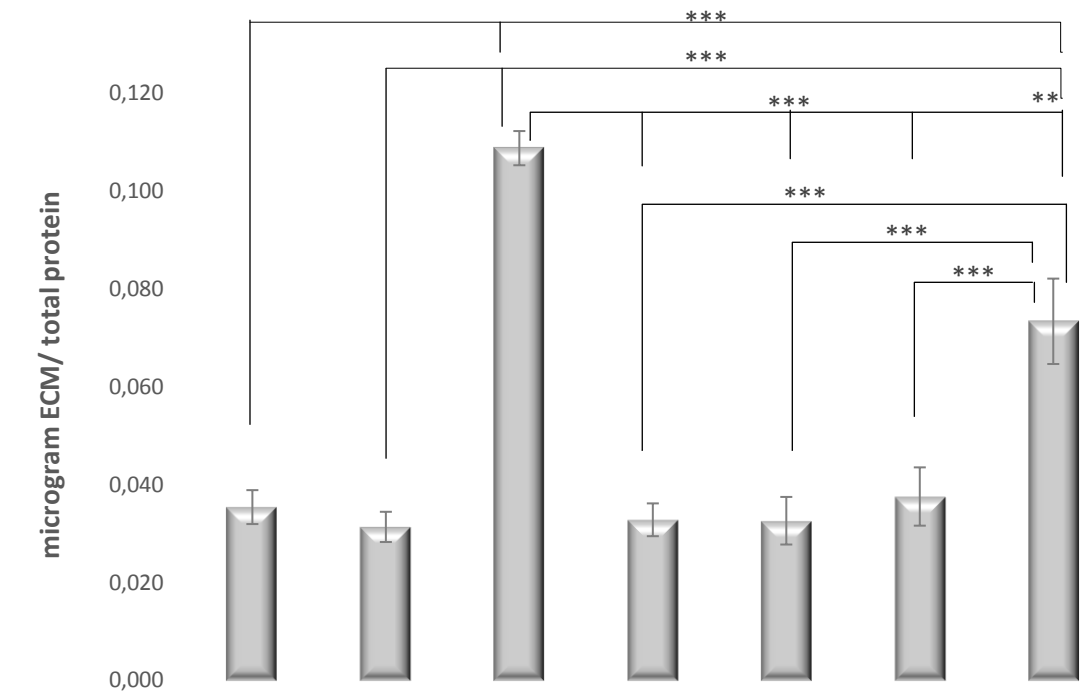

Glucose 30mM	-	+	+	+	+	+	+
H_2O_2 0.5 mM	-	-	+	+	+	-	-
Liraglutide 10nM	-	-	-	+	-	+	-
Liraglutide 20nM	-	-	-	-	+	-	+

Figure 5.6.a: Levels of collagen synthesis in experimental LLC-PK1 treated cell lines (control vs HG30 and HG30/H_2O_2; HG30 vs HG30/Lira10 and HG30/Lira20; HG30/H_2O_2 vs HG30/ H_2O_2/Lira10 and HG30/H_2O_2/Lira20). ECM measurements were done by spectrophotometry at 595 nm. One-way ANOVA $_{F(9,26)=49.73,\ p=1.6\times10^{-6}}$ with Tukey HSD post hoc test; *p<0.05, **p<0.01, ***p<0.001. The values are represented in microgram ECM per total protein as average with standard deviation ± SD. Plus (+) sign indicates the addition of compounds and minus (−) sign lack of compounds in the experimental group compared to untreated control. The data shown are representative of at least three independent experiments ECM measurement, pig proximal tubule cell line (LLC-PK1), HG (1.5 mM, 30 mM), H_2O_2 (0.5mM), Liraglutide (10 nM, 20 nM).

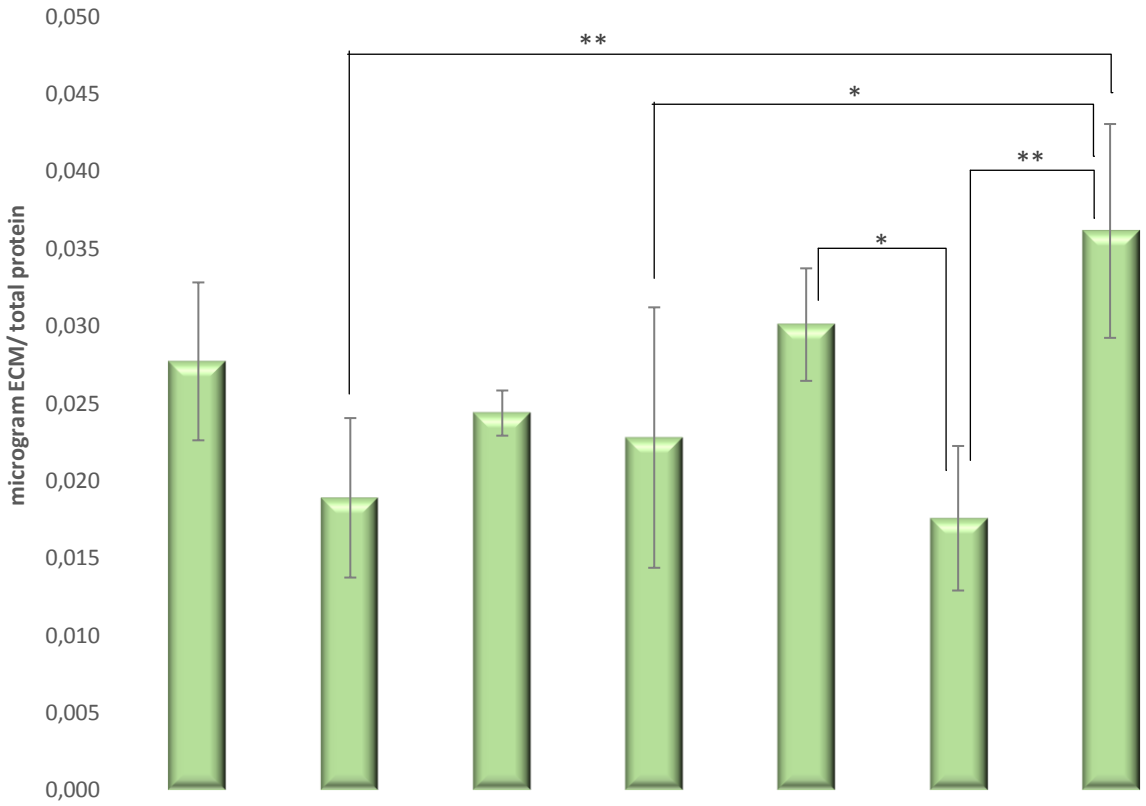

Glucose 30 mM	-	+	+	+	+	+	+
H_2O_2 0.5 mM	-	-	+	+	+	-	-
Empagliflozin 100 nM	-	-	-	+	-	+	-
Empagliflozin 500 nM	-	-	-	-	+	-	+

Figure 5.6.b: Levels of collagen synthesis in treated LLC-PK1 cell lines (control vs HG30 and HG30/H_2O_2; HG30 vs HG30/Empa100 and HG30/Empa500; HG30/H_2O_2 vs HG30/ H_2O_2/Empa100 and HG30/H_2O_2/Empa500). ECM measurements were done by spectrophotometry at 595 nm. One-way ANOVA $_{F(8,79)=4.337,\ p=2.571\times10^{-2}}$ with Tukey HSD post hoc test; *p<0.05, **p<0.01, ***p<0.001. The values are represented in microgram ECM per

total protein as average with standard deviation ± SD. Plus (+) sign indicates the addition of compounds and minus (−) sign lack of compounds in the experimental group compared to untreated control. The data shown are representative of at least three independent experiments ECM measurement, pig proximal tubule cell line (LLC-PK1), HG (1.5 mM, 30 mM), H_2O_2 (0.5mM), Empagliflozin (100 nM, 500 nM).

5.7. Visualization and quantification of the F-actin cytoskelet with Rhodamine Phalloidin stain in a cell culture model of diabetic nephropathy

Distribution and deformation of the F-actin cytoskeleton are involved in the epithelial cells damage. A significant reduction in the amount of F-actin was observed in cells treated with HG30/H_2O_2 ($p<0.01$), yet no difference was present in HG30 treated cells compared to control as shown in Figure 7 A, B. The addition of Liraglutide 10 and 20 nM to HG30 led to a significant decrease in the amount of F-actin compared to cells cultured with HG30 ($p<0.001$ for all). In the HG30/H_2O_2 treated cells addition of Liraglutide 10 nM caused a significant decline of the actin amount, yet 20nM Liraglutide had no impact. The results are shown in Figure 5.7.a.

In the Empagliflozine set of experiments, a significant decrease in the total amount of actin in LLC-PK1 cells treated with HG30 only was observed, while no change was present with the addition of HG30/H2O2. The addition of 100 and 500 nM of Empagliflozin to HG30/H_2O_2 treated cells had no significant effect on the total amount of actin. 100 nM of Empagliflozin decreased the total amount of actin in HG30 treated cells ($p<0.001$), as opposed to 500 nM in Figure 5.7.c.

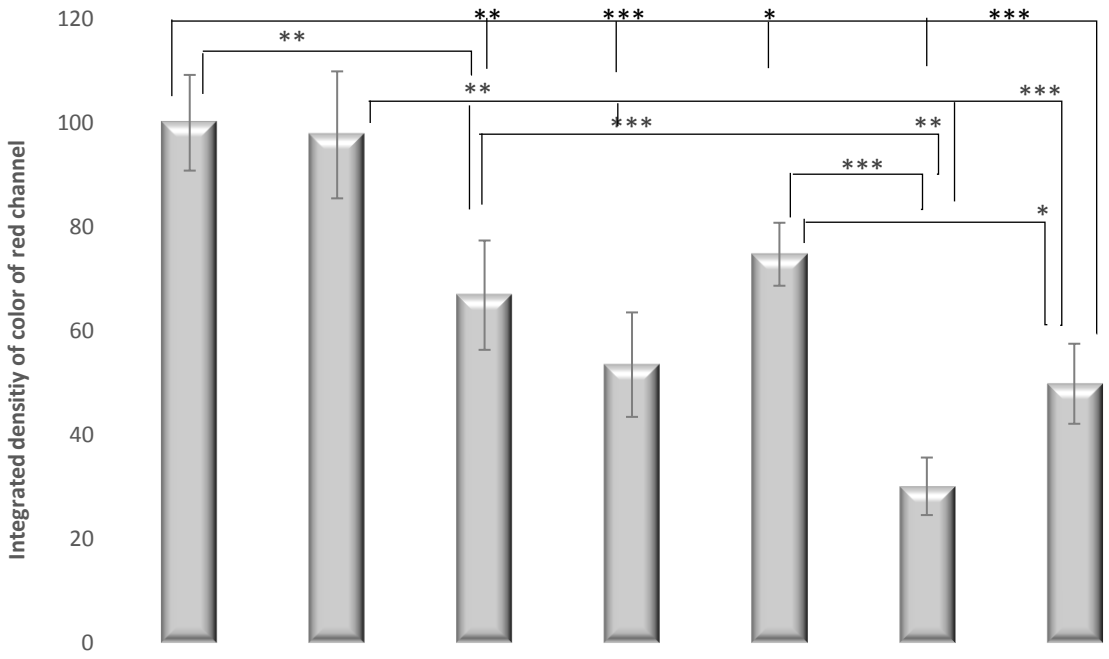

Glucose 30mM	-	+	+	+	+	+	+
H_2O_2 0.5 mM	-	-	+	+	+	-	-
Liraglutide 10nM	-	-	-	+	-	+	-
Liraglutide 20nM	-	-	-	-	+	-	+

Figure 5.7.a: Quantification and Visualization of the F-actin cytoskelet with Rhodamine Phalloidin stain.

(a) Levels of total F actin stained by Phalloidin-Rhodamine in LLC-PK1 treated cell lines (control vs HG30 and HG30/H_2O_2; HG30 vs HG30/Lira10 and HG30/Lira20; HG30/H_2O_2 vs HG30/ H_2O_2/Lira10 and HG30/H_2O_2/Lira20). Data represent the integrated density of red colour of stained actin per single cell. A higher number equals a more intense stain. One-way ANOVA $_{F(8,26)=22.41,\ p=7.46\times10^{-8}}$ with Tukey HSD post hoc test; *p<0.05, **p<0.01, ***p<0.001. The values are represented as means ± SD. Bars assigned with

asterisks are statistically significantly different. Plus (+) sign indicates the addition of compounds and minus (−) sign lack of compounds in the experimental group compared to untreated control. The data shown are representative of at least three independent experiments.

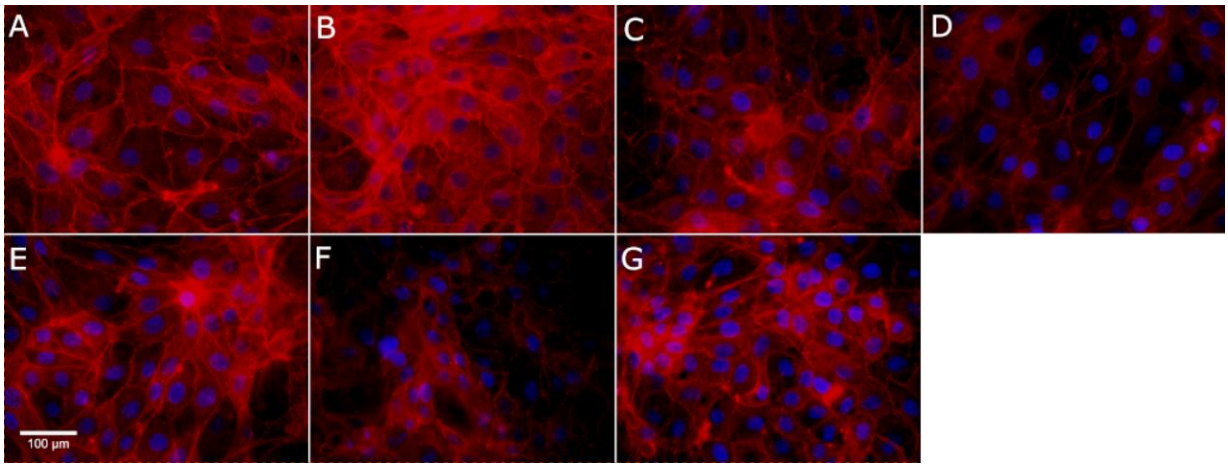

Figure 5.7. b: - LLC-PK1 cells were labeled for F-actin using Rhodamine Phalloidin and nuclei stained with DAPI. A- DMEM (control), B- glucose (HG30mM), C- glucose and H_2O_2 (HG/0.5mM), D- glucose, H_2O_2 and Liraglutide (HG/0.5mM/10nM), E- glucose, H_2O_2 and Liraglutide (HG/0.5mM/20nM), F- glucose and Liraglutide (HG30/10nM), G- glucose and Liraglutide (HG30/20nM). The size bar represents 100 µm.

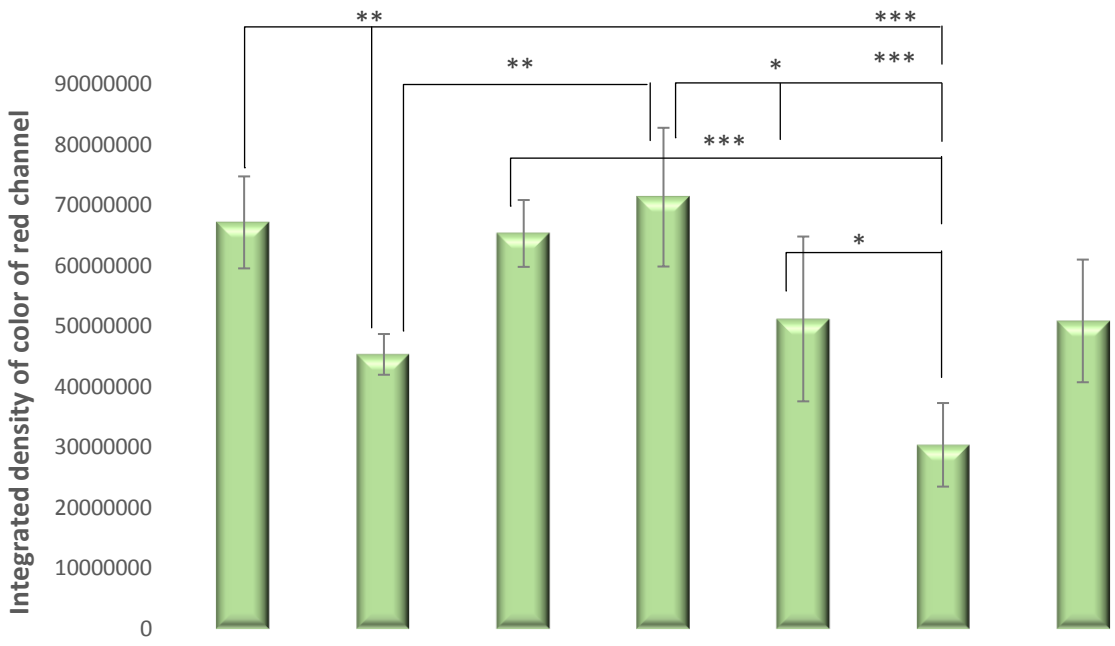

Glucose 30mM	-	+	+	+	+	+	+
H_2O_2 0.5 mM	-	-	+	+	+	-	-
Empagliflozin 100 nM	-	-	-	+	-	+	-
Empagliflozin 500 nM	-	-	-	-	+	-	+

Figure 5.7.c: Levels of total F actin stained by phalloidin-rhodamine in LLC-PK1 treated cell lines (control vs HG30 and HG30/H_2O_2; HG30 vs HG30/Empa100 and HG30/Empa500; HG30/H_2O_2 vs HG30/ H_2O_2/Empa100 and HG30/H_2O_2/Empa500). Data represent the integrated density of red colour of stained actin per single cell. A higher number equals a more intense stain. One-way ANOVA $F(6,32)=12.11, p=1.78\times10^{-6}$ with Tukey HSD post hoc test; *p<0.05, **p<0.01, ***p<0.001. The values are represented as means ± SD. Bars assigned with asterisks are statistically significantly different. Plus (+) sign indicates the addition of compounds and minus (−) sign lack of compounds in the experimental group compared to untreated control The data shown are representative of at least three independent experiments.

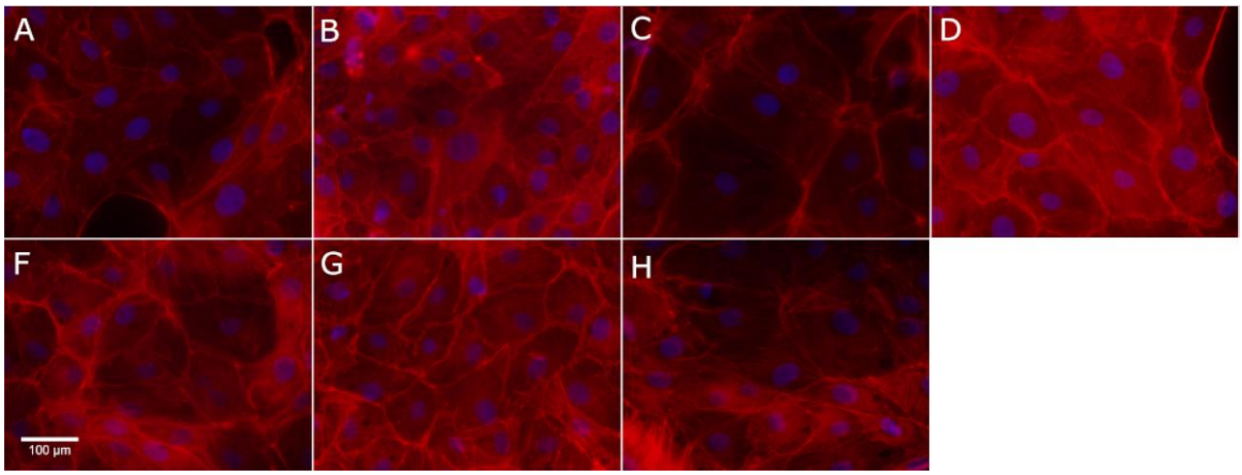

Figure 5.7. d: LLC-PK1 cells were labeled for F-actin using Rhodamine Phalloidin and nuclei stained with DAPI. A- DMEM (control), B- glucose (HG30mM), C- glucose and H_2O_2 (HG/0.5mM), D- glucose, H_2O_2 and Empagliflozin (HG/0.5mM/100 nM), E- glucose, H_2O_2 and Empagliflozin (HG/0.5mM/500 nM), F- glucose and Empagliflozin (HG30/100nM), G- glucose and Empagliflozin (HG30/500nM). The size bar represents 100 µm.

6. DISCUSSION

Diabetic nephropathy is one of the most frequent causes of kidney disease leading to dialysis and transplantation in more developed countries (246). The advancement and development of diabetic nephropathy are greatly influenced by oxidative stress (21). Due to hyperglycemia, reactive oxygen radicals with superoxide anion are produced in the kidneys causing oxidative stress, enhanced by NAD(P)H oxidase, the most significant source of superoxide anions in diabetes (22-24). In the experimental models, the usage of medications that increase cAMP levels, accumulation of cAMP concentration, and stimulation of PKA led to a decrease in NAD(P)H generation. A significant step in the inhibition of NAD(P)H-dependent superoxide generation is the activation of the cAMP-PKA pathway. Moreover, the activation of the GLP-1 receptor triggers adenylate cyclase and increases cAMP production; increased cAMP levels stimulate PKA that consequently decreases NAD(P)H and oxidative stress (26, 27, 58). Similarly, oxidative stress stimulates fibrogenic cytokines, like CTGF and TGF-β1, leading to the proliferation of extracellular matrix and mesangial cells (29, 247). The progression of albuminuria is a consequence of decreased levels of nitric oxide, primarily caused by oxidative stress, resulting in the impairment of the glomerular barrier and endothelium (30, 31). Studies conducted on streptozotocin-induced diabetes mouse models showed that treatment with GLP-1 receptor agonist Liraglutide decreases kidney damage caused by diabetes, including the proliferation of mesangial cells and albuminuria, reduction of oxidative stress and inflammatory cytokines (56, 248, 249).

Many drugs such as SGLT2 inhibitor Empagliflozin used for diabetes treatment additionally benefit renal function in DN (103). The anti-inflammatory potential of SGLT2i has been shown in diabetic animals (127, 128), human studies (130, 131), and in hyperglycemic cell cultures (86). Some in vitro studies using cell cultures like human tubular cells (HK2) or murine tubular epithelial cells explored the effects and underlying pathophysiological mechanisms of Empagliflozin. Few studies have shown that SGLT2 inhibition minimizes the release of inflammatory or fibrotic factors caused by HG while some studies found a positive effect on oxidative stress feedback (86, 250-253). In a recent study by Maayah et al. the anti-inflammatory potential of Empagliflozin independent of antihyperglycemic effects has been demonstrated indicating a survival benefit in mice induced with septic shock treated with Empagliflozin (145).

In patients with T2DM, supra-physiological GLP-1 serum concentrations of 50 to 120 pM have been shown to lower glucose plasma concentrations (254). In the in vitro model of proximal tubular cells, Liraglutide concentrations between 200 pM to 20 nM were used and with 20 nM significant inhibition of sodium re-absorption was demonstrated (255). In our study, we used two different concentrations of Liraglutide: 10 nM and 20 nM. The effect of Liraglutide on the reduction of oxidative stress markers was confirmed by Hendarto, H. et al. demonstrating its role in the expression of NAD(P)H oxidase in renal tissue (Nox4, gp91phox, p22phox, p47phox) of rats with developed DM II, independent of antihyperglycemic effect (249). Also, in the mouse model of diabetic nephropathy, similar conclusions were suggested, focusing on the key role that Liraglutide has in the protection or inhibition of oxidative stress in renal tissue and reduction of the accumulation of fibronectin in glomerular capillary walls (77). As previously specified, NAD(P)H oxidase inhibition and cAMP-PKA pathway activation are molecular mechanisms associated with those processes (77).

In another set of experiments, we used two different concentrations of Empagliflozin: 100 nM and 500 nM based on previous research using Empagliflozin in concentrations (10, 100, and 500 nM) to HG treated cells in *in vitro* experiments on proximal tubular epithelial cells (PTCs). Moreover, another *in vitro* study using human proximal tubular cell lines HK-2 and RPTEC/TERT1 has shown beneficial effects when treated with therapeutic concentrations of 500 nM of Empaglifozin (146, 256).

In our study, treating porcine renal proximal tubular cell line LLC-PK1, routinely used to study the nephrotoxic effects of drugs in humans (242) with HG and H_20_2, caused a decrease in cell viability in both sets of experiments (with Liragutiede and Empagliflozin) assessed by the Erythrosin B color exclusion test and MTT assay. In a study by Tong et al. decrease in cell viability and an increase in cell apoptosis in NRK-52E cell culture was also demonstrated. H_20_2 induces cell death or apoptosis and attenuates cell viability of A549 cells in a concentration and time-dependent manner (257, 258). H_20_2 decreases intracellular ATP levels and activated (259) caspase 3/caspase-7 activity (260) and it also upregulates the expression of cleaved-caspase-9. Oxidative stress induces carboxylation of lipids, DNA, and proteins it represents the first mechanism of damage (261). High concentrations of exogenous H_20_2 are required to elevate intracellular H_20_2 since catalase quickly degrades H_20_2 entering the cells. Exogenous H_20_2 at very high concentrations, such as 3mM, elevates intracellular H_20_2 in distal nephron cells (262) while in this study 0.5 mM of H_20_2 was used. In our study, to

determine the optimal concentration of H_20_2, LLC-PK1 was cultured in 6 well plates for 24 hours in a DMEM medium containing 0.25 mM, 0.5 mM, 1mM, and 2 mM of H_20_2. After that cell viability was measured with an MTT assay and optimal concentration was used in further experiments. According to a study performed by Peruchetti DB et al., 30 mM is the optimal concentration of glucose to mimic DN in LLC-PK1 cell culture (263). This was confirmed with MTT assay where LLC-PK1 cells were cultured in 6 well plates for 24 hours in DMEM medium supplemented with 0, 4.5, 15, 30 and 45 mM of D-glucose.

Treatment with Liraglutide led to improved viability in hypergylcemic conditions measured by the Erythrosin B color exclusion test and MTT levels. In a study by Wang et al. Liraglutide has been shown to improve the mitochondrial function by activating the Sirt1/AMPK/PGC1α pathways in an obesity-induced rat CKD model (264). The study by Zhao et al. proved that Liraglutide ameliorated cell viability in HK-2 cells (human proximal tubular cells) by downregulating caspase-3 expression (40). Yet, in cells treated with H_20_2, Liraglutide did not have a significant effect on the cells due to extensive damage caused by exogenous cell apoptosis (257).

When treated with Empagliflozin, cell viability was significantly increased in hypergylcemic conditions, and oxidative stress was assessed by the Erythrosin B color exclusion test and MTT assay. These results can be compared with the previous study that investigated the protective effects of Empagliflozin 500 nM in HK2 cells exposed to high glucose inducing cell damage through a mitochondrial mechanism. The authors also demonstrated that Empagliflozin did not induce negative effects on PTCs viability cultured in HG (256). Others explored the subcellular pathways underlying the protective effects of Empagliflozin from HG-mediated damage on HK-2 cells (251). The study by Smith et al. has shown that Empaglifozin does not have a cytotoxic, genotoxic, or mitogenic role (252).

In states of oxidative stress, cells try to resist oxidative effects by activating defense enzymes, transcription factors, and structural proteins. Increasing the ratio of oxidized and reduced glutathione (GSH / GSSG ratio, GSH / GSSG) in favor of the oxidized form represents one of the important mechanisms contributing to oxidative stress (265). Supply of cellular gluthatione (GSH) known as non-enzymatic antioxidant system inhibits cell damage due to oxidative stress, while the loss of the glutathione-dependent enzyme pathway due to decreased glutathione levels contributes to the onset and progression of several diseases including DN (266). To a certain level, GSH can control the damage caused by free radicals,

but at one point when hyper saturation occurs, cells are confronted with oxidative stress, and the inclusion of external agents is necessary to maintain cell viability (267). In this study, in both sets of experiments, GSH levels have shown that treatment with HG and H_20_2 increased oxidative stress and both Liraglutide and Empagliflozin relatively reduced oxidative stress. However, the addition of Liraglutide to cells damaged only by hyperglycemia had a modest effect, indicating that the protective effect of the drug is achieved predominantly through the prevention of oxidative stress caused by H2O2. Previous research supports this hypothesis. For example, in a study by Yin et al. recombinant human GLP-1 inhibited protein kinase C (PKC)-β, but increased protein kinase A (PKA), reducing oxidative stress in both glomeruli and tubules (54). The study from Krause et al. demonstrated that Liraglutide significantly improved GSH levels, but did not affect the reactive oxygen species production (268). Therefore, we could hypothesize that GSH has a protective effect upon exposure of cell membrane to free radicals.

Previous research has demonstrated no effect of Empagliflozin in reducing oxidative stress in hyperglycemia-induced cell damage. In a study by Baer, P.C. et al. oxidative stress did not decrease with Empagliflozin treatment (256). However, in our study, Empagliflozin added in both concentrations to HG30 treated cells caused an increase in GSH levels. Furthermore, Empagliflozin 500 nM led to a significant increase of GSH levels when added to HG30/H202 treated cells. Those findings indicate a protective role of Empagliflozin on PTC exposed to oxidative stress conditions. Similarly, in a recently published study, the addition of Empagliflozin to proximal renal tubular cells exposed to high glucose led to an increase of HIF-1α (Hypoxia-inducible factor−1alpha) protein expression, a protein responsible for modulation of hypoxia-induced tissue reaction (269).

In our study, high glucose increased mRNA expression of *TGF β1* in the cell culture model of diabetic nephropathy, but the addition of 10 nM of Liraglutide to cells exposed to high glucose and hydrogen peroxide significantly decreased the expression of *TGF β1*. Previous studies support these results because different *in vitro* studies have examined the advantages of Liraglutide therapy. For instance, the study by Sun Li et al. observed that LLC-PK1 cell culture under high glucose ambience led to increased mRNA expression of *TGF β1* levels (270). A study by Cruz MC et al. clearly demonstrated that H_2O_2 stimulated the expression of TGF-β1 mRNA in human mesangial cells (271). In a study performed by Chen P. et al. Liraglutide inhibited the expression of *TGF β1*. Furthermore, the mRNA expression

of *TGF β1* in diabetic nephropathy treated with Liraglutide clearly showed reduced levels compared to non treated DN group (272).

In a study by Ying Y. et al. adjoining tubule cell-specific removal of P53 increased renal function and debilitated ischemia/reperfusion-induced renal oxidative stress (273). In response to injury, both, glucose-conditioned renal proximal tubular cells and diabetic kidney tissues showed markedly higher p53 induction. Suppression of p53 diminished the sensitivity of high glucose-conditioned cells to acute injury *in vitro* (274). Moreover, several studies indicated that p53 is accountable for the apoptosis of renal cell in DN (274, 275) while other studies discovered that p53 inhibition may decrease TGF-β-induced hypertrophy in mesangial cells (MMCs) (276). However, in a study by Ma Y et al, exposure of PTC to high glucose caused a decline in cell proliferation, along with cell cycle arrest and EMT via stimulation of the p53 signaling pathway (277). Therefore, the regulatory mechanism of p53 in DN-induced renal fibrosis remains elusive (275). Surprisingly, our results demonstrated higher expression of p53 in cells exposed to H202 and HG with the addition of Empa500 relative to HG30/H2O2 and HG30/Empa100 and 500 treated group, but no difference was observed between the control group and all experimental groups. Similar results were observed with the expression of the Pp53 protein. As there was no significant difference in p53 levels between all experimental groups and controls, we can conclude that in this experimental model of diabetic nephropathy the regulation of pathophysiological mechanisms involving p53 molecular pathways had no significant role. However, a significant simultaneous increase in p53 and Pp53 in HG30/ H_20_2/Empa 500-treated cells indicate that high concentrations of Empagliflozin in combination with cell injury increase the gene expression of this cell cycle regulator. These results may also imply potential drug toxicity in combination with extreme cell damage caused by oxidative stress and high concentrations of glucose and hydrogen peroxide, which is difficult to translate into a human model.

In our study, analysis of PPAR-γ protein expression in diabetic nephropathy showed that PPAR-γ protein expression was significantly increased in HG treated cells, hydrogen peroxide, and the highest concentration of Empagliflozin compared to HG/ H_20_2 treated cells. In other groups where both concentrations of Empagliflozin were added, a slight increase in PPAR-γ expression was seen. Such results suggest an increase in PPAR-γ expression with the addition of Empagliflozin. Previous studies have shown that at the time of diabetes onset, PPAR-γ and GLUT4 protein expression levels were decreased (278). Also, increased PPAR-γ and GLUT4 protein expression levels are associated with protective effects against DN (279).

pSTAT3 is directly related to the leptin signaling pathway. In the Western blott analysis of pSTAT3, we have observed the same pattern as for AKT activity. Treatment with HG30 / H202 / Empa500 increased pSTAT3 levels significantly compared to all groups except control indicating that oxidative stress, high glucose concentration, and treatment with Empagliflozin will lead to the activation of the leptin signaling pathway section which in turn will block part of the insulin pathway. These results suggest that this combination of high osmotic and oxidative stress and drugs could also have a potentially detrimental effect on cell metabolism due to dysregulation of the insulin and leptin signaling pathways within cells. Research by Liu et al. reported that acetylation and phosphorylation of p65 and STAT3 were higher in the glomeruli of db/db mice than in those of db/m mice (280). The study also affirmed that acetylation of STAT3 and p65 is necessary for their transcriptional movement through the mutation of the acetylated residues. The technical knockout of sirtuin-1 in podocytes greatly upturned acetylation of p65 due to which the mice and STAT3 were more responsive to DN(150).

The loss of renal Smad7 in the diabetic kidney could develop NF-kB-driven inflammation and TGF-b/Smad-mediated renal fibrosis since Smad7 is an acknowledged inhibitory of TGF-b/Smad signaling and induces an NF-kB inhibitor IkBa to block NF-kB activation (174, 175). This hypothesis is further supported by the research of enhanced diabetic kidney injury such as renal inflammation in Smad7 KO mice, microalbuminuria, and renal fibrosis. In this study, it has been shown that antifibrosis could be a mechanism through which Smad7 preserves kidneys from diabetic injury. Thus, the activation of TGF-b/Smad signaling that has been displayed in the human diabetic kidneys in an experimental way (281, 282) is responsible for ECM development *in vitro* under high glucose and advanced glycation end products conditions (282, 283). Due to the protective role in the diabetic renal injury of Smad7, its overexpression may show an innovative therapy for diabetic kidney complications (284). Analysis of SMAD7 protein expression in our study showed a significant decrease in cells treated with HG and HG and hydrogen peroxide compared to the control. In cells treated with HG and H_20_2 and where a higher concentration of Empagliflozin was added, a significant increase in SMAD7 protein expression was seen compared to all other groups. A study by Li C et al. demonstrated that Empagliflozin downregulated the expression of TGF-β1 and decreased the ratios of p-Smad2/Smad2 and p-Smad3/Smad3 in DM mice. Furthermore, Smad7, the negative inhibitor of the TGF-β/SMAD pathway, was significantly increased with

the addition of Empagliflozin(285). Such results support a protective role of Empagliflozin mediated by an increase in SMAD7 protein expression.

The absence of a significant difference in the AKT levels between the experimental groups indicates that regardless of treatments, basal levels of AKT molecules remain unchanged. However, treatment with HG30/H_20_2/Empa500 significantly increased AKT phosphorylation compared to the group treated with HG30/Empa500 indicating that treatment with Empagliflozin in case of oxidative stress increases the endogenous activity of the insulin signaling pathway which could increase cell survival. In addition, treatment with HG30 and both concentrations of Empagliflozin had no effect on the activity of the insulin signaling pathway compared to the control group, meaning the drug itself does not activate the insulin activation cascade, but only in the state of the oxidative damage. These results could indicate a protective effect of Empagliflozin on kidney tubule cells when exposed to large amounts of oxygen-free radicals. Akt was described as a negative regulator of p38 MAPK activation and p38 MAPK activation in response to HG contributes to hypertrophy of RPTCs. A study by Rane MJ et al. distinctly showed that overexpression of Akt offered protection to RPTCs exposed to hyperglycemia by inhibiting proapoptotic p38 MAPK signaling (184). Accordingly, pharmacological induction of Akt activation may give therapeutic benefits to control p38 MAPK-mediated diabetic impairment. In *in vitro* diabetic model, Rane MJ et al. demonstrated in seeded RPTCs that Akt phosphorylation was significantly increased following 3–9 h of HG exposure, followed by a decrease between 12 and 48 h. This study indicated that downregulation of Akt activation in hyperglycemia can contribute to p38 MAPK activation and RPTC apoptosis (184). The study by Fujita H et al. demonstrated that exposure of LLC-PK1 cells to 25 mM HG for 24 and 72 h significantly increased p38 MAPK phosphorylation at both time points (286).

GSK3β levels were significantly increased in cells treated with HG30/H2O2/Empa500 compared to the HG30 and the HG30/Empa100 and HG30/Empa500 treated groups, once again pointing that the combination of oxidative stress and increased glucose concentration will lead to increased activity of the lower insulin signaling pathway subsequently changing glycogen synthase kinase activity in tubule cells (287). Given that kidney cells are able to synthesize glycogen, transcription activation for GSK3 Beta could be independent of the insulin stimulation whereas environmental factors would be the ones driving its synthesis. There was no difference between the control group and that of glucose only-treated and glucose-treated groups in combination with both Empagliflozin concentrations suggesting that

glucose alone is unable to induce changes in GSK3 Beta expression levels. Furthermore, the effects of Empagliflozin on the GSK 3 Beta activity were dose dependant, meaning that treatment with a higher concentration of Empagliflozin significantly increased activity of GSK3 Beta compared to the group treated with lower concentration. Therefore, we could hypothesize that glucose alone is not able to activate GSK3 Beta, but some exogenous stimulus is needed. In a study by Miyamoto et al. the exposure of H9c2 cells to H_20_2 (500 μM) notably downturned phosphorylation of GSK-3β while it raised phosphorylation of Akt (ser473). The cell death may be prevented through Akt, by phosphorylating its specific targets, consequently changing the function and/or subcellular localizations of proteins, together with Bad [Bcl-2 associated agonist of cell death] and Bax. Moreover, Akt is also able to translocate to the mitochondrial matrix and inhibit mPTP opening thus preventing cell death (185).

The level of oxidative stress-induced in this *in vitro* study cannot be translated into the in vivo conditions since the injury is primarily caused by free radicals generated by hyperglycemia and not by direct damage with an aggressive agent such as H_20_2. Consequently, the level of oxidative stress-induced in this study could have affected both the leptin and insulin pathway disorders to the extent that the addition of the drug at higher and more effective concentration further potentiates cell injury and the toxic effect achieved by adding both, glucose and hydrogen peroxide. Furthermore, in glucose-only treated cells, without hydrogen peroxide, and with the addition of Empagliflozin, no change in GSK3 Beta expression has been observed further supporting this notion. Obviously, in this study, we have revealed signaling pathways involved in cytoprotection and cytotoxicity of the drug itself, and further molecular studies *in vitro* and *vivo* are required to elucidate the complexity of pathophysiological mechanisms of Empagliflozin effects under conditions of hyperglycemia and oxidative stress.

In contrast, cellular viability, GSH, and TGF β levels show that Empagliflozin has protective effects in not only where hyperglycemia is induced, but as well as in conditions where hyperglycemia and oxidative stress are induced simultaneously.

Several studies have suggested that intrinsic renal cells are able to produce inflammatory cytokines and growth factors such as transforming growth factor-beta 1 (TGF-β1) in the progression of DN (288). As a fibrogenic cytokine, TGF-β1 is considered a key mediator in DN (289). In addition, oxidative stress through P13K/Akt and JNK pathways leads to

activation of NF-κB, upregulating expression of TGF-β1 and connective tissue growth factor (35). The results of our study are in agreement with previous research demonstrating a significant increase of TGF-β1 levels in injured cells, both with hyperglycemia and oxidative stress. Also, a study by Cruz MC et al. showed that H2O2 stimulates TGF- β1 production (271). Furthermore, Liraglutide led to a decrease of TGF-beta1 levels when added to cells exposed to hyperglycemia and/or oxidative stress suggesting that the protective effect of Liraglutide was mediated primarily through inhibition of TGF beta 1 expression in this model of diabetic nephropathy. Likewise, previous research demonstrated a protective role of Liraglutide diminishing renal fibrosis induced by TGF-β1 in NRK-52E cells. The proposed pathophysilogical mechanism could be inhibition of TGF-β1/Smad3 and ERK1/2 signaling pathways activation (290). Liraglutide also alleviated renal fibrosis by decreasing transforming growth factor β activity and augmenting ERK activation in renal tubular epithelial cells (291). Likewise, Empagliflozin led to a decrease of TGF-beta1 levels when added to cells exposed to hyperglycemia and/or oxidative stress suggesting that the protective effect of Empagliflozin was mediated through the suppression of TGF beta 1 expression in this model of diabetic nephropathy. In research by Winiarska A. et al., the downstream mediator of TGFβ was as well increased following exposure to HG and normalized by the addition of Empagliflozin (292). In *in vitro* study by Lee et al. Empagliflozin prevented phosphorylation of NFκBa signal transducer and activator of transcription (STAT) 1 and 3, Janus (JAK2) kinase and IKK. Complex interaction mechanisms among SGLT2i and macrophages resulted in the attenuation of systemic inflammation through the downregulation of IKK/NF-κB, MKK7/JNK, and JAK2/STAT1 pathways (293).

Exposure of human proximal tubular cells and cortical fibroblasts to high glucose (HG) concentrations can directly induce cell growth and collagen synthesis, regardless of glomerular, haemodynamic, or vascular pathology (294). Some studies have shown that fibronectin generation in response to HG is mediated by the polyol pathway in LLC-PK1 cells (295) and that flux of glucose in the hexosamine pathway mediates ECM production via stimulation of TGF-β (34). Likewise, it promotes oxidative stress and through P13/Akt pathway leads to tubular dysfunction. Hypoxia increases collagen production, TIMP1 expression and decreases MMP2 activity (ECM accumulation) (33, 35). In our study, H_20_2 may have induced ECM expression by a direct or an indirect effect through activation of the TGF-β system (271). A study by Mali N et al. showed that Liraglutide reduced the accumulation of glomerular extracellular matrix (ECM) and renal injury in DN by

upregulating the signaling of the Wnt/β-catenin pathway and ameliorated renal injury in diabetic nephropathy(296). This is in agreement with our results since an increased amount of collagen was observed in the group treated with high glucose and H202, while a decrease of collagen concentration was noted in groups treated with both concentrations of Liraglutide.

In recently published research, Empagliflozin decreased deposition of extracellular matrix proteins like type I collagen, type III collagen, and αSMA via suppression of TGF-β/SMAD signaling pathway associated with collagen production in a diversity of cell types and organs (285). In a study by Aroor et al., treatment with Empagliflozin led to a decrease of diabetic kidney injury and fibrosis by suppressing macrovascular/microvascular rigidity and enhancing expression of the anti-fibrotic RECK in the kidney(297). In a study by Ndibalema AR et al. TGFβ, fibronectin, and collagen type IV were significantly increased in HK-2 cells grown in HG medium. The addition of Empagliflozin in different concentrations (50nM, 100nM, and 500nM) caused a decrease in TGFβ, fibronectin, and collagen type IV expression in a dose-dependent manner (269).

In our study, there was no change in collagen synthesis in cells exposed to oxidative stress induced by H_20_2 and hyperglycemia relative to the control group. Furthermore, the addition of Empagliflozin had no significant effect on the production of collagen in the glucose only-treated nor in cells treated with a combination of HG and H_20_2, while only Empagliflozin at a dose of 500 nM significantly increased collagen synthesis in cells treated with HG30 compared to cells treated with HG30 only. Therefore, we can conclude that under these experimental conditions Empagliflozin has no significant effect on collagen synthesis.

The major structural component in the proximal tubule is F-actin (298). Previous studies demonstrated that diabetes causes alterations in the cellular matrix, such as fibrosis and changes in the F-actin content and organization (299-301). Proximal cells' function relies on specific actin cytoskeletal systems and connected cytoskeleton proteins which are naturally expressed in the cells (302). Derangement of the actin cytoskeleton was reported to be a critical characteristic of damaged proximal tubular cells (303). Moreover, Xu C. et al. demonstrated that cytoskeletal modifications in proximal tubular cells, manifested by F actin rearrangement was caused by exposure to high glucose (304). Hydrogen peroxide during inflammation causes cell death mainly by disarranging filamentous (polymerized) actin (F-actin). In a study from DalleDonne et al. escalation in H_20_2 concentration used for the treatment of actin monomers, enhanced the number of actin filaments at a steady-state (305).

Furthermore, in *in vitro* study in mouse podocytes, high glucose led to filamentous actin (F-actin) rearrangement and injury (306). Several studies have shown a more disorganized F-actin structure with decreased F-actin content in diabetic animals (307). Accordingly, a significant reduction in the distribution of F-actin was observed in cells treated with HG30/H_2O_2, however, this effect was absent in cells exposed to hyperglycemia alone. Obviously, oxidative stress is the key element in F actin filament disruption. While studies have quantified F-actin fluorescence in diabetic animals, none have quantified F-actin disorganization at present. Data on exendin-4 treatment demonstrated a significant increase in the rearrangement of filamentous-actin with a reduction of cell migration (308). Quite unexpectedly, the addition of Liraglutide to HG30 caused a significant decline of F-actin distribution, while no effect was detected in HG30/H_2O_2 treated cells. Similarly, the addition of Empagliflozin to HG30/H_2O_2 treated cells had no significant effect on the total amount of actin, while 100 nM of Empagliflozin decreased the total amount of actin only in HG30 treated cells. We can only speculate that the reduced distribution of F actin with the addition of Liraglutide or Empagliflozin in hyperglycemic conditions is the result of actin filaments reorganization, increased differentiation, and reduced cell migration, as with the addition of oxidative stress, Liraglutide and Empagliflozin effect on F actin structure is less pronounced.

Our results support a protective role of Liraglutide and Empagliflozin in LLC-PK cells treated with hyperglycemia with and without H_2O_2. This role is mediated primarily via inhibiting TGF-β1 reducing oxidative stress injury.

7. CONCLUSIONS

Based on this study results, the following conclusions can be drawn:

- Model of diabetic nephropathy can be considered valid because induced changes in levels of expression of TGF beta and insulin signaling pathway activity are in line with previously observed data collected in humans and animals thus other experiments have good translational potential.
- Treating cells with Liraglutide or Empagliflozin reduces negative effects of induced diabetic nephropathy increasing cell survival and their oxidative status.
- The addition of Liraglutide led to a decrease of TGF beta gene expression in the cell culture model of diabetic nephropathy.
- The addition of Empagliflozin led to a significant increase of proteins ' (p53, p-p53, PPAR-γ, pSTAT3, pGSK3β, GSK3β, SMAD 7 and p Akt) expression involved in insulin/leptin pathway, except for Akt.
- Liraglutide reduced ECM accumulation induced by high glucose and oxidative stress but Empagliflozin did not affect collagen synthesis in given concentrations.
- The addition of Liraglutide led to a significant decrease while Empagliflozin did not affect the distribution of F-actin.

8. SUMMARY

Objectives*:* Transforming growth factor-beta (TGF- β) has been recently implicated in the development of diabetic nephropathy (DN) causing cell apoptosis induced by oxidative stress, cell proliferation, and migration triggered by hyperglycemia and inflammation. GLP 1 RA and SGLT2i are two antyhyperglycemic drug classes that have direct renoprotective effects, although molecular mechanisms for both drugs are still not clear. This research aimed to assess the effects of Liraglutide (GLP 1 RA) and Empagliflozin (SGLT2i) on cell viability, GSH levels, TGF-β expression and concentration, protein levels involved in insulin signaling pathway and cell damage, and F actin distribution in the LLC-PK1 model of DN.

Study design: In order to mimic DN, cells were exposed to high glucose (HG30 mM) followed by 0,5 mM H_2O_2 and a combination of glucose and H_2O_2 during 24 hours. In the first set of the experiment, the cells were treated with different combinations of glucose and Liraglutide and combinations of glucose, H_2O_2, and Liraglutide. In the second set, cells were treated with different combinations of glucose and Empagliflozin and combinations of glucose, H_2O_2 and Empagliflozin.

Materials and methods: Cell viability was determined by MTT colorimetric test and Erythrosin B color exclusion test. Glutathione (tGSH), ECM expression, and TGF-β1 concentration were measured using spectrophotometric/microplate reader assay and ELISA kit, respectively. Expression of mRNA *TGF- β1* was measured by RT-PCR and β actin was used as an internal control. Western blotting was used to detect the protein level of Akt, pAkt, GSK3β, pGSK3β, p53, p-p53, pSTAT3, SMAD7, and PPAR-γ. F-actin cytoskelet was visualized with Phalloidin stain and subsequently quantified.

Results: Cell viability and GSH levels were decreased in the DN model of cell culture. Liraglutide and Empagliflozin generally improved cell viability and GSH levels. Expression of *TGF- β1* levels were significantly increased in HG30 treated cells. Liraglutide reduced expression of *TGF-β1* except in HG30/H_2O_2 treated cells. A significant reduction of SMAD 7 and pGSK3β in the DN model was noted compared to the control. In HG30/ H_2O_2/Empa500 treated cells significant increase in p53, pp53, PPAR-γ, pSTAT3, pGSK3BETA, GSK3BETA, SMAD 7, and p AKT levels was observed except for AKT. A significant increase of TGF-β1 levels in injured cells was observed and Liraglutid and Empagliflozin treatment led to a decrease of TGF- β1 levels. Liraglutide reduced ECM accumulation

induced by high glucose and oxidative stress, but Empagliflozin did not have any significant effect. The addition of Liraglutide to all treated cell groups led to a significant decrease, while Empagliflozin partially led to a decrease in the distribution of F-actin.

Conclusion: Renal tubular injury in the LLC-PK model of DN is facilitated through TGF beta predominantly stimulating oxidative stress cell damage. Inhibition of TGF beta is mainly responsible for renal benefits of Liraglutide and Empagliflozin.

Keywords: Diabetic nephropathy, oxidative stress, hyperglycemia, Liraglutide, Empagliflozin, LLC-PK1

9. SAŽETAK

Ciljevi: Transformirajući faktor rasta beta (TGF-β) uključen je u razvoj dijabetičke nefropatije (DN) koja uzrokuje staničnu apoptozu uzrokovanu oksidativnim stresom, proliferacijom i migracijom stanica izazvane hiperglikemijom i upalom. GLP 1 RA i SGLT2i dvije su klase antihiperglikemijskih lijekova za koje se pokazalo kako imaju izravne renoprotektivne učinke, iako molekularni mehanizmi za oba lijeka još uvijek nisu jasni. Cilj ovog istraživanja bio je procijeniti učinke Liraglutida (GLP 1 RA) i Empagliflozina (SGLT2i) na vijabilnost stanica, GSH razine, ekspresiju i koncentraciju TGF-β, razine proteina uključenih u signalni put inzulina i oštećenje stanica te distribucija F aktina u LLC-PK1 modelu dijabetičke nefropatije.

Tijek istraživanja: Kako bi se oponašala dijabetička nefropatija, stanice su bile izložene visokoj glukozi (HG30 mM) uz dodavanje 0,5 mM H_2O_2 i kombinaciji glukoze i H_2O_2 tijekom 24 sata. U prvom dijelu pokusa stanice su tretirane različitim kombinacijama glukoze i Liraglutida te kombinacijama glukoze, H_2O_2 i Liraglutida. U drugom dijelu stanice su tretirane različitim kombinacijama glukoze i Empagliflozina te kombinacijama glukoze, H_2O_2 i Empagliflozina.

Materijali i metode: Vijabilnost stanica određena je MTT kolorimetrijskim testom i bojom Eritrozin B. Glutation (tGSH), ekspresija ECM i TGF-β1 koncentracija mjereni su pomoću spektrofotometrijskog/mikroploče čitača i ELISA kompleta. RT-PCR mjerio je ekspresiju mRNA TGF-β1, a β aktin korišten je kao interna kontrola. Western blot korišten je za otkrivanje razine proteina Akt, pAkt, GSK3β, pGSK3β, p53, p-p53, pSTAT3, SMAD7 i PPAR-γ. F-aktinski citoskelet vizualiziran je s faloidin bojom i naknadno kvantificiran.

Rezultati: Vijabilnost stanica i GSH razine smanjene su u DN modelu stanične kulture. Liraglutid i Empagliflozin općenito su poboljšali vitalnost stanica i razine GSH. Ekspresija razina TGF-β1 bila je značajno povećana u stanicama tretiranim HG30. Liraglutid je smanjio ekspresiju TGF-β1 osim u stanicama tretiranim HG30/H_2O_2. Zabilježeno je značajno smanjenje SMAD 7 i pGSK3β u DN modelu u usporedbi s kontrolom. U stanicama tretiranim HG30/H_2O_2/Empa500 uočeno je značajno povećanje razina p53, pp53, PPAR-γ, pSTAT3, pGSK3BETA, GSK3BETA, SMAD 7 i p AKT, osim za AKT. Uočeno je značajno povećanje razine TGF-β1 u ozlijeđenim stanicama, a liječenje Liraglutidom i Empagliflozinom dovelo je do smanjenja razine TGF-β1. Liraglutid je smanjio nakupljanje ECM-a izazvano visokom

glukozom i oksidativnim stresom, ali Empagliflozin nije imao značajan učinak. Dodavanje Liraglutida svim tretiranim skupinama stanica dovelo je do značajnog smanjenja, dok je Empagliflozin djelomično doveo do smanjenja distribucije F-aktina.

Zaključak: Ozljeda bubrežnih tubula u LLC-PK DN modelu omogućena je kroz TGF beta koji pretežno potiče oštećenje stanica oksidativnim stresom. Inhibicija TGF beta uglavnom je odgovorna za bubrežne pozitivne učinke Liraglutida i Empagliflozina.

Ključne riječi: dijabetička nefropatija, Empagliflozin, hiperglikemija, Liraglutid, LLC-PK1, oksidativni stres

10. REFERENCE

1. Thomas B. The Global Burden of Diabetic Kidney Disease: Time Trends and Gender Gaps. Curr Diab Rep. 2019;19(4):18.
2. Hill CJ, Cardwell CR, Patterson CC, Maxwell AP, Magee GM, Young RJ, et al. Chronic kidney disease and diabetes in the national health service: a cross-sectional survey of the U.K. national diabetes audit. Diabet Med. 2014;31(4):448-54.
3. Cao Z, Cooper ME. Pathogenesis of diabetic nephropathy. J Diabetes Investig. 2011;2(4):243-7.
4. Mahmoodnia L, Aghadavod E, Beigrezaei S, Rafieian-Kopaei M. An update on diabetic kidney disease, oxidative stress and antioxidant agents. J Renal Inj Prev. 2017;6(2):153-7.
5. Pichler R, Afkarian M, Dieter BP, Tuttle KR. Immunity and inflammation in diabetic kidney disease: translating mechanisms to biomarkers and treatment targets. Am J Physiol Renal Physiol. 2017;312(4):F716-F31.
6. McDonough CW, Palmer ND, Hicks PJ, Roh BH, An SS, Cooke JN, et al. A genome-wide association study for diabetic nephropathy genes in African Americans. Kidney Int. 2011;79(5):563-72.
7. Wei L, Xiao Y, Li L, Xiong X, Han Y, Zhu X, et al. The Susceptibility Genes in Diabetic Nephropathy. Kidney Dis (Basel). 2018;4(4):226-37.
8. Lindblom R, Higgins G, Coughlan M, de Haan JB. Targeting Mitochondria and Reactive Oxygen Species-Driven Pathogenesis in Diabetic Nephropathy. Rev Diabet Stud. 2015;12(1-2):134-56.
9. Mittal M, Siddiqui MR, Tran K, Reddy SP, Malik AB. Reactive oxygen species in inflammation and tissue injury. Antioxid Redox Signal. 2014;20(7):1126-67.
10. Kizivat T, Smolić M, Marić I, Tolušić Levak M, Smolić R, Bilić Čurčić I, et al. Antioxidant Pre-Treatment Reduces the Toxic Effects of Oxalate on Renal Epithelial Cells in a Cell Culture Model of Urolithiasis. Int J Environ Res Public Health. 2017;14(1).
11. Fioretto P, Caramori ML, Mauer M. The kidney in diabetes: dynamic pathways of injury and repair. The Camillo Golgi Lecture 2007. Diabetologia. 2008;51(8):1347-55.
12. Tervaert TW, Mooyaart AL, Amann K, Cohen AH, Cook HT, Drachenberg CB, et al. Pathologic classification of diabetic nephropathy. J Am Soc Nephrol. 2010;21(4):556-63.

13. Alicic RZ, Rooney MT, Tuttle KR. Diabetic Kidney Disease: Challenges, Progress, and Possibilities. Clin J Am Soc Nephrol. 2017;12(12):2032-45.
14. Tyagi I, Agrawal U, Amitabh V, Jain AK, Saxena S. Thickness of glomerular and tubular basement membranes in preclinical and clinical stages of diabetic nephropathy. Indian J Nephrol. 2008;18(2):64-9.
15. Fioretto P, Mauer M. Histopathology of diabetic nephropathy. Semin Nephrol. 2007;27(2):195-207.
16. Caramori ML, Parks A, Mauer M. Renal lesions predict progression of diabetic nephropathy in type 1 diabetes. J Am Soc Nephrol. 2013;24(7):1175-81.
17. Drummond K, Mauer M, Group IDNS. The early natural history of nephropathy in type 1 diabetes: II. Early renal structural changes in type 1 diabetes. Diabetes. 2002;51(5):1580-7.
18. Osterby R, Tapia J, Nyberg G, Tencer J, Willner J, Rippe B, et al. Renal structures in type 2 diabetic patients with elevated albumin excretion rate. APMIS. 2001;109(11):751-61.
19. Saito Y, Kida H, Takeda S, Yoshimura M, Yokoyama H, Koshino Y, et al. Mesangiolysis in diabetic glomeruli: its role in the formation of nodular lesions. Kidney Int. 1988;34(3):389-96.
20. Stout LC, Kumar S, Whorton EB. Focal mesangiolysis and the pathogenesis of the Kimmelstiel-Wilson nodule. Hum Pathol. 1993;24(1):77-89.
21. Forbes JM, Coughlan MT, Cooper ME. Oxidative stress as a major culprit in kidney disease in diabetes. Diabetes. 2008;57(6):1446-54.
22. Satoh M, Fujimoto S, Haruna Y, Arakawa S, Horike H, Komai N, et al. NAD(P)H oxidase and uncoupled nitric oxide synthase are major sources of glomerular superoxide in rats with experimental diabetic nephropathy. Am J Physiol Renal Physiol. 2005;288(6):F1144-52.
23. Wardle EN. Cellular oxidative processes in relation to renal disease. Am J Nephrol. 2005;25(1):13-22.
24. Gorin Y, Block K, Hernandez J, Bhandari B, Wagner B, Barnes JL, et al. Nox4 NAD(P)H oxidase mediates hypertrophy and fibronectin expression in the diabetic kidney. J Biol Chem. 2005;280(47):39616-26.
25. Saha S, Li Y, Anand-Srivastava MB. Reduced levels of cyclic AMP contribute to the enhanced oxidative stress in vascular smooth muscle cells from spontaneously hypertensive rats. Can J Physiol Pharmacol. 2008;86(4):190-8.

26. Baggio LL, Drucker DJ. Biology of incretins: GLP-1 and GIP. Gastroenterology. 2007;132(6):2131-57.
27. Leech CA, Chepurny OG, Holz GG. Epac2-dependent rap1 activation and the control of islet insulin secretion by glucagon-like peptide-1. Vitam Horm. 2010;84:279-302.
28. Yin W, Jiang Y, Xu S, Wang Z, Peng L, Fang Q, et al. Protein kinase C and protein kinase A are involved in the protection of recombinant human glucagon-like peptide-1 on glomeruli and tubules in diabetic rats. J Diabetes Investig. 2019;10(3):613-25.
29. Blaslov K, Bulum T, Duvnjak L. [Pathophysiological factors in the development of diabetic nephropathy--new insights]. Acta Med Croatica. 2014;68(2):135-40.
30. Kanetsuna Y, Takahashi K, Nagata M, Gannon MA, Breyer MD, Harris RC, et al. Deficiency of endothelial nitric-oxide synthase confers susceptibility to diabetic nephropathy in nephropathy-resistant inbred mice. Am J Pathol. 2007;170(5):1473-84.
31. Prabhakar S, Starnes J, Shi S, Lonis B, Tran R. Diabetic nephropathy is associated with oxidative stress and decreased renal nitric oxide production. J Am Soc Nephrol. 2007;18(11):2945-52.
32. Heldin CH, Landström M, Moustakas A. Mechanism of TGF-beta signaling to growth arrest, apoptosis, and epithelial-mesenchymal transition. Curr Opin Cell Biol. 2009;21(2):166-76.
33. Orphanides C, Fine LG, Norman JT. Hypoxia stimulates proximal tubular cell matrix production via a TGF-beta1-independent mechanism. Kidney Int. 1997;52(3):637-47.
34. Daniels MC, McClain DA, Crook ED. Transcriptional regulation of transforming growth factor beta1 by glucose: investigation into the role of the hexosamine biosynthesis pathway. Am J Med Sci. 2000;319(3):138-42.
35. Li X, Kimura H, Hirota K, Sugimoto H, Yoshida H. Hypoxia reduces constitutive and TNF-alpha-induced expression of monocyte chemoattractant protein-1 in human proximal renal tubular cells. Biochem Biophys Res Commun. 2005;335(4):1026-34.
36. Gentilella R, Pechtner V, Corcos A, Consoli A. Glucagon-like peptide-1 receptor agonists in type 2 diabetes treatment: are they all the same? Diabetes Metab Res Rev. 2019;35(1):e3070.
37. Gallwitz B. Glucagon-like peptide-1 receptor agonists. In: **Gough** S, editor. Handbook of Incretin-based Therapies in Type 2 Diabetes. Switzerland: Springer International Publishing 2016. p. 31-43.

38. Kim HS, Jung CH. Oral Semaglutide, the First Ingestible Glucagon-Like Peptide-1 Receptor Agonist: Could It Be a Magic Bullet for Type 2 Diabetes? Int J Mol Sci. 2021;22(18).
39. Turton MD, O'Shea D, Gunn I, Beak SA, Edwards CM, Meeran K, et al. A role for glucagon-like peptide-1 in the central regulation of feeding. Nature. 1996;379(6560):69-72.
40. Zhao X, Liu G, Shen H, Gao B, Li X, Fu J, et al. Liraglutide inhibits autophagy and apoptosis induced by high glucose through GLP-1R in renal tubular epithelial cells. Int J Mol Med. 2015;35(3):684-92.
41. Nauck MA, Duran S, Kim D, Johns D, Northrup J, Festa A, et al. A comparison of twice-daily exenatide and biphasic insulin aspart in patients with type 2 diabetes who were suboptimally controlled with sulfonylurea and metformin: a non-inferiority study. Diabetologia. 2007;50(2):259-67.
42. Buse JB, Bergenstal RM, Glass LC, Heilmann CR, Lewis MS, Kwan AY, et al. Use of twice-daily exenatide in Basal insulin-treated patients with type 2 diabetes: a randomized, controlled trial. Ann Intern Med. 2011;154(2):103-12.
43. Weissman PN, Carr MC, Ye J, Cirkel DT, Stewart M, Perry C, et al. HARMONY 4: randomised clinical trial comparing once-weekly albiglutide and insulin glargine in patients with type 2 diabetes inadequately controlled with metformin with or without sulfonylurea. Diabetologia. 2014;57(12):2475-84.
44. Wysham C, Blevins T, Arakaki R, Colon G, Garcia P, Atisso C, et al. Efficacy and safety of dulaglutide added onto pioglitazone and metformin versus exenatide in type 2 diabetes in a randomized controlled trial (AWARD-1). Diabetes Care. 2014;37(8):2159-67.
45. Nauck M, Weinstock RS, Umpierrez GE, Guerci B, Skrivanek Z, Milicevic Z. Efficacy and safety of dulaglutide versus sitagliptin after 52 weeks in type 2 diabetes in a randomized controlled trial (AWARD-5). Diabetes Care. 2014;37(8):2149-58.
46. Drucker DJ, Buse JB, Taylor K, Kendall DM, Trautmann M, Zhuang D, et al. Exenatide once weekly versus twice daily for the treatment of type 2 diabetes: a randomised, open-label, non-inferiority study. Lancet. 2008;372(9645):1240-50.
47. Blevins T, Pullman J, Malloy J, Yan P, Taylor K, Schulteis C, et al. DURATION-5: exenatide once weekly resulted in greater improvements in glycemic control compared with exenatide twice daily in patients with type 2 diabetes. J Clin Endocrinol Metab. 2011;96(5):1301-10.

48. Buse JB, Drucker DJ, Taylor KL, Kim T, Walsh B, Hu H, et al. DURATION-1: exenatide once weekly produces sustained glycemic control and weight loss over 52 weeks. Diabetes Care. 2010;33(6):1255-61.
49. Buse JB, Rosenstock J, Sesti G, Schmidt WE, Montanya E, Brett JH, et al. Liraglutide once a day versus exenatide twice a day for type 2 diabetes: a 26-week randomised, parallel-group, multinational, open-label trial (LEAD-6). Lancet. 2009;374(9683):39-47.
50. Abd El Aziz MS, Kahle M, Meier JJ, Nauck MA. A meta-analysis comparing clinical effects of short- or long-acting GLP-1 receptor agonists versus insulin treatment from head-to-head studies in type 2 diabetic patients. Diabetes Obes Metab. 2017;19(2):216-27.
51. Zaccardi F, Htike ZZ, Webb DR, Khunti K, Davies MJ. Benefits and Harms of Once-Weekly Glucagon-like Peptide-1 Receptor Agonist Treatments: A Systematic Review and Network Meta-analysis. Ann Intern Med. 2016;164(2):102-13.
52. DeFronzo RA, Ratner RE, Han J, Kim DD, Fineman MS, Baron AD. Effects of exenatide (exendin-4) on glycemic control and weight over 30 weeks in metformin-treated patients with type 2 diabetes. Diabetes Care. 2005;28(5):1092-100.
53. Lorenz M, Evers A, Wagner M. Recent progress and future options in the development of GLP-1 receptor agonists for the treatment of diabesity. Bioorg Med Chem Lett. 2013;23(14):4011-8.
54. Yin W, Xu S, Wang Z, Liu H, Peng L, Fang Q, et al. Recombinant human GLP-1(rhGLP-1) alleviating renal tubulointestitial injury in diabetic STZ-induced rats. Biochem Biophys Res Commun. 2018;495(1):793-800.
55. Hills CE, Al-Rasheed N, Willars GB, Brunskill NJ. C-peptide reverses TGF-beta1-induced changes in renal proximal tubular cells: implications for treatment of diabetic nephropathy. Am J Physiol Renal Physiol. 2009;296(3):F614-21.
56. Kodera R, Shikata K, Kataoka HU, Takatsuka T, Miyamoto S, Sasaki M, et al. Glucagon-like peptide-1 receptor agonist ameliorates renal injury through its anti-inflammatory action without lowering blood glucose level in a rat model of type 1 diabetes. Diabetologia. 2011;54(4):965-78.
57. Leech CA, Holz GG, Habener JF. Signal transduction of PACAP and GLP-1 in pancreatic beta cells. Ann N Y Acad Sci. 1996;805:81-92; discussion -3.

58. Holz GG. Epac: A new cAMP-binding protein in support of glucagon-like peptide-1 receptor-mediated signal transduction in the pancreatic beta-cell. Diabetes. 2004;53(1):5-13.
59. Savitha G, Salimath BP. Cross-talk between protein kinase C and protein kinase A down-regulates the respiratory burst in polymorphonuclear leukocytes. Cell Signal. 1993;5(2):107-17.
60. Gutzwiller JP, Hruz P, Huber AR, Hamel C, Zehnder C, Drewe J, et al. Glucagon-like peptide-1 is involved in sodium and water homeostasis in humans. Digestion. 2006;73(2-3):142-50.
61. Rieg T, Gerasimova M, Murray F, Masuda T, Tang T, Rose M, et al. Natriuretic effect by exendin-4, but not the DPP-4 inhibitor alogliptin, is mediated via the GLP-1 receptor and preserved in obese type 2 diabetic mice. Am J Physiol Renal Physiol. 2012;303(7):F963-71.
62. Muskiet MHA, Tonneijck L, Smits MM, van Baar MJB, Kramer MHH, Hoorn EJ, et al. GLP-1 and the kidney: from physiology to pharmacology and outcomes in diabetes. Nat Rev Nephrol. 2017;13(10):605-28.
63. Muskiet MH, Smits MM, Morsink LM, Diamant M. The gut-renal axis: do incretin-based agents confer renoprotection in diabetes? Nat Rev Nephrol. 2014;10(2):88-103.
64. Imamura S, Hirai K, Hirai A. The glucagon-like peptide-1 receptor agonist, liraglutide, attenuates the progression of overt diabetic nephropathy in type 2 diabetic patients. Tohoku J Exp Med. 2013;231(1):57-61.
65. Davies MJ, Bain SC, Atkin SL, Rossing P, Scott D, Shamkhalova MS, et al. Efficacy and Safety of Liraglutide Versus Placebo as Add-on to Glucose-Lowering Therapy in Patients With Type 2 Diabetes and Moderate Renal Impairment (LIRA-RENAL): A Randomized Clinical Trial. Diabetes Care. 2016;39(2):222-30.
66. Mann JFE, Ørsted DD, Buse JB. Liraglutide and Renal Outcomes in Type 2 Diabetes. N Engl J Med. 2017;377(22):2197-8.
67. Mather A, Pollock C. Renal glucose transporters: novel targets for hyperglycemia management. Nat Rev Nephrol. 2010;6(5):307-11.
68. Abdul-Ghani MA, DeFronzo RA, Norton L. Novel hypothesis to explain why SGLT2 inhibitors inhibit only 30-50% of filtered glucose load in humans. Diabetes. 2013;62(10):3324-8.

69. Marks J, Carvou NJ, Debnam ES, Srai SK, Unwin RJ. Diabetes increases facilitative glucose uptake and GLUT2 expression at the rat proximal tubule brush border membrane. J Physiol. 2003;553(Pt 1):137-45.
70. Idorn T, Knop FK, Jørgensen M, Jensen T, Resuli M, Hansen PM, et al. Safety and efficacy of liraglutide in patients with type 2 diabetes and end-stage renal disease: protocol for an investigator-initiated prospective, randomised, placebo-controlled, double-blinded, parallel intervention study. BMJ Open. 2013;3(4).
71. de Vos LC, Hettige TS, Cooper ME. New Glucose-Lowering Agents for Diabetic Kidney Disease. Adv Chronic Kidney Dis. 2018;25(2):149-57.
72. Muskiet MHA, Tonneijck L, Huang Y, Liu M, Saremi A, Heerspink HJL, et al. Lixisenatide and renal outcomes in patients with type 2 diabetes and acute coronary syndrome: an exploratory analysis of the ELIXA randomised, placebo-controlled trial. Lancet Diabetes Endocrinol. 2018;6(11):859-69.
73. Fuhrman DY, Schneider MF, Dell KM, Blydt-Hansen TD, Mak R, Saland JM, et al. Albuminuria, Proteinuria, and Renal Disease Progression in Children with CKD. Clin J Am Soc Nephrol. 2017;12(6):912-20.
74. Fox CS, Matsushita K, Woodward M, Bilo HJ, Chalmers J, Heerspink HJ, et al. Associations of kidney disease measures with mortality and end-stage renal disease in individuals with and without diabetes: a meta-analysis. Lancet. 2012;380(9854):1662-73.
75. Lorenzo V, Saracho R, Zamora J, Rufino M, Torres A. Similar renal decline in diabetic and non-diabetic patients with comparable levels of albuminuria. Nephrol Dial Transplant. 2010;25(3):835-41.
76. Marso SP, Bain SC, Consoli A, Eliaschewitz FG, Jódar E, Leiter LA, et al. Semaglutide and Cardiovascular Outcomes in Patients with Type 2 Diabetes. N Engl J Med. 2016;375(19):1834-44.
77. Fujita H, Morii T, Fujishima H, Sato T, Shimizu T, Hosoba M, et al. The protective roles of GLP-1R signaling in diabetic nephropathy: possible mechanism and therapeutic potential. Kidney Int. 2014;85(3):579-89.
78. Choi CI. Sodium-Glucose Cotransporter 2 (SGLT2) Inhibitors from Natural Products: Discovery of Next-Generation Antihyperglycemic Agents. Molecules. 2016;21(9).
79. Mather A, Pollock C. Glucose handling by the kidney. Kidney Int Suppl. 2011(120):S1-6.

80. Gilbert RE, Cooper ME. The tubulointerstitium in progressive diabetic kidney disease: more than an aftermath of glomerular injury? Kidney Int. 1999;56(5):1627-37.
81. Cherney DZ, Perkins BA, Soleymanlou N, Xiao F, Zimpelmann J, Woerle HJ, et al. Sodium glucose cotransport-2 inhibition and intrarenal RAS activity in people with type 1 diabetes. Kidney Int. 2014;86(5):1057-8.
82. Vallon V, Richter K, Blantz RC, Thomson S, Osswald H. Glomerular hyperfiltration in experimental diabetes mellitus: potential role of tubular reabsorption. J Am Soc Nephrol. 1999;10(12):2569-76.
83. Johnson DW, Saunders HJ, Brew BK, Poronnik P, Cook DI, Field MJ, et al. TGF-beta 1 dissociates human proximal tubule cell growth and Na(+)-H+ exchange activity. Kidney Int. 1998;53(6):1601-7.
84. Panchapakesan U, Pollock CA, Chen XM. The effect of high glucose and PPAR-gamma agonists on PPAR-gamma expression and function in HK-2 cells. Am J Physiol Renal Physiol. 2004;287(3):F528-34.
85. Qi W, Chen X, Holian J, Mreich E, Twigg S, Gilbert RE, et al. Transforming growth factor-beta1 differentially mediates fibronectin and inflammatory cytokine expression in kidney tubular cells. Am J Physiol Renal Physiol. 2006;291(5):F1070-7.
86. Panchapakesan U, Pegg K, Gross S, Komala MG, Mudaliar H, Forbes J, et al. Effects of SGLT2 inhibition in human kidney proximal tubular cells--renoprotection in diabetic nephropathy? PLoS One. 2013;8(2):e54442.
87. Scheen AJ. Pharmacokinetic and pharmacodynamic profile of empagliflozin, a sodium glucose co-transporter 2 inhibitor. Clin Pharmacokinet. 2014;53(3):213-25.
88. Scheen AJ. Drug-drug interactions with sodium-glucose cotransporters type 2 (SGLT2) inhibitors, new oral glucose-lowering agents for the management of type 2 diabetes mellitus. Clin Pharmacokinet. 2014;53(4):295-304.
89. Merovci A, Mari A, Solis-Herrera C, Xiong J, Daniele G, Chavez-Velazquez A, et al. Dapagliflozin lowers plasma glucose concentration and improves β-cell function. J Clin Endocrinol Metab. 2015;100(5):1927-32.
90. Del Prato S. Role of glucotoxicity and lipotoxicity in the pathophysiology of Type 2 diabetes mellitus and emerging treatment strategies. Diabet Med. 2009;26(12):1185-92.
91. Wilding JP, Blonde L, Leiter LA, Cerdas S, Tong C, Yee J, et al. Efficacy and safety of canagliflozin by baseline HbA1c and known duration of type 2 diabetes mellitus. J Diabetes Complications. 2015;29(3):438-44.

92. Heerspink HJ, Johnsson E, Gause-Nilsson I, Cain VA, Sjöström CD. Dapagliflozin reduces albuminuria in patients with diabetes and hypertension receiving renin-angiotensin blockers. Diabetes Obes Metab. 2016;18(6):590-7.
93. Johnsson KM, Ptaszynska A, Schmitz B, Sugg J, Parikh SJ, List JF. Urinary tract infections in patients with diabetes treated with dapagliflozin. J Diabetes Complications. 2013;27(5):473-8.
94. Elkinson S, Scott LJ. Canagliflozin: first global approval. Drugs. 2013;73(9):979-88.
95. Polidori D, Sha S, Mudaliar S, Ciaraldi TP, Ghosh A, Vaccaro N, et al. Canagliflozin lowers postprandial glucose and insulin by delaying intestinal glucose absorption in addition to increasing urinary glucose excretion: results of a randomized, placebo-controlled study. Diabetes Care. 2013;36(8):2154-61.
96. Engeli S, Jordan J. Novel metabolic drugs and blood pressure: implications for the treatment of obese hypertensive patients? Curr Hypertens Rep. 2013;15(5):470-4.
97. Nyirjesy P, Zhao Y, Ways K, Usiskin K. Evaluation of vulvovaginal symptoms and Candida colonization in women with type 2 diabetes mellitus treated with canagliflozin, a sodium glucose co-transporter 2 inhibitor. Curr Med Res Opin. 2012;28(7):1173-8.
98. Ferrannini E, Muscelli E, Frascerra S, Baldi S, Mari A, Heise T, et al. Metabolic response to sodium-glucose cotransporter 2 inhibition in type 2 diabetic patients. J Clin Invest. 2014;124(2):499-508.
99. Gerich JE. Role of the kidney in normal glucose homeostasis and in the hyperglycaemia of diabetes mellitus: therapeutic implications. Diabet Med. 2010;27(2):136-42.
100. Cherney DZ, Scholey JW, Jiang S, Har R, Lai V, Sochett EB, et al. The effect of direct renin inhibition alone and in combination with ACE inhibition on endothelial function, arterial stiffness, and renal function in type 1 diabetes. Diabetes Care. 2012;35(11):2324-30.
101. De Nicola L, Gabbai FB, Liberti ME, Sagliocca A, Conte G, Minutolo R. Sodium/glucose cotransporter 2 inhibitors and prevention of diabetic nephropathy: targeting the renal tubule in diabetes. Am J Kidney Dis. 2014;64(1):16-24.
102. Abbiss H, Maker GL, Trengove RD. Metabolomics Approaches for the Diagnosis and Understanding of Kidney Diseases. Metabolites. 2019;9(2).
103. Wanner C, Inzucchi SE, Zinman B. Empagliflozin and Progression of Kidney Disease in Type 2 Diabetes. N Engl J Med. 2016;375(18):1801-2.

104. Perkovic V, de Zeeuw D, Mahaffey KW, Fulcher G, Erondu N, Shaw W, et al. Canagliflozin and renal outcomes in type 2 diabetes: results from the CANVAS Program randomised clinical trials. Lancet Diabetes Endocrinol. 2018;6(9):691-704.
105. Mosenzon O, Wiviott SD, Cahn A, Rozenberg A, Yanuv I, Goodrich EL, et al. Effects of dapagliflozin on development and progression of kidney disease in patients with type 2 diabetes: an analysis from the DECLARE-TIMI 58 randomised trial. Lancet Diabetes Endocrinol. 2019;7(8):606-17.
106. Perkovic V, Jardine MJ, Neal B, Bompoint S, Heerspink HJL, Charytan DM, et al. Canagliflozin and Renal Outcomes in Type 2 Diabetes and Nephropathy. N Engl J Med. 2019;380(24):2295-306.
107. Heerspink HJL, Kosiborod M, Inzucchi SE, Cherney DZI. Renoprotective effects of sodium-glucose cotransporter-2 inhibitors. Kidney Int. 2018;94(1):26-39.
108. Heerspink HJL, Stefánsson BV, Correa-Rotter R, Chertow GM, Greene T, Hou FF, et al. Dapagliflozin in Patients with Chronic Kidney Disease. N Engl J Med. 2020;383(15):1436-46.
109. Packer M, Anker SD, Butler J, Filippatos G, Pocock SJ, Carson P, et al. Cardiovascular and Renal Outcomes with Empagliflozin in Heart Failure. N Engl J Med. 2020;383(15):1413-24.
110. Lv W, Booz GW, Wang Y, Fan F, Roman RJ. Inflammation and renal fibrosis: Recent developments on key signaling molecules as potential therapeutic targets. Eur J Pharmacol. 2018;820:65-76.
111. Rahmoune H, Thompson PW, Ward JM, Smith CD, Hong G, Brown J. Glucose transporters in human renal proximal tubular cells isolated from the urine of patients with non-insulin-dependent diabetes. Diabetes. 2005;54(12):3427-34.
112. Vallon V, Gerasimova M, Rose MA, Masuda T, Satriano J, Mayoux E, et al. SGLT2 inhibitor empagliflozin reduces renal growth and albuminuria in proportion to hyperglycemia and prevents glomerular hyperfiltration in diabetic Akita mice. Am J Physiol Renal Physiol. 2014;306(2):F194-204.
113. Terami N, Ogawa D, Tachibana H, Hatanaka T, Wada J, Nakatsuka A, et al. Long-term treatment with the sodium glucose cotransporter 2 inhibitor, dapagliflozin, ameliorates glucose homeostasis and diabetic nephropathy in db/db mice. PLoS One. 2014;9(6):e100777.

114. Nagata T, Fukuzawa T, Takeda M, Fukazawa M, Mori T, Nihei T, et al. Tofogliflozin, a novel sodium-glucose co-transporter 2 inhibitor, improves renal and pancreatic function in db/db mice. Br J Pharmacol. 2013;170(3):519-31.
115. Lin B, Koibuchi N, Hasegawa Y, Sueta D, Toyama K, Uekawa K, et al. Glycemic control with empagliflozin, a novel selective SGLT2 inhibitor, ameliorates cardiovascular injury and cognitive dysfunction in obese and type 2 diabetic mice. Cardiovasc Diabetol. 2014;13:148.
116. Gangadharan Komala M, Gross S, Mudaliar H, Huang C, Pegg K, Mather A, et al. Inhibition of kidney proximal tubular glucose reabsorption does not prevent against diabetic nephropathy in type 1 diabetic eNOS knockout mice. PLoS One. 2014;9(11):e108994.
117. Tabatabai NM, Sharma M, Blumenthal SS, Petering DH. Enhanced expressions of sodium-glucose cotransporters in the kidneys of diabetic Zucker rats. Diabetes Res Clin Pract. 2009;83(1):e27-30.
118. Tuttle KR, Lakshmanan MC, Rayner B, Busch RS, Zimmermann AG, Woodward DB, et al. Dulaglutide versus insulin glargine in patients with type 2 diabetes and moderate-to-severe chronic kidney disease (AWARD-7): a multicentre, open-label, randomised trial. Lancet Diabetes Endocrinol. 2018;6(8):605-17.
119. Maldonado-Cervantes MI, Galicia OG, Moreno-Jaime B, Zapata-Morales JR, Montoya-Contreras A, Bautista-Perez R, et al. Autocrine modulation of glucose transporter SGLT2 by IL-6 and TNF-α in LLC-PK(1) cells. J Physiol Biochem. 2012;68(3):411-20.
120. Beloto-Silva O, Machado UF, Oliveira-Souza M. Glucose-induced regulation of NHEs activity and SGLTs expression involves the PKA signaling pathway. J Membr Biol. 2011;239(3):157-65.
121. Ghezzi C, Wright EM. Regulation of the human Na+-dependent glucose cotransporter hSGLT2. Am J Physiol Cell Physiol. 2012;303(3):C348-54.
122. Osorio H, Bautista R, Rios A, Franco M, Santamaría J, Escalante B. Effect of treatment with losartan on salt sensitivity and SGLT2 expression in hypertensive diabetic rats. Diabetes Res Clin Pract. 2009;86(3):e46-9.
123. Doblado M, Moley KH. Facilitative glucose transporter 9, a unique hexose and urate transporter. Am J Physiol Endocrinol Metab. 2009;297(4):E831-5.
124. Cain L, Shankar A, Ducatman AM, Steenland K. The relationship between serum uric acid and chronic kidney disease among Appalachian adults. Nephrol Dial Transplant. 2010;25(11):3593-9.

125. Komala MG, Panchapakesan U, Pollock C, Mather A. Sodium glucose cotransporter 2 and the diabetic kidney. Curr Opin Nephrol Hypertens. 2013;22(1):113-9.
126. Gallo LA, Ward MS, Fotheringham AK, Zhuang A, Borg DJ, Flemming NB, et al. Erratum: Once daily administration of the SGLT2 inhibitor, empagliflozin, attenuates markers of renal fibrosis without improving albuminuria in diabetic db/db mice. Sci Rep. 2016;6:28124.
127. Kawanami D, Matoba K, Takeda Y, Nagai Y, Akamine T, Yokota T, et al. SGLT2 Inhibitors as a Therapeutic Option for Diabetic Nephropathy. Int J Mol Sci. 2017;18(5).
128. Wang XX, Levi J, Luo Y, Myakala K, Herman-Edelstein M, Qiu L, et al. SGLT2 Protein Expression Is Increased in Human Diabetic Nephropathy: SGLT2 PROTEIN INHIBITION DECREASES RENAL LIPID ACCUMULATION, INFLAMMATION, AND THE DEVELOPMENT OF NEPHROPATHY IN DIABETIC MICE. J Biol Chem. 2017;292(13):5335-48.
129. Ishibashi Y, Matsui T, Yamagishi S. Tofogliflozin, A Highly Selective Inhibitor of SGLT2 Blocks Proinflammatory and Proapoptotic Effects of Glucose Overload on Proximal Tubular Cells Partly by Suppressing Oxidative Stress Generation. Horm Metab Res. 2016;48(3):191-5.
130. Heerspink HJL, Perco P, Mulder S, Leierer J, Hansen MK, Heinzel A, et al. Canagliflozin reduces inflammation and fibrosis biomarkers: a potential mechanism of action for beneficial effects of SGLT2 inhibitors in diabetic kidney disease. Diabetologia. 2019;62(7):1154-66.
131. Dekkers CCJ, Petrykiv S, Laverman GD, Cherney DZ, Gansevoort RT, Heerspink HJL. Effects of the SGLT-2 inhibitor dapagliflozin on glomerular and tubular injury markers. Diabetes Obes Metab. 2018;20(8):1988-93.
132. Chonchol M, Shlipak MG, Katz R, Sarnak MJ, Newman AB, Siscovick DS, et al. Relationship of uric acid with progression of kidney disease. Am J Kidney Dis. 2007;50(2):239-47.
133. Kitagawa K, Wada T, Furuichi K, Hashimoto H, Ishiwata Y, Asano M, et al. Blockade of CCR2 ameliorates progressive fibrosis in kidney. Am J Pathol. 2004;165(1):237-46.
134. Sassy-Prigent C, Heudes D, Mandet C, Bélair MF, Michel O, Perdereau B, et al. Early glomerular macrophage recruitment in streptozotocin-induced diabetic rats. Diabetes. 2000;49(3):466-75.
135. Giunti S, Barutta F, Perin PC, Gruden G. Targeting the MCP-1/CCR2 System in diabetic kidney disease. Curr Vasc Pharmacol. 2010;8(6):849-60.

136. Tam FW, Riser BL, Meeran K, Rambow J, Pusey CD, Frankel AH. Urinary monocyte chemoattractant protein-1 (MCP-1) and connective tissue growth factor (CCN2) as prognostic markers for progression of diabetic nephropathy. Cytokine. 2009;47(1):37-42.
137. Kohan DE, Pollock DM. Endothelin antagonists for diabetic and non-diabetic chronic kidney disease. Br J Clin Pharmacol. 2013;76(4):573-9.
138. Boels MGS, Koudijs A, Avramut MC, Sol WMPJ, Wang G, van Oeveren-Rietdijk AM, et al. Systemic Monocyte Chemotactic Protein-1 Inhibition Modifies Renal Macrophages and Restores Glomerular Endothelial Glycocalyx and Barrier Function in Diabetic Nephropathy. Am J Pathol. 2017;187(11):2430-40.
139. Chow FY, Nikolic-Paterson DJ, Ozols E, Atkins RC, Rollin BJ, Tesch GH. Monocyte chemoattractant protein-1 promotes the development of diabetic renal injury in streptozotocin-treated mice. Kidney Int. 2006;69(1):73-80.
140. Tarabra E, Giunti S, Barutta F, Salvidio G, Burt D, Deferrari G, et al. Effect of the monocyte chemoattractant protein-1/CC chemokine receptor 2 system on nephrin expression in streptozotocin-treated mice and human cultured podocytes. Diabetes. 2009;58(9):2109-18.
141. Dhaun N, Webb DJ. Endothelins in cardiovascular biology and therapeutics. Nat Rev Cardiol. 2019;16(8):491-502.
142. Spires D, Poudel B, Shields CA, Pennington A, Fizer B, Taylor L, et al. Prevention of the progression of renal injury in diabetic rodent models with preexisting renal disease with chronic endothelin A receptor blockade. Am J Physiol Renal Physiol. 2018;315(4):F977-F85.
143. Wenzel RR, Littke T, Kuranoff S, Jürgens C, Bruck H, Ritz E, et al. Avosentan reduces albumin excretion in diabetics with macroalbuminuria. J Am Soc Nephrol. 2009;20(3):655-64.
144. Kohan DE, Pritchett Y, Molitch M, Wen S, Garimella T, Audhya P, et al. Addition of atrasentan to renin-angiotensin system blockade reduces albuminuria in diabetic nephropathy. J Am Soc Nephrol. 2011;22(4):763-72.
145. Maayah ZH, Ferdaoussi M, Takahara S, Soni S, Dyck JRB. Empagliflozin suppresses inflammation and protects against acute septic renal injury. Inflammopharmacology. 2021;29(1):269-79.

146. Pirklbauer M, Sallaberger S, Staudinger P, Corazza U, Leierer J, Mayer G, et al. Empagliflozin Inhibits IL-1β-Mediated Inflammatory Response in Human Proximal Tubular Cells. Int J Mol Sci. 2021;22(10).
147. Moynihan KA, Grimm AA, Plueger MM, Bernal-Mizrachi E, Ford E, Cras-Méneur C, et al. Increased dosage of mammalian Sir2 in pancreatic beta cells enhances glucose-stimulated insulin secretion in mice. Cell Metab. 2005;2(2):105-17.
148. Umino H, Hasegawa K, Minakuchi H, Muraoka H, Kawaguchi T, Kanda T, et al. High Basolateral Glucose Increases Sodium-Glucose Cotransporter 2 and Reduces Sirtuin-1 in Renal Tubules through Glucose Transporter-2 Detection. Sci Rep. 2018;8(1):6791.
149. Elibol B, Kilic U. High Levels of SIRT1 Expression as a Protective Mechanism Against Disease-Related Conditions. Front Endocrinol (Lausanne). 2018;9:614.
150. Zhong Y, Lee K, He JC. SIRT1 Is a Potential Drug Target for Treatment of Diabetic Kidney Disease. Front Endocrinol (Lausanne). 2018;9:624.
151. Kumar S, Lombard DB. Mitochondrial sirtuins and their relationships with metabolic disease and cancer. Antioxid Redox Signal. 2015;22(12):1060-77.
152. Perico L, Morigi M, Rota C, Breno M, Mele C, Noris M, et al. Human mesenchymal stromal cells transplanted into mice stimulate renal tubular cells and enhance mitochondrial function. Nat Commun. 2017;8(1):983.
153. Tian J, Zhang M, Suo M, Liu D, Wang X, Liu M, et al. Dapagliflozin alleviates cardiac fibrosis through suppressing EndMT and fibroblast activation via AMPKα/TGF-β/Smad signalling in type 2 diabetic rats. J Cell Mol Med. 2021;25(16):7642-59.
154. Lerrer B, Gertler AA, Cohen HY. The complex role of SIRT6 in carcinogenesis. Carcinogenesis. 2016;37(2):108-18.
155. Morigi M, Perico L, Benigni A. Sirtuins in Renal Health and Disease. J Am Soc Nephrol. 2018;29(7):1799-809.
156. Stark GR, Darnell JE. The JAK-STAT pathway at twenty. Immunity. 2012;36(4):503-14.
157. Darnell JE. STATs and gene regulation. Science. 1997;277(5332):1630-5.
158. Kawai M, Namba N, Mushiake S, Etani Y, Nishimura R, Makishima M, et al. Growth hormone stimulates adipogenesis of 3T3-L1 cells through activation of the Stat5A/5B-PPARgamma pathway. J Mol Endocrinol. 2007;38(1-2):19-34.
159. Richard AJ, Stephens JM. The role of JAK-STAT signaling in adipose tissue function. Biochim Biophys Acta. 2014;1842(3):431-9.

160. Wegrzyn J, Potla R, Chwae YJ, Sepuri NB, Zhang Q, Koeck T, et al. Function of mitochondrial Stat3 in cellular respiration. Science. 2009;323(5915):793-7.
161. Tontonoz P, Hu E, Graves RA, Budavari AI, Spiegelman BM. mPPAR gamma 2: tissue-specific regulator of an adipocyte enhancer. Genes Dev. 1994;8(10):1224-34.
162. Wasik AA, Dumont V, Tienari J, Nyman TA, Fogarty CL, Forsblom C, et al. Septin 7 reduces nonmuscle myosin IIA activity in the SNAP23 complex and hinders GLUT4 storage vesicle docking and fusion. Exp Cell Res. 2017;350(2):336-48.
163. Astapova O, Leff T. Adiponectin and PPARγ: cooperative and interdependent actions of two key regulators of metabolism. Vitam Horm. 2012;90:143-62.
164. Rosen ED, Walkey CJ, Puigserver P, Spiegelman BM. Transcriptional regulation of adipogenesis. Genes Dev. 2000;14(11):1293-307.
165. Tontonoz P, Spiegelman BM. Fat and beyond: the diverse biology of PPARgamma. Annu Rev Biochem. 2008;77:289-312.
166. Christodoulides C, Vidal-Puig A. PPARs and adipocyte function. Mol Cell Endocrinol. 2010;318(1-2):61-8.
167. Eeckhoute J, Oger F, Staels B, Lefebvre P. Coordinated Regulation of PPARγ Expression and Activity through Control of Chromatin Structure in Adipogenesis and Obesity. PPAR Res. 2012;2012:164140.
168. Ge J, Miao JJ, Sun XY, Yu JY. Huangkui capsule, an extract from Abelmoschus manihot (L.) medic, improves diabetic nephropathy via activating peroxisome proliferator-activated receptor (PPAR)-α/γ and attenuating endoplasmic reticulum stress in rats. J Ethnopharmacol. 2016;189:238-49.
169. Ong ALC, Ramasamy TS. Role of Sirtuin1-p53 regulatory axis in aging, cancer and cellular reprogramming. Ageing Res Rev. 2018;43:64-80.
170. Saito R, Rocanin-Arjo A, You YH, Darshi M, Van Espen B, Miyamoto S, et al. Systems biology analysis reveals the role of MDM2 in diabetic nephropathy. JCI Insight. 2016;1(17):e87877.
171. Menini S, Iacobini C, Oddi G, Ricci C, Simonelli P, Fallucca S, et al. Increased glomerular cell (podocyte) apoptosis in rats with streptozotocin-induced diabetes mellitus: role in the development of diabetic glomerular disease. Diabetologia. 2007;50(12):2591-9.
172. Mishra M, Flaga J, Kowluru RA. Molecular Mechanism of Transcriptional Regulation of Matrix Metalloproteinase-9 in Diabetic Retinopathy. J Cell Physiol. 2016;231(8):1709-18.

173. Ma F, Wu J, Jiang Z, Huang W, Jia Y, Sun W, et al. P53/NRF2 mediates SIRT1's protective effect on diabetic nephropathy. Biochim Biophys Acta Mol Cell Res. 2019;1866(8):1272-81.
174. Wang W, Huang XR, Li AG, Liu F, Li JH, Truong LD, et al. Signaling mechanism of TGF-beta1 in prevention of renal inflammation: role of Smad7. J Am Soc Nephrol. 2005;16(5):1371-83.
175. Hayashi H, Abdollah S, Qiu Y, Cai J, Xu YY, Grinnell BW, et al. The MAD-related protein Smad7 associates with the TGFbeta receptor and functions as an antagonist of TGFbeta signaling. Cell. 1997;89(7):1165-73.
176. Kavsak P, Rasmussen RK, Causing CG, Bonni S, Zhu H, Thomsen GH, et al. Smad7 binds to Smurf2 to form an E3 ubiquitin ligase that targets the TGF beta receptor for degradation. Mol Cell. 2000;6(6):1365-75.
177. Ka SM, Huang XR, Lan HY, Tsai PY, Yang SM, Shui HA, et al. Smad7 gene therapy ameliorates an autoimmune crescentic glomerulonephritis in mice. J Am Soc Nephrol. 2007;18(6):1777-88.
178. Huang XR, Chung AC, Zhou L, Wang XJ, Lan HY. Latent TGF-beta1 protects against crescentic glomerulonephritis. J Am Soc Nephrol. 2008;19(2):233-42.
179. Meng XM, Tang PM, Li J, Lan HY. TGF-β/Smad signaling in renal fibrosis. Front Physiol. 2015;6:82.
180. Lan HY. Diverse roles of TGF-β/Smads in renal fibrosis and inflammation. Int J Biol Sci. 2011;7(7):1056-67.
181. Cho H, Thorvaldsen JL, Chu Q, Feng F, Birnbaum MJ. Akt1/PKBalpha is required for normal growth but dispensable for maintenance of glucose homeostasis in mice. J Biol Chem. 2001;276(42):38349-52.
182. Yang K, Chen Z, Gao J, Shi W, Li L, Jiang S, et al. The Key Roles of GSK-3β in Regulating Mitochondrial Activity. Cell Physiol Biochem. 2017;44(4):1445-59.
183. Jing D, Bai H, Yin S. Renoprotective effects of emodin against diabetic nephropathy in rat models are mediated via PI3K/Akt/GSK-3β and Bax/caspase-3 signaling pathways. Exp Ther Med. 2017;14(5):5163-9.
184. Rane MJ, Song Y, Jin S, Barati MT, Wu R, Kausar H, et al. Interplay between Akt and p38 MAPK pathways in the regulation of renal tubular cell apoptosis associated with diabetic nephropathy. Am J Physiol Renal Physiol. 2010;298(1):F49-61.

185. Zhang X, Lu Z, Abdul KSM, Changping MA, Tan KS, Jovanovi A, et al. Isosteviol sodium protects heart embryonic H9c2 cells against oxidative stress by activating Akt/GSK-3β signaling pathway. Pharmazie. 2020;75(1):36-40.
186. de Zeeuw D, Remuzzi G, Parving HH, Keane WF, Zhang Z, Shahinfar S, et al. Proteinuria, a target for renoprotection in patients with type 2 diabetic nephropathy: lessons from RENAAL. Kidney Int. 2004;65(6):2309-20.
187. Yale JF, Bakris G, Cariou B, Yue D, David-Neto E, Xi L, et al. Efficacy and safety of canagliflozin in subjects with type 2 diabetes and chronic kidney disease. Diabetes Obes Metab. 2013;15(5):463-73.
188. Kojima N, Williams JM, Takahashi T, Miyata N, Roman RJ. Effects of a new SGLT2 inhibitor, luseogliflozin, on diabetic nephropathy in T2DN rats. J Pharmacol Exp Ther. 2013;345(3):464-72.
189. Goicoechea M, de Vinuesa SG, Verdalles U, Ruiz-Caro C, Ampuero J, Rincón A, et al. Effect of allopurinol in chronic kidney disease progression and cardiovascular risk. Clin J Am Soc Nephrol. 2010;5(8):1388-93.
190. Iseki K, Oshiro S, Tozawa M, Iseki C, Ikemiya Y, Takishita S. Significance of hyperuricemia on the early detection of renal failure in a cohort of screened subjects. Hypertens Res. 2001;24(6):691-7.
191. Hovind P, Rossing P, Johnson RJ, Parving HH. Serum uric acid as a new player in the development of diabetic nephropathy. J Ren Nutr. 2011;21(1):124-7.
192. Kang DH, Nakagawa T, Feng L, Watanabe S, Han L, Mazzali M, et al. A role for uric acid in the progression of renal disease. J Am Soc Nephrol. 2002;13(12):2888-97.
193. Cefalu WT, Leiter LA, Yoon KH, Arias P, Niskanen L, Xie J, et al. Efficacy and safety of canagliflozin versus glimepiride in patients with type 2 diabetes inadequately controlled with metformin (CANTATA-SU): 52 week results from a randomised, double-blind, phase 3 non-inferiority trial. Lancet. 2013;382(9896):941-50.
194. Bailey CJ, Gross JL, Pieters A, Bastien A, List JF. Effect of dapagliflozin in patients with type 2 diabetes who have inadequate glycaemic control with metformin: a randomised, double-blind, placebo-controlled trial. Lancet. 2010;375(9733):2223-33.
195. Wilding JP, Ferrannini E, Fonseca VA, Wilpshaar W, Dhanjal P, Houzer A. Efficacy and safety of ipragliflozin in patients with type 2 diabetes inadequately controlled on metformin: a dose-finding study. Diabetes Obes Metab. 2013;15(5):403-9.

196. Schernthaner G, Schernthaner-Reiter MH, Schernthaner GH. EMPA-REG and Other Cardiovascular Outcome Trials of Glucose-lowering Agents: Implications for Future Treatment Strategies in Type 2 Diabetes Mellitus. Clin Ther. 2016;38(6):1288-98.
197. Zinman B, Wanner C, Lachin JM, Fitchett D, Bluhmki E, Hantel S, et al. Empagliflozin, Cardiovascular Outcomes, and Mortality in Type 2 Diabetes. N Engl J Med. 2015;373(22):2117-28.
198. Neuen BL, Young T, Heerspink HJL, Neal B, Perkovic V, Billot L, et al. SGLT2 inhibitors for the prevention of kidney failure in patients with type 2 diabetes: a systematic review and meta-analysis. Lancet Diabetes Endocrinol. 2019;7(11):845-54.
199. Kalra S, Singh V, Nagrale D. Sodium-Glucose Cotransporter-2 Inhibition and the Glomerulus: A Review. Adv Ther. 2016;33(9):1502-18.
200. Molitch ME, Adler AI, Flyvbjerg A, Nelson RG, So WY, Wanner C, et al. Diabetic kidney disease: a clinical update from Kidney Disease: Improving Global Outcomes. Kidney Int. 2015;87(1):20-30.
201. Anker SD, Butler J, Filippatos G, Ferreira JP, Bocchi E, Böhm M, et al. Empagliflozin in Heart Failure with a Preserved Ejection Fraction. N Engl J Med. 2021;385(16):1451-61.
202. McMurray JJV, Solomon SD, Inzucchi SE, Køber L, Kosiborod MN, Martinez FA, et al. Dapagliflozin in Patients with Heart Failure and Reduced Ejection Fraction. N Engl J Med. 2019;381(21):1995-2008.
203. Cherney DZI, Bakris GL. Novel therapies for diabetic kidney disease. Kidney Int Suppl (2011). 2018;8(1):18-25.
204. Bloomgarden Z. The kidney and cardiovascular outcome trials. J Diabetes. 2018;10(2):88-9.
205. León Jiménez D, Cherney DZI, Bjornstad P, Guerra LC, Miramontes González JP. Antihyperglycemic agents as novel natriuretic therapies in diabetic kidney disease. Am J Physiol Renal Physiol. 2018;315(5):F1406-F15.
206. Marso SP, Daniels GH, Brown-Frandsen K, Kristensen P, Mann JF, Nauck MA, et al. Liraglutide and Cardiovascular Outcomes in Type 2 Diabetes. N Engl J Med. 2016;375(4):311-22.
207. Hernandez AF, Green JB, Janmohamed S, D'Agostino RB, Granger CB, Jones NP, et al. Albiglutide and cardiovascular outcomes in patients with type 2 diabetes and cardiovascular disease (Harmony Outcomes): a double-blind, randomised placebo-controlled trial. Lancet. 2018;392(10157):1519-29.

208. Gerstein HC, Colhoun HM, Dagenais GR, Diaz R, Lakshmanan M, Pais P, et al. Dulaglutide and cardiovascular outcomes in type 2 diabetes (REWIND): a double-blind, randomised placebo-controlled trial. Lancet. 2019;394(10193):121-30.
209. Pfeffer MA, Claggett B, Diaz R, Dickstein K, Gerstein HC, Køber LV, et al. Lixisenatide in Patients with Type 2 Diabetes and Acute Coronary Syndrome. N Engl J Med. 2015;373(23):2247-57.
210. Holman RR, Bethel MA, Mentz RJ, Thompson VP, Lokhnygina Y, Buse JB, et al. Effects of Once-Weekly Exenatide on Cardiovascular Outcomes in Type 2 Diabetes. N Engl J Med. 2017;377(13):1228-39.
211. Koska J, Sands M, Burciu C, D'Souza KM, Raravikar K, Liu J, et al. Exenatide Protects Against Glucose- and Lipid-Induced Endothelial Dysfunction: Evidence for Direct Vasodilation Effect of GLP-1 Receptor Agonists in Humans. Diabetes. 2015;64(7):2624-35.
212. Rakipovski G, Rolin B, Nøhr J, Klewe I, Frederiksen KS, Augustin R, et al. The GLP-1 Analogs Liraglutide and Semaglutide Reduce Atherosclerosis in ApoE. JACC Basic Transl Sci. 2018;3(6):844-57.
213. Aravindhan K, Bao W, Harpel MR, Willette RN, Lepore JJ, Jucker BM. Cardioprotection Resulting from Glucagon-Like Peptide-1 Administration Involves Shifting Metabolic Substrate Utilization to Increase Energy Efficiency in the Rat Heart. PLoS One. 2015;10(6):e0130894.
214. Noyan-Ashraf MH, Momen MA, Ban K, Sadi AM, Zhou YQ, Riazi AM, et al. GLP-1R agonist liraglutide activates cytoprotective pathways and improves outcomes after experimental myocardial infarction in mice. Diabetes. 2009;58(4):975-83.
215. Striepe K, Jumar A, Ott C, Karg MV, Schneider MP, Kannenkeril D, et al. Effects of the Selective Sodium-Glucose Cotransporter 2 Inhibitor Empagliflozin on Vascular Function and Central Hemodynamics in Patients With Type 2 Diabetes Mellitus. Circulation. 2017;136(12):1167-9.
216. Chilton R, Tikkanen I, Cannon CP, Crowe S, Woerle HJ, Broedl UC, et al. Effects of empagliflozin on blood pressure and markers of arterial stiffness and vascular resistance in patients with type 2 diabetes. Diabetes Obes Metab. 2015;17(12):1180-93.
217. Li H, Shin SE, Seo MS, An JR, Choi IW, Jung WK, et al. The anti-diabetic drug dapagliflozin induces vasodilation via activation of PKG and Kv channels. Life Sci. 2018;197:46-55.

218. Santos-Gallego CG, García-Ropero Á, Badimon JJ. Spark That Lights the Fire: Infection Triggers Cardiovascular Events. J Am Heart Assoc. 2018;7(22):e011175.
219. Kappel BA, Lehrke M, Schütt K, Artati A, Adamski J, Lebherz C, et al. Effect of Empagliflozin on the Metabolic Signature of Patients With Type 2 Diabetes Mellitus and Cardiovascular Disease. Circulation. 2017;136(10):969-72.
220. Packer M, Anker SD, Butler J, Filippatos G, Zannad F. Effects of Sodium-Glucose Cotransporter 2 Inhibitors for the Treatment of Patients With Heart Failure: Proposal of a Novel Mechanism of Action. JAMA Cardiol. 2017;2(9):1025-9.
221. Uthman L, Baartscheer A, Bleijlevens B, Schumacher CA, Fiolet JWT, Koeman A, et al. Class effects of SGLT2 inhibitors in mouse cardiomyocytes and hearts: inhibition of Na. Diabetologia. 2018;61(3):722-6.
222. Baartscheer A, Schumacher CA, Wüst RC, Fiolet JW, Stienen GJ, Coronel R, et al. Empagliflozin decreases myocardial cytoplasmic Na. Diabetologia. 2017;60(3):568-73.
223. Lee TM, Chang NC, Lin SZ. Dapagliflozin, a selective SGLT2 Inhibitor, attenuated cardiac fibrosis by regulating the macrophage polarization via STAT3 signaling in infarcted rat hearts. Free Radic Biol Med. 2017;104:298-310.
224. Packer M. Epicardial Adipose Tissue May Mediate Deleterious Effects of Obesity and Inflammation on the Myocardium. J Am Coll Cardiol. 2018;71(20):2360-72.
225. Packer M. Do sodium-glucose co-transporter-2 inhibitors prevent heart failure with a preserved ejection fraction by counterbalancing the effects of leptin? A novel hypothesis. Diabetes Obes Metab. 2018;20(6):1361-6.
226. Garvey WT, Van Gaal L, Leiter LA, Vijapurkar U, List J, Cuddihy R, et al. Effects of canagliflozin versus glimepiride on adipokines and inflammatory biomarkers in type 2 diabetes. Metabolism. 2018;85:32-7.
227. Sato T, Aizawa Y, Yuasa S, Kishi S, Fuse K, Fujita S, et al. The effect of dapagliflozin treatment on epicardial adipose tissue volume. Cardiovasc Diabetol. 2018;17(1):6.
228. Wanner C, Lachin JM, Inzucchi SE, Fitchett D, Mattheus M, George J, et al. Empagliflozin and Clinical Outcomes in Patients With Type 2 Diabetes Mellitus, Established Cardiovascular Disease, and Chronic Kidney Disease. Circulation. 2018;137(2):119-29.
229. Neal B, Perkovic V, Matthews DR. Canagliflozin and Cardiovascular and Renal Events in Type 2 Diabetes. N Engl J Med. 2017;377(21):2099.
230. Wiviott SD, Raz I, Bonaca MP, Mosenzon O, Kato ET, Cahn A, et al. Dapagliflozin and Cardiovascular Outcomes in Type 2 Diabetes. N Engl J Med. 2019;380(4):347-57.

231. Zelniker TA, Wiviott SD, Raz I, Im K, Goodrich EL, Bonaca MP, et al. SGLT2 inhibitors for primary and secondary prevention of cardiovascular and renal outcomes in type 2 diabetes: a systematic review and meta-analysis of cardiovascular outcome trials. Lancet. 2019;393(10166):31-9.
232. Toyama T, Neuen BL, Jun M, Ohkuma T, Neal B, Jardine MJ, et al. Effect of SGLT2 inhibitors on cardiovascular, renal and safety outcomes in patients with type 2 diabetes mellitus and chronic kidney disease: A systematic review and meta-analysis. Diabetes Obes Metab. 2019;21(5):1237-50.
233. Cosentino F, Grant PJ, Aboyans V, Bailey CJ, Ceriello A, Delgado V, et al. 2019 ESC Guidelines on diabetes, pre-diabetes, and cardiovascular diseases developed in collaboration with the EASD. Eur Heart J. 2019.
234. Hull RN, Cherry WR, Weaver GW. The origin and characteristics of a pig kidney cell strain, LLC-PK. In Vitro. 1976;12(10):670-7.
235. Nielsen R, Birn H, Moestrup SK, Nielsen M, Verroust P, Christensen EI. Characterization of a kidney proximal tubule cell line, LLC-PK1, expressing endocytotic active megalin. J Am Soc Nephrol. 1998;9(10):1767-76.
236. Rabito CA. Occluding junctions in a renal cell line (LLC-PK1) with characteristics of proximal tubular cells. Am J Physiol. 1986;250(4 Pt 2):F734-43.
237. Zhu XJ, Gong Z, Li SJ, Jia HP, Li DL. Long non-coding RNA Hottip modulates high-glucose-induced inflammation and ECM accumulation through miR-455-3p/WNT2B in mouse mesangial cells. Int J Clin Exp Pathol. 2019;12(7):2435-45.
238. Masella R, Di Benedetto R, Varì R, Filesi C, Giovannini C. Novel mechanisms of natural antioxidant compounds in biological systems: involvement of glutathione and glutathione-related enzymes. J Nutr Biochem. 2005;16(10):577-86.
239. Jones DP, Carlson JL, Mody VC, Cai J, Lynn MJ, Sternberg P. Redox state of glutathione in human plasma. Free Radic Biol Med. 2000;28(4):625-35.
240. Valko M, Leibfritz D, Moncol J, Cronin MT, Mazur M, Telser J. Free radicals and antioxidants in normal physiological functions and human disease. Int J Biochem Cell Biol. 2007;39(1):44-84.
241. Sapiro JM, Monks TJ, Lau SS. All-. Am J Physiol Renal Physiol. 2017;313(6):F1200-F8.
242. Gunness P, Aleksa K, Kosuge K, Ito S, Koren G. Comparison of the novel HK-2 human renal proximal tubular cell line with the standard LLC-PK1 cell line in studying drug-induced nephrotoxicity. Can J Physiol Pharmacol. 2010;88(4):448-55.

243. Milorad Z. Effects of changes in glycolipid

cell membrane composition on the composition of lipid rafts in SH-SY5Y human

neuroblastoma cell line. Osijek: Faculty of Medicine, J.J. Strossmayer University of Osijek; 2021.

244. Gallicchio MA, Bach LA. Uptake of advanced glycation end products by proximal tubule epithelial cells via macropinocytosis. Biochim Biophys Acta. 2013;1833(12):2922-32.

245. Zjalić M, Mustapić M, Glumac Z, Prološčić I, Blažetić S, Vuković A, et al. Construction of AC/DC magnetic syringe device for stimulated drug release, injection and ejection of nanocarriers and testing cytotoxicity. MethodsX. 2021;8:101312.

246. Brownlee M. The pathobiology of diabetic complications: a unifying mechanism. Diabetes. 2005;54(6):1615-25.

247. Elmarakby AA, Sullivan JC. Relationship between oxidative stress and inflammatory cytokines in diabetic nephropathy. Cardiovasc Ther. 2012;30(1):49-59.

248. Mima A, Hiraoka-Yamomoto J, Li Q, Kitada M, Li C, Geraldes P, et al. Protective effects of GLP-1 on glomerular endothelium and its inhibition by PKCβ activation in diabetes. Diabetes. 2012;61(11):2967-79.

249. Hendarto H, Inoguchi T, Maeda Y, Ikeda N, Zheng J, Takei R, et al. GLP-1 analog liraglutide protects against oxidative stress and albuminuria in streptozotocin-induced diabetic rats via protein kinase A-mediated inhibition of renal NAD(P)H oxidases. Metabolism. 2012;61(10):1422-34.

250. Yao D, Wang S, Wang M, Lu W. Renoprotection of dapagliflozin in human renal proximal tubular cells via the inhibition of the high mobility group box 1- receptor for advanced glycation end products- nuclear factor- κB signaling pathway. Mol Med Rep. 2018;18(4):3625-30.

251. Lee WC, Chau YY, Ng HY, Chen CH, Wang PW, Liou CW, et al. Empagliflozin Protects HK-2 Cells from High Glucose-Mediated Injuries via a Mitochondrial Mechanism. Cells. 2019;8(9).

252. Smith JD, Huang Z, Escobar PA, Foppiano P, Maw H, Loging W, et al. A Predominant Oxidative Renal Metabolite of Empagliflozin in Male Mice Is Cytotoxic in Mouse Renal Tubular Cells but not Genotoxic. Int J Toxicol. 2017;36(6):440-8.

253. Uthman L, Homayr A, Juni RP, Spin EL, Kerindongo R, Boomsma M, et al. Empagliflozin and Dapagliflozin Reduce ROS Generation and Restore NO

Bioavailability in Tumor Necrosis Factor α-Stimulated Human Coronary Arterial Endothelial Cells. Cell Physiol Biochem. 2019;53(5):865-86.

254. Nauck MA, Meier JJ. Glucagon-like peptide 1 and its derivatives in the treatment of diabetes. Regul Pept. 2005;128(2):135-48.
255. Schlatter P, Beglinger C, Drewe J, Gutmann H. Glucagon-like peptide 1 receptor expression in primary porcine proximal tubular cells. Regul Pept. 2007;141(1-3):120-8.
256. Baer PC, Koch B, Freitag J, Schubert R, Geiger H. No Cytotoxic and Inflammatory Effects of Empagliflozin and Dapagliflozin on Primary Renal Proximal Tubular Epithelial Cells under Diabetic Conditions In Vitro. Int J Mol Sci. 2020;21(2).
257. Chen JP, Xu DG, Yu XY, Zhao FM, Xu DQ, Zhang X, et al. Discrepancy between the effects of morronside on apoptosis in human embryonic lung fibroblast cells and lung cancer A549 cells. Oncol Lett. 2014;7(4):927-32.
258. Tong Y, Liu S, Gong R, Zhong L, Duan X, Zhu Y. Ethyl Vanillin Protects against Kidney Injury in Diabetic Nephropathy by Inhibiting Oxidative Stress and Apoptosis. Oxid Med Cell Longev. 2019;2019:2129350.
259. Cui J, Mo J, Luo M, Yu Q, Zhou S, Li T, et al. c-Myc-activated long non-coding RNA H19 downregulates miR-107 and promotes cell cycle progression of non-small cell lung cancer. Int J Clin Exp Pathol. 2015;8(10):12400-9.
260. Kaushik N, Uddin N, Sim GB, Hong YJ, Baik KY, Kim CH, et al. Responses of solid tumor cells in DMEM to reactive oxygen species generated by non-thermal plasma and chemically induced ROS systems. Sci Rep. 2015;5:8587.
261. Mukherjee K, Chio TI, Sackett DL, Bane SL. Detection of oxidative stress-induced carbonylation in live mammalian cells. Free Radic Biol Med. 2015;84:11-21.
262. Lee E, Lee HS. Peroxidase expression is decreased by palmitate in cultured podocytes but increased in podocytes of advanced diabetic nephropathy. J Cell Physiol. 2018;233(12):9060-9.
263. Peruchetti DB, Silva-Aguiar RP, Siqueira GM, Dias WB, Caruso-Neves C. High glucose reduces megalin-mediated albumin endocytosis in renal proximal tubule cells through protein kinase B. J Biol Chem. 2018;293(29):11388-400.
264. Wang C, Li L, Liu S, Liao G, Chen Y, Cheng J, et al. GLP-1 receptor agonist ameliorates obesity-induced chronic kidney injury via restoring renal metabolism homeostasis. PLoS One. 2018;13(3):e0193473.
265. Birben E, Sahiner UM, Sackesen C, Erzurum S, Kalayci O. Oxidative stress and antioxidant defense. World Allergy Organ J. 2012;5(1):9-19.

266. Tan BL, Norhaizan ME, Liew WP, Sulaiman Rahman H. Antioxidant and Oxidative Stress: A Mutual Interplay in Age-Related Diseases. Front Pharmacol. 2018;9:1162.
267. Huang HS, Ma MC, Chen J, Chen CF. Changes in the oxidant-antioxidant balance in the kidney of rats with nephrolithiasis induced by ethylene glycol. J Urol. 2002;167(6):2584-93.
268. Krause GC, Lima KG, Dias HB, da Silva EFG, Haute GV, Basso BS, et al. Liraglutide, a glucagon-like peptide-1 analog, induce autophagy and senescence in HepG2 cells. Eur J Pharmacol. 2017;809:32-41.
269. Ndibalema AR, Kabuye D, Wen S, Li L, Li X, Fan Q. Empagliflozin Protects Against Proximal Renal Tubular Cell Injury Induced by High Glucose via Regulation of Hypoxia-Inducible Factor 1-Alpha. Diabetes Metab Syndr Obes. 2020;13:1953-67.
270. Sun L, Dutta RK, Xie P, Kanwar YS. myo-Inositol Oxygenase Overexpression Accentuates Generation of Reactive Oxygen Species and Exacerbates Cellular Injury following High Glucose Ambience: A NEW MECHANISM RELEVANT TO THE PATHOGENESIS OF DIABETIC NEPHROPATHY. J Biol Chem. 2016;291(11):5688-707.
271. Iglesias-De La Cruz MC, Ruiz-Torres P, Alcamí J, Díez-Marqués L, Ortega-Velázquez R, Chen S, et al. Hydrogen peroxide increases extracellular matrix mRNA through TGF-beta in human mesangial cells. Kidney Int. 2001;59(1):87-95.
272. Chen P, Shi X, Xu X, Lin Y, Shao Z, Wu R, et al. Liraglutide ameliorates early renal injury by the activation of renal FoxO1 in a type 2 diabetic kidney disease rat model. Diabetes Res Clin Pract. 2018;137:173-82.
273. Ying Y, Kim J, Westphal SN, Long KE, Padanilam BJ. Targeted deletion of p53 in the proximal tubule prevents ischemic renal injury. J Am Soc Nephrol. 2014;25(12):2707-16.
274. Peng J, Li X, Zhang D, Chen JK, Su Y, Smith SB, et al. Hyperglycemia, p53, and mitochondrial pathway of apoptosis are involved in the susceptibility of diabetic models to ischemic acute kidney injury. Kidney Int. 2015;87(1):137-50.
275. Wang J, Pan J, Li H, Long J, Fang F, Chen J, et al. lncRNA ZEB1-AS1 Was Suppressed by p53 for Renal Fibrosis in Diabetic Nephropathy. Mol Ther Nucleic Acids. 2018;12:741-50.
276. Deshpande SD, Putta S, Wang M, Lai JY, Bitzer M, Nelson RG, et al. Transforming growth factor-β-induced cross talk between p53 and a microRNA in the pathogenesis of diabetic nephropathy. Diabetes. 2013;62(9):3151-62.

277. Ma Y, Yan R, Wan Q, Lv B, Yang Y, Lv T, et al. Inhibitor of growth 2 regulates the high glucose-induced cell cycle arrest and epithelial-to-mesenchymal transition in renal proximal tubular cells. J Physiol Biochem. 2020;76(3):373-82.
278. Irudayaraj SS, Stalin A, Sunil C, Duraipandiyan V, Al-Dhabi NA, Ignacimuthu S. Antioxidant, antilipidemic and antidiabetic effects of ficusin with their effects on GLUT4 translocation and PPARγ expression in type 2 diabetic rats. Chem Biol Interact. 2016;256:85-93.
279. Zhou Z, Wan J, Hou X, Geng J, Li X, Bai X. MicroRNA-27a promotes podocyte injury via PPARγ-mediated β-catenin activation in diabetic nephropathy. Cell Death Dis. 2017;8(3):e2658.
280. Tikoo K, Singh K, Kabra D, Sharma V, Gaikwad A. Change in histone H3 phosphorylation, MAP kinase p38, SIR 2 and p53 expression by resveratrol in preventing streptozotocin induced type I diabetic nephropathy. Free Radic Res. 2008;42(4):397-404.
281. Hong SW, Isono M, Chen S, Iglesias-De La Cruz MC, Han DC, Ziyadeh FN. Increased glomerular and tubular expression of transforming growth factor-beta1, its type II receptor, and activation of the Smad signaling pathway in the db/db mouse. Am J Pathol. 2001;158(5):1653-63.
282. Li JH, Huang XR, Zhu HJ, Oldfield M, Cooper M, Truong LD, et al. Advanced glycation end products activate Smad signaling via TGF-beta-dependent and independent mechanisms: implications for diabetic renal and vascular disease. FASEB J. 2004;18(1):176-8.
283. Li JH, Huang XR, Zhu HJ, Johnson R, Lan HY. Role of TGF-beta signaling in extracellular matrix production under high glucose conditions. Kidney Int. 2003;63(6):2010-9.
284. Chen HY, Huang XR, Wang W, Li JH, Heuchel RL, Chung AC, et al. The protective role of Smad7 in diabetic kidney disease: mechanism and therapeutic potential. Diabetes. 2011;60(2):590-601.
285. Li C, Zhang J, Xue M, Li X, Han F, Liu X, et al. SGLT2 inhibition with empagliflozin attenuates myocardial oxidative stress and fibrosis in diabetic mice heart. Cardiovasc Diabetol. 2019;18(1):15.
286. Fujita H, Omori S, Ishikura K, Hida M, Awazu M. ERK and p38 mediate high-glucose-induced hypertrophy and TGF-beta expression in renal tubular cells. Am J Physiol Renal Physiol. 2004;286(1):F120-6.

287. McManus EJ, Sakamoto K, Armit LJ, Ronaldson L, Shpiro N, Marquez R, et al. Role that phosphorylation of GSK3 plays in insulin and Wnt signalling defined by knockin analysis. EMBO J. 2005;24(8):1571-83.
288. Navarro-González JF, Mora-Fernández C. The role of inflammatory cytokines in diabetic nephropathy. J Am Soc Nephrol. 2008;19(3):433-42.
289. Qiao YC, Chen YL, Pan YH, Ling W, Tian F, Zhang XX, et al. Changes of transforming growth factor beta 1 in patients with type 2 diabetes and diabetic nephropathy: A PRISMA-compliant systematic review and meta-analysis. Medicine (Baltimore). 2017;96(15):e6583.
290. Wang D, Hu B, Hu C, Zhu F, Liu X, Zhang J, et al. Clinical Characteristics of 138 Hospitalized Patients With 2019 Novel Coronavirus-Infected Pneumonia in Wuhan, China. JAMA. 2020.
291. Zhou H, Zhu P, Guo J, Hu N, Wang S, Li D, et al. Ripk3 induces mitochondrial apoptosis via inhibition of FUNDC1 mitophagy in cardiac IR injury. Redox Biol. 2017;13:498-507.
292. Winiarska A, Knysak M, Nabrdalik K, Gumprecht J, Stompór T. Inflammation and Oxidative Stress in Diabetic Kidney Disease: The Targets for SGLT2 Inhibitors and GLP-1 Receptor Agonists. Int J Mol Sci. 2021;22(19).
293. Lee N, Heo YJ, Choi SE, Jeon JY, Han SJ, Kim DJ, et al. Anti-inflammatory Effects of Empagliflozin and Gemigliptin on LPS-Stimulated Macrophage via the IKK/NF-. J Immunol Res. 2021;2021:9944880.
294. Jones SC, Saunders HJ, Pollock CA. High glucose increases growth and collagen synthesis in cultured human tubulointerstitial cells. Diabet Med. 1999;16(11):932-8.
295. Morrisey K, Steadman R, Williams JD, Phillips AO. Renal proximal tubular cell fibronectin accumulation in response to glucose is polyol pathway dependent. Kidney Int. 1999;55(6):2548-72.
296. Zhang NMSGF. Efficacy of Liraglutide in Patients With Diabetic Nephropathy: A Meta-Analysis of Randomized Controlled Trials. This work is licensed under a Creative Commons Attribution 40 International License. 2021:14.
297. Aroor AR, Das NA, Carpenter AJ, Habibi J, Jia G, Ramirez-Perez FI, et al. Glycemic control by the SGLT2 inhibitor empagliflozin decreases aortic stiffness, renal resistivity index and kidney injury. Cardiovasc Diabetol. 2018;17(1):108.
298. Figueiredo JF, Bertels IM, Gontijo JA. Actin cytoskeletal and functional studies of the proximal convoluted tubules after preservation. Transplant Proc. 2008;40(10):3311-5.

299. Chen PY, Shih NL, Hao WR, Chen CC, Liu JC, Sung LC. Inhibitory Effects of Momordicine I on High-Glucose-Induced Cell Proliferation and Collagen Synthesis in Rat Cardiac Fibroblasts. Oxid Med Cell Longev. 2018;2018:3939714.
300. Guo S, Meng XW, Yang XS, Liu XF, Ou-Yang CH, Liu C. Curcumin administration suppresses collagen synthesis in the hearts of rats with experimental diabetes. Acta Pharmacol Sin. 2018;39(2):195-204.
301. Xie XW. Liquiritigenin attenuates cardiac injury induced by high fructose-feeding through fibrosis and inflammation suppression. Biomed Pharmacother. 2017;86:694-704.
302. Perico L, Conti S, Benigni A, Remuzzi G. Podocyte-actin dynamics in health and disease. Nat Rev Nephrol. 2016;12(11):692-710.
303. Motonishi S, Nangaku M, Wada T, Ishimoto Y, Ohse T, Matsusaka T, et al. Sirtuin1 Maintains Actin Cytoskeleton by Deacetylation of Cortactin in Injured Podocytes. J Am Soc Nephrol. 2015;26(8):1939-59.
304. Xu C, Zhou X, Xie T, Zhou Y, Zhang Q, Jiang S, et al. Renal tubular Bim mediates the tubule-podocyte crosstalk via NFAT2 to induce podocyte cytoskeletal dysfunction. Theranostics. 2020;10(15):6806-24.
305. DalleDonne I, Milzani A, Colombo R. H2O2-treated actin: assembly and polymer interactions with cross-linking proteins. Biophys J. 1995;69(6):2710-9.
306. Lv Z, Hu M, Ren X, Fan M, Zhen J, Chen L, et al. Fyn Mediates High Glucose-Induced Actin Cytoskeleton Reorganization of Podocytes via Promoting ROCK Activation In Vitro. J Diabetes Res. 2016;2016:5671803.
307. Nemoto O, Kawaguchi M, Yaoita H, Miyake K, Maehara K, Maruyama Y. Left ventricular dysfunction and remodeling in streptozotocin-induced diabetic rats. Circ J. 2006;70(3):327-34.
308. Romanelli G, Varela R, Benech JC. Diabetes induces differences in the F-actin spatial organization of striated muscles. Cytoskeleton (Hoboken). 2020;77(5-6):202-13.

11. CURRICULUM VITAE

Name and surname:	**Vjera Ninčević**
Date and place of birth:	31. srpnja 1990., Zagreb, Croatia
Nationality:	Croatian
Home address:	Senjska 2b, Karlovac
E-mail:	vnincevic@mefos.hr; vnincevic@fdmz.hr

Education:

2021 – present	Resident in General internal medicine, Cardiology, Clinical Hospital Osijek
2015 – 2021	Postgraduate doctoral study of Biomedicine and health
2009 – 2015	Medical doctor, Faculty of Medicine Osijek, University of J.J. Strossmayer in Osijek

Work experience:

2021 – present	Resident in General internal medicine, Cardiology, Faculty of Dental Medicine and Health, J.J. Strossmayer in Osijek
2018	Internship, Health Center Osijek
2017 – present	Research/Teaching Assistant, Department of Pharmacology and Biochemistry, Faculty of Dental Medicine and Health, J.J. Strossmayer in Osijek
2015- 2021	Research/Teaching Assistant, Department of Pharmacology, Faculty of Medicine Osijek, University of J.J. Strossmayera in Osijek

2016-2017 Postdoctoral Fellow, Department of Medicine, Division of Gastroenterology - Hepatology, University of Connecticut Health Center, Farmington, CT, USA.

Book chapters:

- M. Austria, Alyssa; **Ninčević, Vjera**; Y. Wu, George.
  A Brief Update on the Treatment of Hepatitis C // Update on Hepatitis C / Smolić, Martina; Včev, Aleksandar ; Y. Wu, George (ur.). Rijeka : InTech, 2017. Str. 3-16

Scientific articles:

- **Vjera Ninčević;** Milorad Zjalić; Tea Omanović Kolarić; Martina Smolić; Tomislav Kizivat; Lucija Kuna; Aleksandar Vcev; Ashraf A. Tabll; Ines Bilić Ćurčić has been accepted in Curr. Issues Mol. Biol.(ISSN 1467-3045) on 23 February 2022, Renoprotective effect of Liraglutide is mediated via inhibition of TGF-beta 1 in LLC-PK1 cell model of diabetic nephropathy, Q2, IF 2.081

- Kuna L, Zjalic M, Kizivat T, Roguljic H, **Nincevic V**, Omanovic Kolaric T, Wu CH, Vcev A, Smolic M*, Smolic R. Pretreatment of Garlic Oil Extracts Hampers Epithelial Damage in Cell Culture Model of Peptic Ulcer Disease. *Medicina (Kaunas)*. 2022 Jan 7;58(1):91. doi: 10.3390/medicina58010091. IF 2.430, Q2

- Tea Omanovic Kolaric*, **Vjera Nincevic***, Lucija Kuna, Kristina Duspara, Kristina Bojanic, Sonja Vukadin, Nikola Raguz-Lucic, George Y Wu, Martina Smolic. Drug-induced Fatty Liver Disease: Pathogenesis and Treatment. Journal of Clinical and Translational Hepatology. 2021 September, 9(5) 731-737. IF 4.108, Q2

- Kristina Duspara, Kristina Bojanic, Josipa Ivanusic Pejic, Lucija Kuna, Tea Omanovic Kolaric, **Vjera Nincevic**, Robert Smolic, Aleksandar Vcev, Marija Glasnovic, Ines Bilic Curcic and Martina Smolic. Targeting the Wnt Signaling Pathway in Liver Fibrosis for Drug Options: An Update. Journal of Clinical and Translational Hepatology. 2021 September. DOI: 10.14218/JCTH.2021.00065. IF 4.108, Q2
- Roguljic H, **Nincevic V**, Bojanic K, Kuna L, Smolic R, Vcev A, Primorac D, Vceva A, Wu GY, Smolic M. Impact of DAA Treatment on Cardiovascular Disease Risk in

Chronic HCV Infection: An Update. Front Pharmacol. 2021 May 11;12:678546. IF 5.810, Q1

- **Ninčević V**, Omanović Kolarić T, Roguljić H, Kizivat T, Smolić M, Bilić Ćurčić I. Renal Benefits of SGLT 2 Inhibitors and GLP-1 Receptor Agonists: Evidence Supporting a Paradigm Shift in the Medical Management of Type 2 Diabetes. Int J Mol Sci. 2019 Nov 20;20(23)., IF 4,331, Q1

- Omanović Kolarić, Tea; **Ninčević, Vjera**; Smolić, Robert; Smolić, Martina; Wu, George Y. Mechanisms of Hepatic Cholestatic Drug Injury. Journal of Clinical and Translational Hepatology, 7 (2019), Q2, IF 3.489

- Lucic, Nikola Raguz, Jakab, Jelena, Smolic, Martina, Milas, Ana-Maria, Kolaric, Tea Omanovic, **Nincevic, Vjera**, Bojanic, Kralik, Kristina, Miskulin, Maja, Wu, George Y., Smolic, Robert. Primary Care Provider Counseling Practices about Adverse Drug Reactions and Interactions in Croatia 2018, JOURNAL OF CLINICAL MEDICINE, IF 5.688, Q1

- **Vjera Ninčević**, Tomislav Kizivat, Tea Omanović Kolarić, Lucija Kuna, Anita Cindrić, Anamarija Banovac, Ines Bilić Ćurčić, Sandra Tucak-Zorić, Martina Smolić. Influence of Caffeine on Crystallization and Amelioration of Oxidative Stress on in vitro Model of Urolithiasis. Coll. Antropol. 44 (2020) 3: 121-125, Q4

Active participation in conferences:

- **Vjera Ninčević**, Milorad Zjalić, Tea Omanović Kolarić, Lucija Kuna, Tomislav Kizivat, Martina Smolić, Ines Bilić Ćurčić. Molecular mechanisms of renal effect of liraglutide on cellular model of proximal tubular cells. 8th European Virtual Congress of Pharmacology (EPHAR 2021), December 6-8, 2021.
- Omanović Kolarić Tea, **Ninčević Vjera**, Kizivat Tomislav, Kuna Lucija, Zjalić Milorad, Bilić Ćurčić Ines, Vukadin Sonja, Roguljić Hrvoje, Včev Aleksandar, Smolić

Martina. Amiodarone and tamoxifen induced fatty liver injury and possible in vitro protective effect of GLP-1RA cotreatment. 8th European Virtual Congress of Pharmacology (EPHAR 2021), December 6-8, 2021.

- Kuna Lucija, Zjalic Milorad, Kizivat Tomislav, Roguljic Hrvoje, **Nincevic Vjera**, Omanovic Kolaric Tea, Vcev Aleksandar, Smolic Martina, Smolic Robert. Garlic extracts act synergistically with lansoprazole against sodium taurocholate-induced ulcer disease in AGS cell culture model. 8th European Virtual Congress of Pharmacology (EPHAR 2021), December 6-8, 2021.
- Kuna Lucija, Smolic Robert, Martina Smolic, Kizivat Tomislav, Zjalic Milorad, **Nincevic Vjera**, Roguljic Hrvoje, Vukadin Sonja, Omanovic Kolaric Tea, Vcev Aleksandar. PREDTRETMAN ČEŠNJAKOVIM ULJEM SMANJUJE OŠTEĆENJE NASTALO DJELOVANJEM NaT-a U AGS MODELU ULKUSNE BOLESTI. 13. međunarodni znanstveno-stručni skup HRANOM DO ZDRAVLJA, 16-17 rujan, 2021.
- Roguljić Hrvoje, Smolić Martina, Kuna Lucija, Smolić Robert, Arambašić Jerko, Kizivat Tomislav, **Ninčević Vjera**, Vukadin Sonja, Omanovic Kolaric Tea, Bilić Ćurčić Ines, Včev Aleksandar. LJUTA PAPRIKA „STARA PRIJATELJICA“ S NOVOM ULOGOM. 13. međunarodni znanstveno-stručni skup HRANOM DO ZDRAVLJA, 16-17 rujan, 2021.
- Kizivat, Tomislav; **Ninčević, Vjera**; Cindrić, Anita; Omanović Kolarić, Tea; Kuna, Lucija; Smolić, Robert; Bilić-Ćurčić, Ines; Smolić, Martina
  EFFECTS OF CAFFEINE ON DEVELOPMENT OF OXIDATIVE STRESS AND CRYSTALLIZATION ON IN VITRO MODEL OF OXALATE UROLITHIASIS. // 9. Hrvatski kongres farmakologije s međunarodnim sudjelovanjem Zagreb, 2019. str. 132-132 (poster, međunarodna recenzija, sažetak, znanstveni)

- Kuna, Lucija; Kizivat, Tomislav; Smolić, Robert; Omanović Kolarić, Tea; **Ninčević, Vjera**; Včev, Aleksandar; Smolić, Martina
  THE ACTIVITY OF GARLIC EXTRACTS (ALLIUM SATIVUM) TO THE EPITHELIAL DAMAGE CAUSED BY SODIUM TAUROCHOLATE IN A CELL CULTURE MODEL OF ULCER DISEASE. // 9. Hrvatski kongres farmakologije s međunarodnim sudjelovanjem Zagreb, 2019. str. 136-136 (poster, međunarodna recenzija, sažetak, znanstveni)

- Omanović Kolarić, Tea; Raguž-Lučić, Nikola; **Ninčević, Vjera**; Smolić, Martina; Stavovi liječnika obiteljske medicine o stalnoj provedbi kontrole farmakoterapije. // Knjiga sažetaka X. Kongresa Društva nastavnika obiteljske medicine "SMJERNICE U PRAKSI OBITELJSKOG LIJEČNIKA"
  Zagreb, Hrvatska, 2019. str. 180-181 (poster, podatak o recenziji nije dostupan, sažetak, ostalo)

- Omanović Kolarić, Tea; **Ninčević, Vjera**; Raguž- Lučić, Nikola; Jakab, Jelena; Kuna, Lucija; Smolić, Robert; Bilić-Ćurčić, Ines; Včev, Aleksandar; Smolić, Martina Seniority of primary care physicians is associated with positive attitudes toward regular pharmacotherapy control habits. // PROGRAM AND ABSTRACTS- 11th ISABS Conference on Forensic and Anthropologic Genetics and Mayo Clinic Lectures in Individualized Medicine / Primorac, Dragan ; Schanfield, Moses ; Vuk-Pavlović, Stanimir ; Kayser, Manfred ; Ordog, Tamas (ur.). Zagreb, 2019. str. 165-165 (poster, međunarodna recenzija, sažetak, ostalo)

- Omanović Kolarić, Tea; **Ninčević, Vjera**; Kuna, Lucija; Kizivat, Tomislav; Včev, Aleksandar; Smolić, Martina
  KLINIČKI ZNAČAJNE INTERAKCIJE HRANE I LIJEKOVA. // Knjiga sažetaka s 12. međunarodnog znanstveno- stručnog skupa HRANOM DO ZDRAVLJA
  Osijek, Hrvatska, 2019. str. 75-75 (poster, međunarodna recenzija, sažetak, znanstveni)

- **Ninčević, Vjera**; Kizivat, Tomislav; Cindrić, Anita; Omanović Kolarić, Tea; Kuna, Lucija; Smolić, Robert; Bilić Ćurčić, Ines; Smolić, Martina
  POTENTIAL OF CAFFEINE TREATMENT ON OXIDATIVE STRESS AND CRYSTALLIZATION INHIBITION IN CELL CULTURE MODEL OF OXALATE UROLITHIASIS. // Knjiga sažetaka s 12. međunarodnog znanstveno- stručnog skupa HRANOM DO ZDRAVLJA
  Osijek, Hrvatska, 2019. str. 73-73 (poster, međunarodna recenzija, sažetak, znanstveni)

- Kuna, Lucija; Kizivat, Tomislav; Smolic, Robert; Omanovic Kolaric, Tea; **Nincevic, Vjera**; Vcev, Aleksandar; Smolic, Martina
  GASTROPROTECTIVE EFFECT OF GARLIC EXTRACTS (ALLIUM SATIVUM) ON AMELIORATING DAMAGE CAUSED BY SODIUM TAUROCHOLATE IN A

CELL MODEL OF ULCER DISEASE. // Knjiga sažetaka s 12. međunarodnog znanstveno- stručnog skupa HRANOM DO ZDRAVLJA
Osijek, Hrvatska, 2019. str. 66-66 (poster, međunarodna recenzija, sažetak, znanstveni)

- Omanović Kolarić, Tea; **Ninčević, Vjera**; Kuna, Lucija; Kizivat, Tomislav; Smolić, Robert; Smolić, Martina
  ASSESSMENT OF HEPATOSTEATOGENIC EFFECTS IN CELL CULTURE MODEL OF DRUG INDUCED FATTY LIVER DISEASE. // 9. Hrvatski kongres farmakologije s međunarodnim sudjelovanjem
  Zagreb, 2019. str. 135-135 (poster, međunarodna recenzija, sažetak, znanstveni)

- Jakab, Jelena; Omanović Kolarić, Tea; Kuna, Lucija; **Ninčević, Vjera**; Kizivat, Tomislav; Volarić, Nikola; Žulj, Marinko; Smolić, Robert; Včev, Aleksandar; Bilić-Čurčić, Ines; Smolić, Martina
  Establishing the model of adipogenesis in vitro. // Abstract book: 7th Croatian Congress of Obesity.
  Opatija, Hrvatska: Hrvatsko društvo za debljinu, 2018. str. 29-30 (poster, domaća recenzija, sažetak, znanstveni)

- Omanović Kolarić, Tea; **Ninčević, Vjera**; Smolić, Martina
  Assessment of the relevance of the specific scientific skills at Postgraduate doctoral study of Biomedicine and Health in Osijek. // ORPHEUS conference 2018
  Rejkjavik, Island, 2018. str. 38-38 (poster, podatak o recenziji nije dostupan, sažetak, ostalo)

- Omanović Kolarić, Tea; , **Ninčević, Vjera**; Jakab, Jelena; Kuna, Lucija; Kizivat, Tomislav; Raguž- Lučič, Nikola; Abičić, Ivan; Smolić, Robert; Včev, Aleksandar; Bilić- Ćurčić, Ines; Smolić, Martina
  In vitro assessment of molecular mechanisms of free fatty acids-induced and drugs-induced fatty liver disease. // Abstract book: 7th Croatian Congress of Obesity.
  Opatija, Hrvatska, 2018. str. 11-12 (poster, domaća recenzija, sažetak, znanstveni)

- Omanović, Tea; Kizivat, Tomislav; Raguž-Lučić, Nikola; **Ninčević, Vjera**; Jakab, Jelena; Kuna, Lucija; Smolić, Robert; Bilić-Čurčić, Ines; Včev, Aleksandar; Smolić, Martina

Evaluation of molecular mechanism differences in in vitro models of drug induced and fatty-acids induced NAFLD. // The 1st International Conference on Fatty Liver Abstracts / Safadi, Rifaat; Sanyal, Arun ; Anstee, Quentin (ur.).
Basel: Karger, 2017. str. 83-83 (poster, međunarodna recenzija, sažetak, znanstveni)

- Raguž-Lučić, Nikola; Milas, Ana Maria; Jakab, Jelena; Kralik, Kristina; Omanović, Tea; **Ninčević, Vjera**; Smolić, Martina
  Knowledge, attitudes and counseling about drug- drug interactions among primary care physicians (PCPs) in Croatia.. // Pharmacology
  London, Engleska, 2017. (poster, podatak o recenziji nije dostupan, neobjavljeni rad, znanstveni)

- Bilić-Ćurčić, Ines; Smolić, Martina; Smolić, Robert; **Ninčević, Vjera**; Omanović, Tea; Včev, Aleksandar
  Bone Mineral Density in Relation to Components of Metabolic Syndrome in Postmenopausal Women with Diabetes Type 2. // IUAES - World anthropologies and privatization of knowledge: engaing anthropology in public
  Dubrovnik, Hrvatska, 2016. (poster, sažetak, ostalo)

Awards:

- **2019**.- Award „VATROSLAV FLORSCHUTZ" for the best scientific article published in 2019 in the category of young scientist; Faculty of Medicine Osijek, University of J.J. Strossmayera in Osijek;
  Ninčević V, Omanović Kolarić T, Roguljić H, Kizivat T, Smolić M, Bilić Ćurčić I. „Renal Benefits of SGLT 2 Inhibitors and GLP-1 Receptor Agonists: Evidence Supporting a Paradigm Shift in the Medical Management of Type 2 Diabetes", International Journal of Molecular Sciences, IF: 4.183, Q1".

Membership in scientific and professional societies:

- Croatian Medical Chamber
- Croatian Society of Personalized Medicine
- Croatian Society of Human Genetics
- Croatian Pharmacological Society
- Croatian Catholic Medical Society

- International Society for Applied Biological Sciences (ISABS) Membership and Publication Committee

Courses:

- Workshop for mentors, December 7, 2016., Osijek, Croatia
- 10.06.2017 The Impact of CRISPR on Imprinting Disorders, University of CT Institute for Systems Genomics and The Health Care Genetics Professional Science Master'S Degree Program, USA.
- 26.8.2017-4.9.2017.Summer School of Clinical Pharmacology, Ohrid, Macedonia
- 26-30/9/2017 Workshop of International School of Pharmacology on "Adventures in the lipidome" heldin Erice, Sicily

Certified laboratory skills:

- Laboratory Animal Science Course, FELASA cat C equivalent, Zagreb, Croatia, March 2020.
- Laboratory imminotechniques in molecular biology research, University of Pecs, Medical School, Pecs, Hungary (14-18 December 2015.)
- May 10th, 2019., Certificate of Attendance to the 1 st Pecs-Osijek PhD symposium. Title of the presentation: Molecular mechanisms of renoprotective effect of SGLT2 and GLP1 analogue on cellular model of proximal tubule of healthy human kidney (HK2).

Participation in exchange programmes as a guest scientist or student

- Erasmus Programme, University of Pecs Medical School/Department of Immunology and Biotechnology in Hungry, 13.-19.6.2016.

Foreign languages:

- English C1
- German A2